7-1-2019

Extreme oxygen isotope zoning in garnet and zircon from a metachert block in melange reveals metasomatism at the peak of subduction metamorphism

F. Zeb Page
Oberlin College, Zeb.Page@oberlin.edu

Emilia M. Cameron

Clara Margaret Flood

Jeffrey W. Dobbins

Michael J. Spicuzza

See next page for additional authors

Repository Citation
Page, F. Zeb, Emilia M. Cameron, Clara Margaret Flood, et al. 2019. "Extreme oxygen isotope zoning in garnet and zircon from a metachert block in melange reveals metasomatism at the peak of subduction metamorphism." Geology 47(7): 655-658.

Authors

F. Zeb Page, Emilia M. Cameron, Clara Margaret Flood, Jeffrey W. Dobbins, Michael J. Spicuzza, Kouki Kitajima, Ariel Strickland, Takayuki Ushikubo, Christopher G. Mattinson, and John W. Valley

Extreme oxygen isotope zoning in garnet and zircon from a metachert block in mélange reveals metasomatism at the peak of subduction metamorphism

F. Zeb Page[1], Emilia M. Cameron[1,2], Clara Margaret Flood[1], Jeffrey W. Dobbins[1], Michael J. Spicuzza[2], Kouki Kitajima[2], Ariel Strickland[2], Takayuki Ushikubo[2*], Christopher G. Mattinson[3], and John W. Valley[2]**

[1] Geology Department, Oberlin College, Oberlin, Ohio 44074, USA
[2] WiscSIMS, Department of Geoscience, University of Wisconsin -Madison, Wisconsin 53706, USA
[3]Department of Geological Sciences, Central Washington University, Ellensburg, Washington 98926
**** Present Address: Kochi Institute for Core Sample Research, JAMSTEC 200 Monobe-otsu, Nankoku, Kochi 783-8502 Japan*

Post-Review revision
April 17, 2019

ABSTRACT

A tectonic block of garnet quartzite in the amphibolite-facies mélange of the Catalina Schist (Santa Catalina Island, California, USA) records the metasomatic pre-treatment of high-$\delta^{18}O$ sediments as they enter the subduction zone. The block is primarily quartz, but contains two generations of garnet that record extreme oxygen isotope disequilibrium and inverse fractionations between garnet cores and matrix quartz. Rare mm-scale garnet crystals record prograde cation zoning patterns, whereas more abundant ~200-μm diameter crystals have the same composition as rims on the larger garnets. Garnets of both generations have high $\delta^{18}O$ cores (20.8-26.3‰, VSMOW) that require an unusually high–$\delta^{18}O$ protolith, and lower–$\delta^{18}O$, less variable rims (10.0-11.2‰). Matrix quartz values are homogeneous (13.6‰). Zircon crystals contain detrital cores ($\delta^{18}O$ = 4.7-8.5‰, 124.6 +1.4/-2.9 Ma), with characteristic igneous trace-element composition likely sourced from arc-volcanics, surrounded by zircon with metamorphic age (115.1 ± 2.5 Ma) and trace-element compositions that suggest growth in the presence of garnet. Metamorphic zircon decreases in $\delta^{18}O$ from near-core (24.1‰) to rim (12.4‰), in equilibrium with zoned garnets.

Collectively, the data document the subduction of a mixed high-$\delta^{18}O$ siliceous ooze/volcanic ash protolith reaching temperatures of 550-625 °C prior to the nucleation of small garnets without influence from external fluids. Metasomatism is recorded in rims of both garnet and zircon populations as large volumes of broadly homogeneous subduction fluids stripped matrix quartz of its extremely high oxygen isotope signature. Zoned garnet and zircon in high-$\delta^{18}O$ subducted sediments offer a detailed window into subduction fluids.

INTRODUCTION

The nature and timing of mass transfer between the subducting plate and the sub-arc mantle is critical to our understanding of crustal formation at convergent margins and its geochemical signatures. Chemical and mechanical hybridization within subduction mélange plays an important role in these processes (e.g., Bebout and Penniston-Dorland, 2016), giving rise to models suggesting that partial melting of diapirs of hybridized mélange rocks are responsible for the classic trace element signature of arc rocks (Marschall and Schumacher, 2012) and the diversity of magma series found at convergent margins (Cruz-Uribe et al., 2018). Adding to these complications is the recent discovery that some sediments have entered the mantle and melted without mixing or hybridization, preserving extreme oxygen isotope signatures of surface weathering in their neoformed igneous zircon (Spencer et al., 2017). If subducted sediment can regularly carry its characteristically enriched oxygen isotope signature ($\delta^{18}O$ = ~7 - 42‰, VSMOW [Vienna standard mean ocean water]; Kolodny and Epstein, 1976; Eiler et al., 2001; Payne et al, 2015) into the mantle ($\delta^{18}O_{Ol}$ = 5.1‰, Eiler et al., 2000), it is surprising that oxygen isotope variability within the subarc mantle is so subtle and challenging to measure (Eiler et al., 1998). A solution to this discrepancy may be found in the fluid metasomatism of subducted sediments.

The first and perhaps most dramatic illustrations of a high degree of fluid flow within subduction mélange were studies of the oxygen isotope ratios of quartz and carbonate in veins within the Catalina Schist subduction complex (California, USA) suggesting km-scale oxygen isotope homogenization driven by large fluid fluxes (Bebout and Barton, 1989; Bebout, 1991). Over the last quarter century, the Catalina Schist has served as a laboratory for the study of subduction mélange, with numerous studies detailing fluid metasomatism and mechanical mixing processes in the subduction channel by means of stable isotopes (e.g., Bebout, 1991; Penniston-Dorland et al., 2012), major and trace elements (e.g., Sorenson and Barton, 1987; Hickmott et al., 1992; Penniston-Dorland et al., 2014) and radiogenic isotopes (King et al., 2006).

The in-situ analysis of oxygen isotopes in garnet is a powerful tool with which to decipher complex or extremely subtle fluid histories and tie them to the metamorphic record. In rocks that have experienced significant metasomatism, the extremely slow intragranular diffusion of oxygen in garnet allows it to preserve a robust geochemical record through all but the hottest and longest of metamorphic events (Vielzeuf et al., 2005). Oxygen isotope variability in garnets from eclogite has illustrated signals of infiltration by mantle (Russell et al., 2013) and supracrustal (e.g., Page et al., 2014; Martin et al., 2014; Rubatto and Angiboust, 2015) fluids that were previously undetectable using bulk methods.

Chert and siliceous schist are high–δ^{18}O lithologies (Eiler et al., 2001) that are found within the amphibolite-facies Catalina Schist mélange (Platt, 1975). In this contribution, we explore the metasomatism of a high–δ^{18}O garnet- and zircon- bearing metachert from a classic subduction mélange, in order to better understand the timing and metamorphic conditions of subduction fluid metasomatism, and to gain a more complete picture of how fluids mitigate the influence of high-δ^{18}O subduction inputs.

CATALINA GARNET QUARTZITE

Although much less numerous than the better-studied garnet-hornblende lithology, tectonic blocks of garnet quartzite are also found within the amphibolite-facies metasedimentary mélange of the Catalina Schist (Santa Catalina Island, California, USA), as well as in more coherent, faultbounded sheets (Platt, 1975; Bebout, 1991). In this study, we report on one exceptional sample of garnet quartzite collected from a meter-scale tectonic block hosted in a shale-matrix mélange from Upper Cottonwood Canyon (33°23'46.20"N, 118°24'52.80"W, Fig. 1A). The quartzite is composed primarily of quartz (93%), garnet (6%), and chlorite (<0.5%), with trace rutile, apatite, amphibole, and zircon (Fig. 1B). Garnet is present in two populations: copious fine-grained (<200µm-diameter) crystals dispersed throughout the sample and a smaller number of larger garnets (1-3mm-diameter, Fig. 1B). The larger crystals have abundant inclusions, which are primarily quartz and apatite. X-ray mapping and major element traverses show that the larger garnets display classic prograde cation-zoning profiles with decreasing Mn and increasing Mg# from core to rim, and with rim compositions similar to smaller, more homogenous (in cations) garnets in the same rock (Figs. 2A, B).

Oxygen Isotopes of Quartz and Garnet

Ion microprobe analysis of garnets (Page et al., 2010, see GSA Data Repository for full data, Tables DR-1, DR-2, and methods) shows extreme oxygen isotope zoning; values of $\delta^{18}O$ are 20.8-26.3‰ in garnet cores and 10.0-11.2‰ in garnet rims (Fig. 2A). Both large and small garnets in this sample show a similar range in $\delta^{18}O$, despite the difference in cation zoning and crystal size. Zoning in oxygen isotopes is sharp, with up to a 7‰ drop in $\delta^{18}O$ over a few micrometers, whereas cation zonation is much more gradual with slightly increased Ca and Mg in the rims of larger garnets (Fig. 2). Smaller garnets are nearly homogeneous with a slight increase in Mg# from core to rim. Matrix quartz has no systematic zoning in cathodoluminescence imaging (CL) and is homogeneous in $\delta^{18}O$ with ion microprobe analyses (13.5‰) identical (within uncertainty) to bulk (~2mg) analysis by laser fluorination (13.6‰).

Garnet-core and quartz pairs yield reversed fractionations ($\delta^{18}O_{grt} > \delta^{18}O_{qz}$), indicating profound disequilibrium. Eleven analyses of quartz inclusions in large garnet cores yield $\delta^{18}O$ = 13.8-16.2‰, higher than matrix quartz, but not in equilibrium with host garnet. Inclusions were generally >50µm, and commonly along cracks and so are unlikely to preserve their original values.

Oxygen Isotopes in Zircon

Zircons were separated from the sample and mounted in epoxy for analysis (see GSA Data Repository). CL imaging (Fig. 3A) reveal oscillatory-zoned cores, often as fragments of crystals, containing inclusions of quartz, K-feldspar, and biotite. These detrital cores are surrounded by annuli of variable intensity, somewhat mottled zircon, containing inclusions of quartz, biotite, sphene, and rutile. Outside of this mottled zone, zircons typically have darker-intensity-CL oscillatory-zoned rims, with rare crystals containing a brighter outer rim with faint oscillatory zoning.

Zircons were analyzed for their oxygen isotope ratios by ion microprobe using both a ~15- and a sub-1-µm diameter beam (Tables DR-4, -5). Highly precise and accurate oxygen isotope ratios from the larger analysis pits are correlated with CL zonation and inclusion population. Zircon cores (n=7) have $\delta^{18}O$ from 4.7 to 8.4‰ (Figs. 3A, 3B). Zircon with mottled CL immediately outside of detrital cores (n=17) has an extremely high $\delta^{18}O$ (Fig. 3A, 3B) of 22.6 ±3.3‰ (2 SD, sample) if one anomalously low analysis is discounted. Intermediate-intensity oscillatory-zoned rims (n=20) have lower $\delta^{18}O$ values (17.3 ±3.9‰), and rare bright outer rims have lower-still $\delta^{18}O$ values (12.9 ±3.3‰). To further determine if there is a systematic zoning pattern in zircon like that found in garnet, 29 sub-1-µm analyses (following the method of Page et al., 2007) were made in traverses across a single zircon (Fig. 3A). These high-spatial resolution (but less precise, ±0.9-1.7‰, 2S.D.) analyses confirm the presence of a low $\delta^{18}O$ core (6.3 ±1.1‰, 2S.D., n=6), surrounded by an extremely high-$\delta^{18}O$ mottled CL region (22.6 ±2.4‰, n=15), indistinguishable within the uncertainty of the sub-1-µm data from the 15-µm-diameter analyses of the same zones. An outer, darker oscillatory-zoned rim has $\delta^{18}O$ of 17.0 ±2.5‰, n=8). The zircon chosen for this analysis does not have an outermost, lighter rim.

PRESSURE, TEMPERATURE, AND TIME HISTORY

The limited mineralogy of this sample coupled with its metasomatic history and zoned minerals, makes thermobarometry challenging. However, an equilibrium assemblage diagram calculated using an estimate of the bulk composition and the computer package Perple_X (Connolly, 2009; Fig. DR-1) yields reasonable results. The observed assemblage (qz+grt+ru±chl) is predicted to form at pressures greater than 8kbar and temperatures greater than 550˚C. The core to rim increase of Mg# observed in the large garnets is consistent with growth during increasing temperatures in the presence of chlorite, and is predicted by the model to have taken place at ~550-650˚C, at pressures of greater than 11kbar, consistent with existing pressure and temperature estimates of amphibolite blocks in the same mélange and [Zr]-in-rutile thermometry from this same sample (Sorenson and Barton, 1987; Hartley et al., 2016; Penniston-Dorland et al., 2018). The closeness between the conditions predicted by the model and existing thermobarometry from Catalina suggests that the metasomatism of this block did not involve substantial change in cation composition. Regardless of the precise conditions of metamorphism, the concomitant decrease in $\delta^{18}O$ with increasing Mg# in garnet requires metasomatism as the sample increased in temperature within the subduction environment.

Zircons were additionally analyzed by SHRIMP-RG for U-Pb isotopes and select trace elements (GSA Data Repository). Detrital zircon cores have more elevated Th/U ratios (0.36-0.89), and are older than rims; 8 of 9 analyses yield a coherent ^{204}Pb-corrected ^{206}Pb*/^{238}U age of 124.6 +1.4/-2.9 Ma (Fig. 3C). Th/U ratios of rims are lower (0.02-0.13) and yield an age of 115.1±2.4 Ma consistent with an igneous origin for zircon cores, and a metamorphic one for the rims (Fig. 3C). Zircon rims also have smaller Eu-anomalies (Eu/Eu* close to 1) and flatter HREE patterns, consistent with a metamorphic origin in a garnet-present, plagioclase-absent high-pressure environment (Fig. 3D).

DISCUSSION

Taken together, the P-T-t-fluid data preserved in garnet and zircon from this sample provide a detailed record of metasomatic events within the subduction channel. A mixed-lithology protolith containing both extremely high-δ^{18}O siliceous material intermixed with intermediate/mafic igneous material including detrital igneous zircon grains was subducted in the Catalina trench. The most plausible interpretation is that the protolith was a mixture of chert or siliceous ooze mixed with ~124 Ma arc volcanoclastic material. The relative purity of the quartzite and the narrow range of zircon core ages seems to preclude weathering of plutonic source material as an origin for the inherited cores. This mixed sediment was subducted and metamorphosed initially as a closed system, with larger, prograde garnet cores having high and unchanging δ^{18}O values. The extreme oxygen isotope ratio of this sample (quartz in equilibrium with garnet cores at 550˚C would have been greater than 30‰, Valley et al., 2003) makes it highly sensitive to infiltration from external fluids with lower δ^{18}O. A second generation of garnets nucleated near the peak of metamorphism, but their growth was not initiated by an external fluid, as core $\delta^{18}O$ compositions are identical to larger garnets. As metamorphic temperatures reached their peak, an external fluid permeated the sample, perhaps due to introduction of the block into the subduction mélange, shifting matrix quartz $\delta^{18}O$ from ~30‰ to 13.6‰. Slow rates of intragranular diffusion preserve a record of the original high-$\delta^{18}O$ composition of garnet and zircon, and their continued growth documents decreasing $\delta^{18}O$ from ~24‰ to ~17‰ to ~11‰ VSMOW, possibly in two discreet pulses. Fractionation between matrix quartz and garnet rim compositions yield temperatures of ~600-750˚C (Valley et al., 2003), consistent with estimates of peak metamorphic temperatures for the block and the region. Likewise, garnet cation composition records increasing temperature (pressure is not well constrained) during metasomatism. Perhaps upwelling within the subduction channel stopped quartz recrystallization and garnet growth simultaneously, effectively ending the record preserved in this sample.

The limited range of $\delta^{18}O$ in quartz and calcite veins within the Catalina Schist first reported by Bebout and Barton (1989) suggests that the entire package of subduction rocks on Catalina Island interacted with a remarkably homogeneous supracrustal fluid reservoir derived from metamorphic dehydration of minerals deeper along the subducting slab with an oxygen isotope composition of 13±1.0‰ VSMOW. The quartz $\delta^{18}O$ value for the block in mélange in this study (13.6‰ VSMOW) yields a calculated water $\delta^{18}O$ value of 12.3‰ VSMOW (650˚C, Friedman and O'Neil, 1977) in close agreement with the range reported by Bebout and Barton.

Although high−$\delta^{18}O$ sediments make up a volumetrically small portion of subducted material, the extreme contrast between their isotope ratios and those of the mantle make them likely candidates for introducing fine-scale isotope anomalies in the sub-arc mantle. Indeed, the recent discovery of high−$\delta^{18}O$ S-type granite within supra-subduction-zone mantle as well as this contribution show that this can happen (Spencer et al., 2017). The sample documented in this study is an example of the most extreme contrast in $\delta^{18}O$ that one might expect to be subducted, with an estimated protolith $\delta^{18}O$ of 30‰. However, the metasomatic processes documented by garnet and zircon zonation in this metachert from Catalina show that subduction fluids can all but wipe out extremely high–$\delta^{18}O$ inputs to subduction zones. Given the modest modal proportion of garnet (7%) with respect to quartz (93%) in this sample, and assuming $\delta^{18}O$ values of 24‰ for garnet and 14‰ for quartz, the whole rock $\delta^{18}O$ of this rock must be less than 15‰, a value that can also be found in the much more abundant subducted metabasalts with protoliths enriched in ^{18}O by low-temperature interaction with sea water (Eiler, 2001). Subduction fluids play a vital role in the generation of arc magmatism and continental growth, but is also seems that they play an important role in buffering the $\delta^{18}O$ of rocks that are recycled into the mantle by subduction, with only strongly refractory (and volumetrically minor) phases such as zircon and garnet able to carry extreme oxygen isotope ratios into the mantle.

ACKNOWLEDGMENTS

We thank Eric Essene, who provided mentorship, assistance in the field, and partial funding for SIMS analysis, S. Penniston-Dorland, E. Walsh and the 2012 Keck Catalina Project (NSF-REU-1062720) students for assistance with fieldwork on Catalina Island, and the Catalina Island Conservancy for access and field support. Comments from Christopher Spencer, two anonymous reviewers and editor Chris Clarke improved this manuscript and are gratefully acknowledged. Assistance with EPMA and laser fluorination analyses were provided by G. Moore (University of Michigan) and Mike Spicuzza (University of Wisconsin). The WiscSIMS ion microprobe laboratory is supported by National Science Foundation (EAR-1355590, 1658823) and the University of Wisconsin–Madison. FZP, EMC, CMF and JWD gratefully acknowledge financial support from Oberlin College and NSF (EAR-1249778). JWV is supported by NSF (EAR-1524336).

REFERENCES CITED

Bebout, G. E., 1991, Field-based evidence for devolatilization in subduction zones: implications for arc magmatism: Science, v. 251, p. 413-416.

Bebout, G. E., and Barton, M. D., 1989, Fluid flow and metasomatism in a subduction zone hydrothermal system: Catalina Schist terrane, California: Geology, v. 17, p. 976-980.

Bebout, G. E., and Penniston-Dorland, S. C., 2016, Fluid and mass transfer at subduction interfaces—The field metamorphic record: Lithos, v. 240-243, p. 228–258, doi: 10.1016/j.lithos.2015.10.007.

Connolly, J. A. D. (2009) The geodynamic equation of state: what and how: Geochemistry, Geophysics, Geosystems, v. 10:Q10014, doi:10.1029/2009GC002540.

Cruz-Uribe, A.M., Marschall, H.R., Gaetani, G.A., and Le Roux, V., 2018, Generation of alkaline magmas in subduction zones by partial melting of mélange diapirs—An experimental study: Geology, v. 46, p. 343–346, doi: 10.1130/G39956.1.

Eiler, J.M., 2001, Oxygen isotope variations of basaltic lavas and upper mantle rocks, *in* Valley, J.W. and Cole, D.R. eds., Reviews in Mineralogy & Geochemistry Vol. 43: Stable Isotope Geochemistry: Mineralogical Society of America, p. 319–364, https://doi.org/10.2138/gsrmg.43.1.319.

Eiler, J.M., McInnes, B., Valley, J.W., Graham, C.M., and Stolper, E.M., 1998, Oxygen isotope evidence for slab-derived fluids in the sub-arc mantle: Nature, v. 393, p. 777–781, https://doi.org/10.1038/31679.

Eiler, J.M., Schiano, P., Kitchen, N., and Stolper, E.M., 2000, Oxygen-isotope evidence for recycled crust in the sources of mid-ocean-ridge basalts: Nature, v. 403, p. 530–534, https://doi.org/10.1038/35000553.

Friedman, I. and O'Neil, J. R., 1977, Compilation of stable isotope fractionation factors of geochemical interest: U.S. Geological Survey Professional Paper, v. 440-KK.

Hartley, E.S., Pereira, I., Moreira, H., Page, F.Z., and Storey, C.D., 2016, Petrology and trace element thermometry of garnet-quartzite from the Catalina Schist, Geological Society of America Abstracts with Programs, v.48, n.7. Abst. 258-3.

Hickmott, D., Sorensen, S. S., and Rogers, P., 1992, Metasomatism in a subduction complex; constraints from microanalysis of trace elements in minerals from garnet amphibolite from the Catalina Schist: Geology, v. 20, p. 347–350.

King, R. L., Bebout, G. E., Moriguti, T., and Nakamura, E., 2006, Elemental mixing systematics and Sr-Nd isotope geochemistry of melange formation: Obstacles to identification of fluid sources to arc volcanics: Earth and Planetary Science Letters, v. 246, p. 288–304.

Kolodny, Y., and Epstein, S., 1976, Stable isotope geochemistry of deep sea cherts: Geochimica et Cosmochimica Acta, v. 40, p. 1195-1209.

Marschall, H.R., and Schumacher, J.C., 2012, Arc magmas sourced from mélange diapirs in subduction zones: Nature Geoscience, v. 5, p. 862–867, doi: 10.1038/ngeo1634.

Martin, L.A., Rubatto, D., Crépisson, C., Hermann, J., Putlitz, B., and Vitale Brovarone, A., 2014, Garnet oxygen analysis by SHRIMP-SI: Matrix corrections and application to high-pressure metasomatic rocks from Alpine Corsica: Chemical Geology, v. 374-375, p. 25–36, doi: 10.1016/j.chemgeo.2014.02.010.

Page, F. Z., Ushikubo, T., Kita, N. T., Riciputi, L. R., and Valley, J. W., 2007, High-precision oxygen isotope analysis of picogram samples reveals 2 μm gradients and slow diffusion in zircon: American Mineralogist, v. 92, p. 1772-1775.

Page, F. Z., Kita, N. T., and Valley, J. W., 2010, Ion microprobe analysis of oxygen isotopes in garnets of complex chemistry: Chemical Geology, v. 270, p. 9-19.
Page, F.Z., Essene, E.J., Mukasa, S.B., and Valley, J.W., 2014, A garnet-zircon oxygen isotope record of subduction and exhumation fluids from the Franciscan Complex, California: Journal of Petrology, v. 55, p. 103–131.
Payne, J.L., Hand, M., Pearson, N.J., Barovich, K.M., and McInerney, D.J., 2015, Crustal thickening and clay: Controls on O isotope variation in global magmatism and siliciclastic sedimentary rocks: Earth and Planetary Science Letters, v. 412, p. 70–76, doi: 10.1016/j.epsl.2014.12.037.
Penniston-Dorland, S. C., Bebout, G. E., Pogge von Strandmann, P. A. E., Elliott, T., and Sorensen, S. S., 2012, Lithium and its isotopes as tracers of subduction fluids and metasomatic processes: Evidence from the Catalina Schist, California, USA: Geochimica et Cosmochimica Acta, v. 77, p. 530-545.
Penniston-Dorland, S. C., Gorman, J. K., Bebout, G. E., Piccoli, P. M., and Walker, R. J., 2014, Reaction rind formation in the Catalina Schist: Deciphering a history of mechanical mixing and metasomatic alteration: Chemical Geology, v. 384, p. 47–61.
Penniston-Dorland, S.C., Kohn, M.J., and Piccoli, P.M., 2018, A mélange of subduction temperatures: Evidence from Zr-in-rutile thermometry for strengthening of the subduction interface: Earth and Planetary Science Letters, v. 482, p. 525–535, doi: 10.1016/j.epsl.2017.11.005.
Platt, J., 1975, Metamorphic and deformational processes in the Franciscan Complex, California: some insights from the Catalina Schist terrane: Bulletin of the Geological Society of America, v. 86, p. 1337–1347.
Rubatto, D., and Angiboust, S., 2015, Oxygen isotope record of oceanic and high-pressure metasomatism: a P–T–time–fluid path for the Monviso eclogites (Italy): Contributions to Mineralogy and Petrology, v.170:44, p. 1–16, doi: 10.1007/s00410-015-1198-4.
Russell, A. K., Kitajima, K., Strickland, A., Medaris, Jr, L. G., Schulze, D. J., and Valley, J.W., 2013, Eclogite-facies fluid infiltration: constraints from $\delta^{18}O$ zoning in garnet: Contributions to Mineralogy and Petrology, v. 165, p. 103-116.
Spencer, C.J., Cavosie, A.J., Raub, T.D., Rollinson, H., Jeon, H., Searle, M.P., Miller, J., McDonald, B.J., Evans, N.J., and EIMF, 2017, Evidence for melting mud in Earth's mantle from extreme oxygen isotope signatures in zircon: Geology, v. 45, p. 975-978, doi: 10.1130/G39402.1.
Valley, J. W., 2003, Oxygen isotopes in zircon: Reviews in Mineralogy and Geochemistry, v. 53, p. 343-385.
Vielzeuf, D., Veschambre, M., and Brunet, F., 2005, Oxygen isotope heterogeneities and diffusion profile in composite metamorphic-magmatic garnets from the Pyrenees: American Mineralogist, v. 90, p. 463–472.

FIGURE CAPTIONS

Figure 1. A) Geologic sketch map of Santa Catalina Island, California (after Platt, 1975) showing sample locations. B) Polished thick section of a garnet quartzite showing two garnet sizes. (grt1 – larger, cation-zoned garnet, grt2 – smaller, garnet crystals, homogeneous in cations, qz-quartz, ru – rutile, ap – apatite, chl – chlorite)

Figure 2. A) $\delta^{18}O$ and cation traverse, rim to rim, of a single ~2.5mm dia. garnet. The core region is generally homogeneous at ~25‰ (aquamarine points), transitions to intermediate values (orange) and low, ~10‰ rims (purple) over short intervals, although zoning is asymmetric. Mg/(Mg+Fe) (Mg#, solid line) increases continuously core to rim. B) Ternary diagram of garnet cation compositions, mm-scale garnets are shown as solid circles, ~100µm-scale garnets shown as open circles. Analysis location (core, intermediate, rim) is also correlated with $\delta^{18}O$, and indicated by color, as in A. Larger garnets have greater cation zoning than smaller garnets (dashed arrow), and all oxygen isotope zonation takes place at the most pyrope-rich compositions for both sizes (alm - almandine, pyp – pyrope, grs -- grossular, sps – spessartine).

Figure 3. Catalina quartzite zircon chemistry and age A) CL images (25µm scale bars) of three zircons showing different CL domains (see text for details). Analysis of $\delta^{18}O$ are shown with two spot sizes and labeled with values in VSMOW (~15µm, ±0.2-0.4‰ 2S.D., Table DR-5; <1µm, ± 2.5‰ 2S.D., Table DR-6). B) Histogram of analyses of zircon and garnet with a 15µm diameter spot from sample 05C-09 grouped by CL domain and/or location across a traverse, colors as in Figure 2.

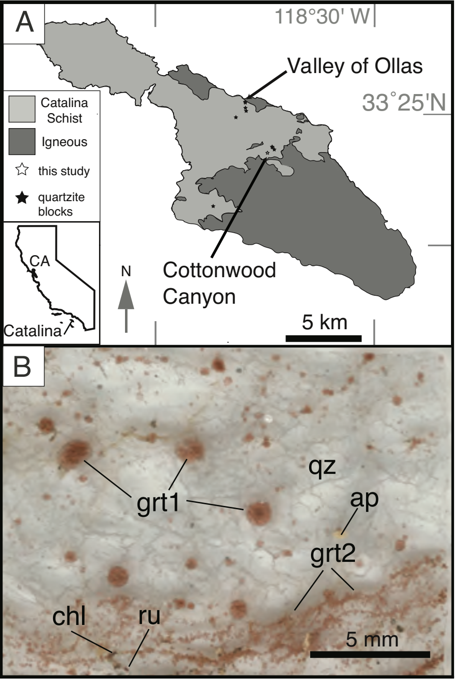
A
118°30' W
Valley of Ollas
33°25'N
Catalina Schist
Igneous
this study
quartzite blocks
CA
Catalina
N
Cottonwood Canyon
5 km
B
qz
grt1
ap
grt2
chl
ru
5 mm

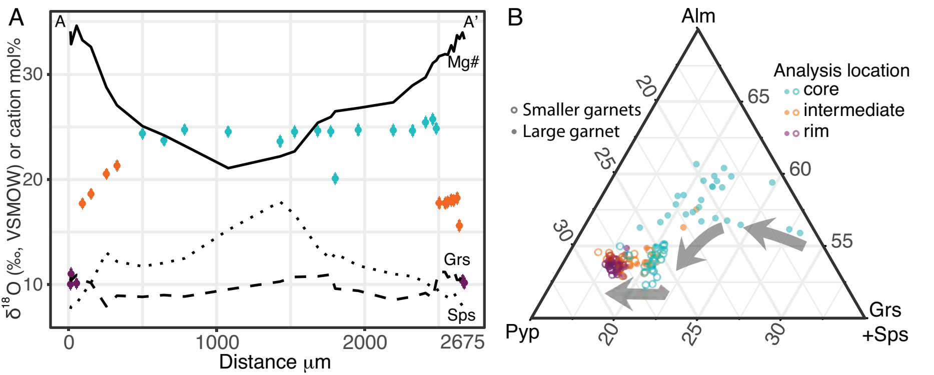

A
A
A'
Mg#
Grs
Sps
δ18O (‰, VSMOW) or cation mol%
30
20
10
0
1000
2000
2675
Distance μm
B
Alm
Pyp
Grs
+Sps
20
25
30
65
60
55
Smaller garnets
Large garnet
Analysis location
core
intermediate
rim

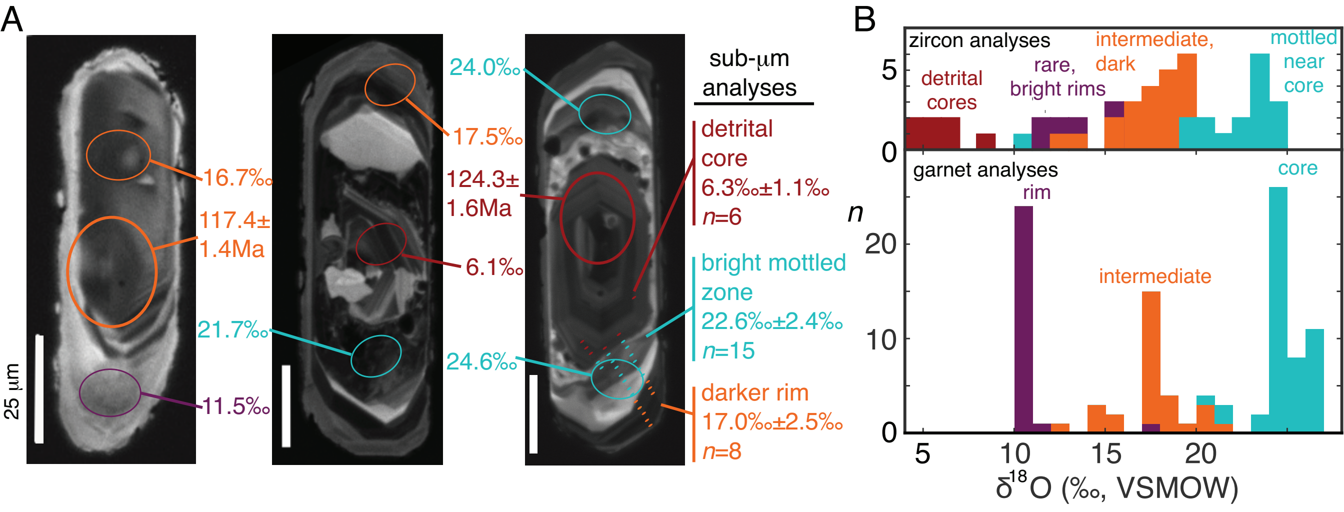

A
16.7‰
117.4±
1.4Ma
21.7‰
11.5‰
25 μm
17.5‰
124.3±
1.6Ma
6.1‰
24.0‰
24.6‰
sub-μm
analyses
detrital
core
6.3‰±1.1‰
n=6
bright mottled
zone
22.6‰±2.4‰
n=15
darker rim
17.0‰±2.5‰
n=8
B
zircon analyses
detrital
cores
rare,
bright rims
intermediate,
dark
mottled
near
core
garnet analyses
rim
intermediate
core
n
δ18O (‰, VSMOW)

GSA Data Repository Item
Methods and Data from Page et al. (2019)

Table of Contents

METHODS

Laser Fluorination

Laser fluorination analyses were performed over two days at the University of Wisconsin – Madison. Samples were crushed by hand to ~500 μm and 1.5 - 2mg of monomineralic, inclusion-free material was hand-picked under a dissecting microscope, pre-treated overnight in a BrF_5 atmosphere and then heated by CO_2 laser (λ = 10.6 µm) in the presence of BrF_5. Unknown analyses were standardized against 4 analyses each day of the UWG-2 standard (Valley et al., 1995) and are reported in standard permil notation on the VSMOW scale. The average of the four UWG-2 analyses on day 1 was 5.64±0.11 (2SD) yielding a correction of +0.16‰. The average of the four UWG-2 analyses on day 2 was 5.71±0.15 (2SD) yielding a correction of +0.09‰.

Oxygen isotope analysis of garnet and quartz by ion microprobe

Oxygen isotope analyses of garnet and quartz were performed on the WiscSIMS CAMECA ims-1280 multi-collector ion microprobe at the University of Wisconsin—Madison in two sessions. All garnet and quartz analyses by ion microprobe were measured within 5mm of the center point of 2.54cm round thin sections with garnet (UWG-2; Valley et al., 1995) and quartz (UWQ-1; Kelley et al., 2007) standard materials embedded in the samples and polished to be co-planar with the thin sections. Analysis conditions were the same as described in Kita et al. (2009) and Valley and Kita (2009). A 2–3 nA Cs^+ primary ion beam (20 kV total accelerating voltage) was focused to a diameter of 10-15μm on the gold-coated sample surface. Mass calibrations were performed every 12 hours. Compositionally-dependent bias correction for garnets was performed according to the method of Page et al. (2010). At the start of each analytical session, a bias correction curve was determined by analyses of compositional standards (Table DR-1 and embedded figures, see Page et al., 2010 for more information on the technique and standards used). Ion probe analyses of garnet and quartz are presented in Table DR-2.

Garnet cation compositions (Table DR-3) were determined using the CAMECA SX100 electron microprobe at the University of Michigan using a point beam with 15 kV accelerating voltage and 20 nA beam current. Natural and synthetic silicate and oxide standards were used and a Cameca-type PAP correction was applied. Elemental analyses were made directly adjacent, but more than 5μm away from to ion probe analysis pits after $\delta^{18}O$ analysis.

Instrument stability during analytical sessions was documented by repeated analyses of the UWG-2 (or UWQ-1) standard in groups of four analyses every 10-12 unknown analyses. Each bracket of unknowns is corrected for instrumental bias based on the average of eight bracketing standard analyses without the application of a drift correction. Garnet analyses are additionally corrected for instrumental bias due to chemical differences between the unknown garnets and the UWG-2 standard following the method of Page et al. (2010). The uncertainty of each unknown quartz analysis is calculated as two standard deviations of the average of the eight standards that bracket a series of unknowns. The precision of garnet analyses is taken as the analytical uncertainty (as calculated for quartz) but with an additional uncertainty for the cation matrix correction of 0.3‰ added in quadrature.

Oxygen isotope analysis of zircon by ion microprobe

Oxygen isotope analyses of zircon were performed on the WiscSIMS CAMECA ims-1280 multi-collector ion microprobe at the University of Wisconsin— Madison in two analytical sessions. Zircons were separated from sample 05C-09 using standard gravimetric and magnetic techniques, mounted in epoxy with the KIM-5 standard (Cavosie et al., 2005) within 5mm of the central point of the 2.54cm diameter mount, and polished until an approximately equatorial section was exposed. Zircons were imaged using panchromatic cathodoluminescence (CL) at the University of Wisconsin-Madison. For the first analytical session, analysis conditions and technique were as reported above for garnet and quartz, with standardization and analytical uncertainty measured using the KIM-5 zircon standard. Zircons were analyzed using the same surface as SHRIMP pits (see next section) Standard and unknown data are presented in Table DR-5. After analysis, pit morphology was examined using secondary electron imaging, and a new sample surface was exposed by hand polishing. A single zoned zircon was selected for sub-micron pit-size analysis and reimaged in CL.

Sub-micron pit oxygen isotope analyses were made at WiscSIMS using the same technique as Page et al. (2007) with the exception that all zircon analyses were normalized using standard KIM-5 (Valley et al., 2003; Cavosie et al., 2005). Analysis setup followed the same protocols as described above, with the following exceptions: the primary ion beam was focused to smaller than 1 μm, confirmed by imaging of a calibrated Si wafer. Because ion probe pits are generally longer in the X-direction (in the plane of both the primary and secondary ion beams) the sample was inserted so that planned traverses would be in the Y-direction, allowing for the highest spatial resolution. Secondary electron images of the pits show pit dimensions of 600 nm x 900 nm with a shallow halo of ~1.5 x 2 μm due to primary beam aberration. The intensity of ^{16}O was (1-2) x10^6 cps, depending on the primary beam intensity, which ranged from 2 to 1 pA over the analytical session. ^{18}O was measured using a miniaturized Hamamatsu electron multiplier (EM) in the multicollector. The dead time of the detector is estimated to be 68ns, which is very close to the hardware setting of the counting system. The pulse height distribution of the EM detector was adjusted to peak at 280mV before the KIM5 standard analyses and was not changed during the session because relatively lower ^{18}O ion currents (2,000-4,000 cps) are unlikely to cause aging of the EM detector during a single day of analyses. The use of an EM/FC configuration for these analyses results in rather different raw $\delta^{18}O$ values than those measured using the FC/FC configuration of the 7 and 10 μm analyses as would be predicted based on the different properties of these detectors. Total analytical time per spot was about 24 minutes including pre-sputtering (360 sec), automatic retuning of the secondary beam (ca. 60 sec), and analysis (1000 sec).

Uranium-lead isotope and trace element analysis of zircon by ion microprobe

Analysis of U-Pb isotopes and trace elements (Th, U, La, Ce, Nd, Sm, Eu, Gd, Dy, Er, Yb, Hf) were conducted in one session at the Stanford University/USGS SHRIMP-RG ion microprobe using the same epoxy mount described in the section above. Analyses were guided by CL, and standardized to zircons R33 and CZ3, and followed the methods described in Gilotti et al. (2011). Data were reduced using the software SQUID and ISOPLOT (Ludwig, 2001,2003).

EQUILIBRIUM ASSEMBLAGE MODELLING

An equilibrium assemblage diagram (EAD) was constructed for the sample in the MnCFMASHT system using Perple_X v. 6.6.8 (Connolly, 2009). The modelled bulk composition was determined by collecting 75 low-magnification back-scattered electron images uniformly distributed across the thin section. Mineral modes were determined using image analysis software and bulk composition. K_2O and Na_2O contents were negligible and were excluded from the model. The bulk composition (SiO_2 96.1, TiO_2 0.1, Al_2O_3 1.4, FeO 1.4, MnO 0.2, MgO 0.6, CaO 0.2, wt.%) was corrected to exclude CaO found in apatite. SiO_2 and H_2O were modeled as saturated components. We used solution models Gt(HP), Chl(HP), Cpx(HP), Opx(HP), Pheng(HP), cAmph(DP2), oAmph(DP), IlGkPy and melt(HP) and the thermodynamic data file hp02ver.dat (Holland and Powell, 1998). The resulting EAD (Fig. DR-1) matches observed mineralogy with the exception of the prediction of trace kyanite in all fields, and is likely an artifact of error in the estimation of bulk composition. The peak metamorphic assemblage of qz+grt+ru±chl spans a large range of P-T space, but is consistent with existing estimates of peak metamorphic conditions (10-15kbar, 650-700˚C) on Catalina based on thermobarometry of amphibolite blocks (Sorensen and Barton, 1987). A lower pressure limit of 8kbar is based on rutile (rather than ilmenite) stability is predited by the model. Compositional isopleths show that large garnets record increasing prograde temperatures of 600˚-650˚, with small garnets forming at the high end of that pressure range. The high-Mg garnet isopleths are at the high T end of the chlorite-bearing field, consistent with the small modal content of chlorite. Garnet of the composition found in this sample is predicted by the model not to form in the presence of rutile below ~14 kbar, and providing a minimum estimate of pressure. Despite the evidence of substantial late fluids resetting oxygen isotopes in quartz, these P-T estimates are broadly consistent with previous estimates (Sorensen and Barton, 1987), and are within ~75˚C of [Zr] in rutile thermometry of both similar lithologies and garnet hornblende blocks on Catalina (Hartley et al., 2016; Penniston-Dorland et al., 2016). If the bulk composition of this block was shifted by late fluid metasomatism, then it was likely minimal given these P-T results.

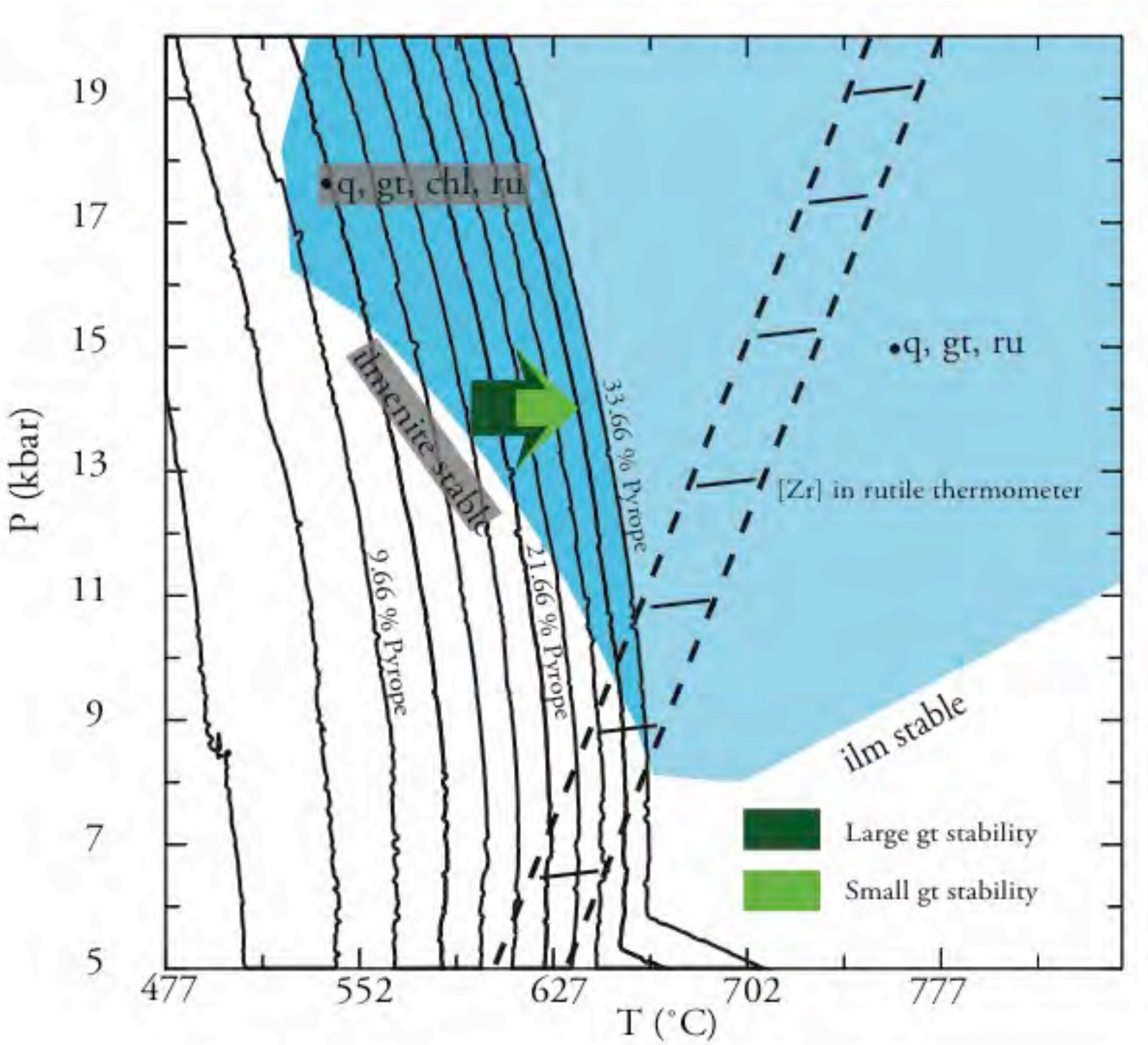

Figure DR- 1 Equilibrium Assemblage Diagram for Catalina Quartzite 05C-09. The peak metamorphic assemblage is qz + gt + ru ±chl, and is shown in blue. A low P limit is established by the stability field of rutile. Garnet isopleth thermometry is shown for large and small garnets as green arrows. Given the inherent uncertainties in thermobarometry and the late metasomatic history of the rock, the diagram is conservatively interpreted to show garnet growth during prograde heating of the sample. [Zr] in rutile thermometry range is from Hartley et al. (2016).

References

Cavosie, A.J., Valley, J.W., Wilde, S.A., and EIMF, 2005, Magmatic $\delta^{18}O$ in 4400-3900 Ma detrital zircons: A record of the alteration and recycling of crust in the Early Archean: Earth and Planetary Science Letters, v. 235, no. 3-4, p. 663–681.

Connolly, J.A.D., 2009, The geodynamic equation of state: What and how: Geochemistry Geophysics Geosystems, v. 10, p. Q10014, doi: 10.1029/2009GC002540.

Gilotti, J.A., and McClelland, W.C., 2011, Geochemical and Geochronological Evidence That the North-East Greenland Ultrahigh-Pressure Terrane Is Laurentian Crust: Journal of Geology, v. 119, no. 5, p. 439–456, doi: 10.1086/660867.

Hartley, E.S., Pereira, I., Moreira, H., Page, F.Z., and Storey, C.D., 2016, Petrology and trace element thermometry of garnet-quartzite from the Catalina Schist: Geological Society of America Abstracts with Programs, v. 48, no. 7, Abstract 258–3, doi: 10.1130/abs/2016AM-282181.

Holland, T.J.B., and Powell, R., 1998, An internally consistent thermodynamic data set for phases of petrological interest: Journal of Metamorphic Geology, v. 16, p. 309–343.

Kita, N.T., Ushikubo, T., Fu, B., and Valley, J.W., 2009, High precision SIMS oxygen isotope analysis and the effect of sample topography: Chemical Geology, v. 264, no. 1-4, p. 43–57, doi: 10.1016/j.chemgeo.2009.02.012.

Kelly, J.L., Fu, B., Kita, N.T., and Valley, J.W., 2007, Optically continuous silcrete quartz cements of the St. Peter Sandstone: High precision oxygen isotope analysis by ion microprobe: Geochimica et Cosmochimica Acta, v. 71, p. 3812–3832, doi: 10.1016/j.gca.2007.05.014.

Ludwig, K.R., 2001, Squid 1.02: a user's manual: Berkeley Geochronology Center Special Publication No. 2, Berkeley, California.

Ludwig, K.R., 2003, Users manual for ISOPLOT/EX, version 3. A geochronological toolkit for Microsoft Excel: Berkeley Geochronology Center Special Publication No. 4, Berkeley, CA.

Page, F.Z., Kita, N.T., and Valley, J.W., 2010, Ion microprobe analysis of oxygen isotopes in garnets of complex chemistry: Chemical Geology, v. 270, no. 1-4, p. 9–19, doi: 10.1016/j.chemgeo.2009.11.001.

Page, F.Z., Ushikubo, T., Kita, N.T., Riciputi, L., and Valley, J.W., 2007, High-precision oxygen isotope analysis of picogram samples reveals 2 μm gradients and slow diffusion in zircon: American Mineralogist, v. 92, no. 10, p. 1772–1775.

Penniston-Dorland, S.C., Kohn, M.J., and Piccoli, P.M., 2016, A mélange of subduction temperatures: Zr-in-rutile thermometry of the Catalina Schist: Goldschmidt Abstracts, p. 2465.

Sorensen, S.S., and Barton, M., 1987, Metasomatism and Partial Melting in a Subduction Complex - Catalina Schist, Southern-California: Geology, v. 15, no. 2, p. 115–118.

Valley, J.W., 2003, Oxygen isotopes in zircon, *in* Reviews in Mineralogy & Geochemistry Vol. 53 Zircon, p. 343–385.
Valley, J.W., and Kita, N.T., 2009, In situ oxygen isotope geochemistry by ion microprobe: Mineralogical Association of Canada Short Course 41, p. 19-61.
Valley, J.W., Kitchen, N., Kohn, M.J., Niendorf, C., and Spicuzza, M.J., 1995, UWG-2, a garnet standard for oxygen isotope ratios: strategies for high precision and accuracy with laser heating: Geochimica et Cosmochimica Acta, v. 59, no. 24, p. 5223–5231.

TABLE DR-1. δ18O ANALYSES OF GARNET COMPOSITIONAL STANDARDS BY ION MICROPROBE

Analysis Number	Spot name	δ18O VSMOW ‰	Average δ18O Raw ‰	2SD	Average bias ‰	Average bias rel. UWG-2 ‰	δ18O Raw ‰	Internal precision ‰
sample: WI-STD-24								
~~1~~	~~UWG-2 (yield, background and dead time are unchecked)~~						~~112.14~~	~~0.27~~
2	UWG-2						8.83	0.25
3	UWG-2						8.64	0.20
4	UWG-2						9.17	0.25
5	UWG-2						8.73	0.29
6	UWG-2						8.70	0.39
7	UWG-2						8.97	0.26
8	UWG-2						8.78	0.22
9	UWG-2						8.80	0.23
10	UWG-2						9.03	0.33
		5.80	8.85	0.35	3.03	**—**		
11	UWG-2						9.54	0.11
12	UWG-2						9.41	0.16
13	UWG-2						9.46	0.25
14	UWG-2						9.45	0.20
15	UWG-2						9.32	0.21
16	UWG-2						9.32	0.11
		5.80	9.41	0.17	3.59	**—**		
17	GrsSe						10.13	0.19
18	GrsSe						10.32	0.21
19	GrsSe						10.17	0.19
20	GrsSe						10.23	0.26
		3.80	10.21	0.17	6.39	**2.95**		
21	Bal509						14.81	0.22
22	Bal509						14.70	0.20
23	Bal509						~~20.01~~	0.33
24	Bal509						14.84	0.21
25	Bal509						14.92	0.24
		12.30	14.82	0.19	2.49	**-0.94**		
26	UWG-2						9.30	0.19
27	UWG-2						9.06	0.24
28	UWG-2						9.21	0.21
29	UWG-2						8.94	0.20
		5.80	9.12	0.32	3.31	**—**		
	bracket	**5.80**	9.25	0.39	3.43	**—**		
30	SpeSe						7.92	0.22
31	SpeSe						8.08	0.16
32	SpeSe						8.08	0.16
33	SpeSe						8.22	0.16
		5.40	8.07	0.24	2.66	**-0.68**		
34	PyDM						8.09	0.20
35	PyDM						8.35	0.15
36	PyDM						8.21	0.21
37	PyDM						8.26	0.21
		5.60	8.23	0.22	2.61	**-0.73**		
38	UWG-2						9.13	0.16
39	UWG-2						9.33	0.17
40	UWG-2						9.21	0.23
41	UWG-2						9.14	0.20
		5.80	9.20	0.18	3.38	**—**		
	bracket	**5.80**	9.16	0.26	3.34	**—**		
sample: WI-STD-23								
42	UWG-2						10.58	0.14
43	UWG-2						10.43	0.17
44	UWG-2						10.45	0.15
45	UWG-2						10.42	0.19
46	UWG-2						10.25	0.17
47	UWG-2						10.40	0.18
		5.80	10.38	0.18	4.55	**—**		
48	13-63-21						9.41	0.17
49	13-63-21						9.60	0.18
50	13-63-21						9.25	0.16
51	13-63-21						9.24	0.24
		4.55	9.37	0.33	4.80	**0.20**	9.37	0.33

TABLE DR-1 (CONTINUED). δ18O ANALYSES OF GARNET COMPOSITIONAL STANDARDS BY ION MICROPROBE

Analysis Number	Spot name	$\delta^{18}O$ VSMOW ‰	Average $\delta^{18}O$ Raw ‰	2SD	Average bias ‰	Average bias rel. UWG-2 ‰	$\delta^{18}O$ Raw ‰	Internal precision ‰
52	UWG-2						10.56	0.22
53	UWG-2						10.39	0.23
54	UWG-2						10.34	0.15
55	UWG-2						10.59	0.21
		5.80	10.47	0.24	4.64	—		
	bracket	**5.80**	10.43	0.22	4.60	—		
56	13-36-20						10.15	0.18
57	13-36-20						10.01	0.18
58	13-36-20						10.13	0.18
59	13-36-20						10.03	0.20
		6.14	10.08	0.14	3.91	**-0.68**		
60	UWG-2						10.40	0.23
61	UWG-2						10.53	0.23
62	UWG-2						10.19	0.17
63	UWG-2						10.44	0.23
		5.80	10.39	0.28	4.56	—		
	bracket	**5.80**	10.43	0.26	4.60	—		
sample: WI-STD-70								
64	epoxy				on epoxy		-33.66	3.52
65	UWG-2						8.98	0.20
66	UWG-2						9.00	0.22
67	UWG-2						8.92	0.24
68	UWG-2						8.85	0.24
69	UWG-2						8.78	0.25
sample: WI-STD-23								
70	UWG-2						9.40	0.20
71	UWG-2						9.19	0.18
72	UWG-2						9.24	0.22
73	UWG-2						9.20	0.23
74	UWG-2						9.19	0.21
75	UWG-2						9.28	0.19
		5.80	9.23	0.09	3.41	—		
76	13-63-21						9.17	0.22
77	13-63-21						9.16	0.22
78	13-63-21						9.08	0.16
79	13-63-21						9.07	0.18
		4.55	9.12	0.11	4.55	**1.17**		
80	UWG-2						9.16	0.23
81	UWG-2						9.25	0.19
82	UWG-2						9.01	0.22
83	UWG-2						9.23	0.19
		5.80	9.16	0.21	3.34	—		
	bracket	**5.80**	9.19	0.17	3.37	—		
84	UWG-2						8.99	0.18
85	UWG-2						8.90	0.17
86	UWG-2						8.83	0.19
87	UWG-2						9.07	0.20
Analysis Number	**Spot name**	**$\delta^{18}O$ VSMOW ‰**	**Average $\delta^{18}O$ Raw ‰**	**2SD**	**Average bias ‰**	**Average bias rel. UWG-2 ‰**	**$\delta^{18}O$ Raw ‰**	**Internal precision ‰**
		5.80	8.95	0.21	3.13	—		
88	R-53						11.25	0.23
89	R-53						11.18	0.20
90	R-53						11.22	0.22
91	R-53						11.27	0.18
		5.33	11.23	0.08	5.87	**2.65**		
92	UWG-2						9.23	0.18
93	UWG-2						9.16	0.16
94	UWG-2						9.13	0.27
95	UWG-2						8.93	0.24
		5.80	9.11	0.26	3.29	—		
	bracket	**5.80**	9.03	0.28	3.21	—		

TABLE DR-1 (CONTINUED). $\delta^{18}O$ ANALYSES OF GARNET COMPOSITIONAL STANDARDS BY ION MICROPROBE

SUMMARY BIAS DATA FOR GARNET STANDARDS		
Standard	Mole Fraction Grossular	Bias Relative to UWG-2
GrsSE	0.94	2.95
Bal509	0.03	-0.94
UWG-2	0.14	0
SpsSE	0	-0.68
PypDM	0	-0.73
13-63-21	0.31	1.17
R-53	0.6	2.65

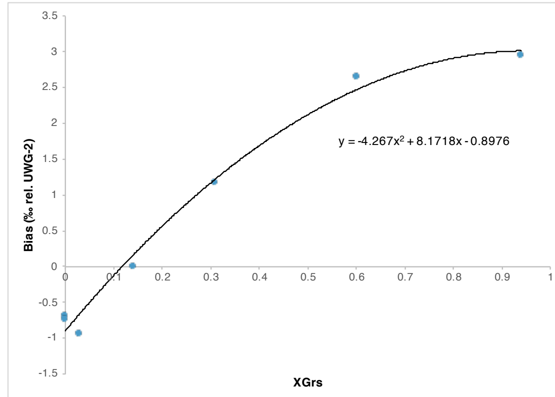

Fig. DR-2 Calibration curve for compositional correction of SIMS garnet analyses

TABLE DR-2. δ18O ANALYSES OF CATALINA QUARTZITE GARNETS AND QUARTZ BY ION MICROPROBE

Analysis Number	Spot name	$\delta^{18}O$ ‰ VSMOW	2 S.D. UWG-2 bracket	$\delta^{18}O$ ‰ Raw	2 S.E. measurement	Alm	Pyp	Sps	Grs
sample: 05C-09aOB									
Calibration curve:	Bias = aXGrs^2 + bXGrs + c a = -4.267 b = 8.1718 c = -0.8976								
93	UWG2			8.918	0.203				
94	UWG2			8.895	0.141				
95	UWG2			8.931	0.214				
96	UWG2			8.931	0.188				
	average		0.03	8.919					
97	05C09aOBg1_1_core	26.09	0.18	29.258	0.198	54.52	24.68	8.62	12.18
98	05C09aOBg1_2_rim	10.16	0.18	13.213	0.169	53.59	27.96	7.24	11.21
99	05C09aOBg1_3	15.09	0.18	18.108	0.177	53.82	27.81	7.84	10.54
100	05C09aOBg1_4	24.56	0.18	27.694	0.165	53.59	26.41	8.20	11.79
101	05C09aOBg1_5	17.98	0.18	21.060	0.274	53.98	26.79	7.91	11.32
102	05C09aOBg1_6	17.53	0.18	20.470	0.203	54.09	28.43	8.01	9.47
103	05C09aOBg1_7	14.97	0.18	18.026	0.158	54.12	27.38	7.37	11.13
104	05C09aOBg1_8	10.27	0.18	13.251	0.252	54.07	27.98	7.73	10.22
105	05C09aOBg1_9	10.35	0.18	13.330	0.187	54.13	28.04	7.52	10.31
106	05C09aOBg1_10	26.07	0.18	29.214	0.183	54.99	24.58	8.65	11.78
107	UWG2			8.854	0.205				
108	UWG2			8.853	0.161				
109	UWG2			8.659	0.247				
110	UWG2			8.937	0.236				
	average		0.24	**8.826**					
	bracket 93-96, 107-110		0.18	**8.872**					
111	05C09aOBg1_11	10.36	0.18	13.339	0.188	53.37	28.56	7.69	10.38
112	05C09aOBg1_12	10.21	0.18	13.184	0.196	53.99	28.33	7.32	10.36
113	05C09aOBg1_13	17.24	0.18	20.261	0.159	54.24	27.43	7.61	10.72
114	05C09aOBg1_14	26.15	0.18	29.323	0.130	53.64	25.94	8.01	12.42
115	05C09aOBg1_15	26.15	0.18	29.315	0.186	55.06	24.56	8.11	12.27
116	05C09aOBg1_16	26.07	0.18	29.215	0.179	54.38	25.34	8.23	12.06
117	05C09aOBg1_17	24.59	0.18	27.732	0.190	53.20	26.58	8.22	11.99
118	05C09aOBg1_18	19.71	0.18	22.754	0.186	53.75	27.29	8.10	10.86
119	05C09aOBg1_19	17.54	0.18	20.659	0.177	53.81	26.21	7.95	12.03
120	05C09aOBg1_20	14.94	0.18	17.897	0.218	54.54	28.07	7.50	9.90
121	05C09aOBg1_21	10.25	0.18	13.215	0.162	54.32	28.12	7.30	10.26
122	UWG2			8.902	0.211				
123	UWG2			8.943	0.175				
124	UWG2			8.877	0.136				
125	UWG2			8.867	0.137				
	average		0.07	**8.897**					
	bracket 107-110, 122-125		0.18	**8.862**					
126	05C09aOBg1b_b	25.58	0.11	28.602	0.194	54.99	27.19	7.48	10.35
127	05C09aOBg1b_b	10.51	0.11	13.474	0.157	53.63	28.53	7.60	10.23
128	05C09aOBg1b_b	17.83	0.11	20.850	0.168	53.86	28.24	7.33	10.56
129	05C09aOBg1b_b	10.36	0.11	13.349	0.164	53.86	28.24	7.33	10.56
130	05C09aOBg1b_b	20.03	0.11	23.089	0.198	53.45	27.92	7.59	11.05
131	05C09aOBg1b_b	10.18	0.11	13.214	0.199	53.58	27.96	7.27	11.18
132	05C09aOBg1_22	10.26	0.11	13.257	0.185	54.06	27.87	7.48	10.58
133	05C09aOBg1_23	26.18	0.11	29.343	0.163	53.26	26.04	8.52	12.18
134	05C09aOBg1_24	10.26	0.11	13.209	0.149	53.74	28.67	7.55	10.03
135	05C09aOBg1_25	10.26	0.11	13.269	0.193	53.21	28.30	7.65	10.84
136	05C09aOBg1_26	26.18	0.11	29.313	0.161	54.45	24.87	8.86	11.82
137	05C09aOBg1_27	26.19	0.11	29.318	0.232	53.68	26.01	8.59	11.71
138	05C09aOBg1_28	17.86	0.11	20.834	0.191	53.95	27.75	8.32	9.98
139	05C09aOBg1_29	26.17	0.11	29.332	0.171	55.06	24.56	8.11	12.27
140	UWG2			8.898	0.149				
141	UWG2			8.797	0.172				
142	UWG2			8.786	0.208				
143	UWG2			8.827	0.124				
	average		0.10	**8.827**					
	bracket 122-125, 140-143		0.11	**8.862**					
144	05C09aOBg2_1	26.13	0.19	29.248	0.229	54.72	24.69	8.91	11.68
145	05C09aOBg2_2	21.92	0.19	25.022	0.216	55.13	24.48	8.82	11.57
146	05C09aOBg2_3	10.02	0.19	13.008	0.251	53.59	28.54	7.38	10.49
147	05C09aOBg2_4	10.26	0.19	13.256	0.174	53.01	28.64	7.72	10.63
148	05C09aOBg2_5	24.44	0.19	27.580	0.151	54.87	25.08	8.05	12.00
149	05C09aOBg2_6	17.88	0.19	20.921	0.107	54.47	26.59	7.97	10.98
150	05C09aOBg2_7	17.16	0.19	20.272	0.123	54.66	25.58	7.78	11.97
151	05C09aOBg2_8	14.58	0.19	17.543	0.178	54.31	28.09	7.62	9.98
152	05C09aOBg2_9	25.80	0.19	28.942	0.163	54.06	25.20	8.76	11.98

TABLE DR-2 (CONTINUED). δ18O ANALYSES OF CATALINA QUARTZITE GARNETS AND QUARTZ BY ION MICROPROBE

Analysis Number	Spot name	δ18O ‰ VSMOW	2 S.D. UWG-2 bracket	δ18O ‰ Raw	2 S.E. measurement	Alm	Pyp	Sps	Grs
153	05C09aOBg2_10	10.61	0.19	13.629	0.192	53.71	27.66	7.75	10.89
154	05C09aOBg2_11	26.06	0.19	29.179	0.184	54.11	25.59	8.66	11.64
155	05C09aOBg2_12	21.82	0.19	24.814	0.193	54.35	26.98	8.50	10.17
156	05C09aOBg2_13	24.76	0.19	27.894	0.145	54.36	25.64	8.13	11.87
157	UWG2			8.908	0.160				
158	UWG2			8.799	0.133				
159	UWG2			9.058	0.165				
160	UWG2			8.777	0.203				
	average		0.26	**8.886**					
	bracket 140-143, 157-160		0.19	**8.860**					
sample: 05C-09aUW									
216	05C9aUW UWG2			8.825	0.168				
217	05C9aUW UWG2			8.706	0.157				
218	05C9aUW UWG2			8.535	0.221				
219	05C9aUW UWG2			8.581	0.187				
	average		0.26	**8.662**					
220	05C9aUW UWG2		0.30	8.779	0.233				
221	05C9aUWg2_1	10.04	0.30	12.882	0.216	53.37	28.19	7.83	10.61
222	05C9aUWg2_2	10.32	0.30	13.164	0.178	53.28	28.11	8.06	10.55
223	05C9aUWg1_1	11.02	0.30	13.854	0.122	54.85	26.85	7.91	10.39
224	05C9aUWg1_2	10.37	0.30	13.236	0.135	53.56	27.56	7.98	10.89
225	05C9aUWg1_3	23.62	0.30	26.478	0.160	55.90	15.94	17.88	10.28
226	05C9aUWg1_4	24.71	0.30	27.504	0.211	57.69	21.11	11.80	9.41
227	05C9aUWg1_5	24.63	0.30	27.384	0.138	57.12	23.26	10.77	8.85
228	05C9aUWg1_6	17.76	0.30	20.668	0.154	54.31	25.22	9.26	11.21
229	05C9aUWg1_7	18.03	0.30	20.919	0.177	53.89	26.25	9.02	10.85
230	05C9aUWg1_8	18.23	0.30	21.084	0.228	53.60	27.26	8.69	10.45
231	05C9aUWg1_9	15.60	0.30	18.447	0.172	54.08	27.09	8.39	10.44
232	05C9aUWg1_10	10.17	0.30	13.017	0.207	54.41	27.20	7.73	10.67
233	05C9aUW-UWG2			8.521	0.184				
234	05C9aUW-UWG2			8.859	0.191				
235	05C9aUW-UWG2			8.774	0.216				
236	05C9aUW-UWG2			8.901	0.233				
	average		0.34	**8.764**					
	bracket 216-219, 233-236		0.30	**8.713**					
237	05C9aUWg1_11	24.64	0.28	27.591	0.242	56.47	19.22	13.54	10.78
238	05C9aUWg1_12	24.54	0.28	27.493	0.144	56.16	16.46	16.67	10.72
239	05C9aUWg1_13	24.74	0.28	27.613	0.145	57.20	22.14	10.99	9.68
240	05C9aUWg1_14	24.60	0.28	27.414	0.168	57.88	22.39	10.85	8.87
241	05C9aUWg1_15	24.67	0.28	27.457	0.150	58.47	21.99	11.01	8.53
242	05C9aUWg1_16	25.43	0.28	28.270	0.146	56.65	23.94	10.22	9.19
243	05C9aUWg1_17	17.75	0.28	20.717	0.160	54.40	25.50	8.92	11.19
244	05C9aUWg1_18	18.00	0.28	20.984	0.199	53.86	25.55	9.21	11.37
245	05C9aUWg1_19	17.86	0.28	20.793	0.173	54.86	25.65	8.79	10.69
246	05C9aUWg1_20	25.73	0.28	28.531	0.195	56.28	25.36	9.65	8.72
247	05C9aUWg1_21	24.85	0.28	27.772	0.205	54.97	25.07	9.69	10.28
248	05C9aUWg1_22	24.72	0.28	27.590	0.211	56.70	21.45	12.14	9.70
249	05C9aUWg1_23	24.49	0.28	27.307	0.118	58.19	20.72	12.16	8.93
250	05C9aUWg1_24	24.78	0.28	27.504	0.160	58.53	21.61	12.09	7.77
251	05C9aUW-UWG2			8.611	0.182				
252	05C9aUW-UWG2			8.906	0.180				
253	05C9aUW-UWG2			8.857	0.164				
254	05C9aUW-UWG2			8.710	0.170				
	average		0.27	**8.771**					
	bracket 233-236, 251-254		0.28	**8.767**					
255	05C9aUWg1_25	20.09	0.23	22.950	0.156	56.92	20.50	12.96	9.61
256	05C9aUWg1_26	24.73	0.23	27.623	0.197	59.82	18.10	12.25	9.83
257	05C9aUWg1_27	24.82	0.23	27.596	0.171	59.12	19.59	12.94	8.35
258	05C9aUWg1_28	24.39	0.23	27.233	0.129	59.51	19.12	12.16	9.22
259	05C9aUWg1_29	24.53	0.23	27.354	0.151	57.35	21.64	11.98	9.03
260	05C9aUWg1_30	24.74	0.23	27.565	0.162	59.10	19.58	12.32	9.00
261	05C9aUWg1_31	24.68	0.23	27.369	0.135	60.68	19.77	12.29	7.27
262	05C9aUWg1_32	24.37	0.23	27.232	0.168	59.06	19.03	12.45	9.46
263	05C9aUWg1_33	24.57	0.23	27.541	0.182	56.76	19.88	12.41	10.95
264	05C9aUWg1_34	24.54	0.23	27.407	0.225	59.40	15.86	15.20	9.54
265	05C9aUWg1_35	24.73	0.23	27.546	0.202	60.40	18.25	12.49	8.86
266	05C9aUWg1_36	23.71	0.23	26.536	0.201	59.84	19.11	12.05	9.00
267	05C9aUWg1_37	24.37	0.23	27.181	0.172	59.53	19.92	11.73	8.83
268	05C9aUWg1_38	21.31	0.23	24.124	0.182	57.54	21.34	12.19	8.94
269	05C9aUWg1_39	10.03	0.23	12.939	0.146	53.79	27.82	7.69	10.70

TABLE DR-2. $\delta^{18}O$ ANALYSES OF CATALINA QUARTZITE GARNETS AND QUARTZ BY ION MICROPROBE

Analysis Number	Spot name	$\delta^{18}O$ ‰ VSMOW	2 S.D. UWG-2 bracket	$\delta^{18}O$ ‰ Raw	2 S.E. measurement	Alm	Pyp	Sps	Grs
270	05C9aUW_UWG2			8.614	0.206				
271	05C9aUW_UWG2			8.838	0.154				
272	05C9aUW_UWG2			8.798	0.196				
273	05C9aUW_UWG2			8.843	0.173				
	average		0.22	**8.773**					
	bracket 251-254, 270-273		0.23	**8.772**					
274	05C9aUWg2_3	25.06	0.15	28.083	0.136	53.83	25.91	8.72	11.53
275	05C9aUWg2_4	25.35	0.15	28.422	0.257	53.34	26.10	8.43	12.13
276	05C9aUWg2_5	25.33	0.15	28.371	0.192	52.31	26.98	8.94	11.76
277	05C9aUWg2_6	17.75	0.15	20.779	0.209	53.12	26.68	8.25	11.95
278	05C9aUWg2_7	17.96	0.15	20.862	0.198	53.79	28.40	7.71	10.09
279	05C9aUWg2_8	10.14	0.15	13.063	0.152	53.05	28.31	7.96	10.68
280	05C9aUWg2_9	10.15	0.15	13.023	0.197	53.80	28.37	7.80	10.03
281	05C9aUWg2_10	12.80	0.15	15.736	0.261	52.92	28.07	8.20	10.81
282	05C9aUWg2_11	26.29	0.15	29.399	0.158	52.37	26.55	8.51	12.57
283	05C9aUWg2_12	25.86	0.15	28.941	0.185	52.84	26.04	8.78	12.33
284	05C9aUWg2_13	20.82	0.15	23.679	0.187	53.89	28.34	8.34	9.43
285	05C9aUWg2_14	18.01	0.15	20.838	0.145	54.57	28.70	7.61	9.12
286	05C9aUWg2_15	10.24	0.15	13.121	0.111	53.34	28.54	7.90	10.22
287	05C9aUWg1_40	18.62	0.15	21.528	0.168	53.70	25.98	10.16	10.16
288	05C9aUWg1_41	17.71	0.15	20.632	0.192	53.76	26.78	9.03	10.43
289	05C9aUWg1_42	10.12	0.15	13.056	0.173	52.88	28.00	8.21	10.91
290	05C9aUWg1_43	20.53	0.15	23.275	0.204	56.29	22.74	13.04	7.93
291	05C9aUW_UWG2			8.745	0.179				
292	05C9aUW_UWG2			8.837	0.223				
293	05C9aUW_UWG2			8.814	0.177				
294	05C9aUW_UWG2			8.750	0.196				
	average		0.09	**8.787**					
	bracket 270-273, 291-294		0.15	**8.780**					
295	05C9aUW_UWQ1			6.722	0.191				
296	05C9aUW_UWQ1			6.750	0.165				
297	05C9aUW_UWQ1			6.745	0.222				
298	05C9aUW_UWQ1			6.658	0.219				
	average		0.08	**6.719**					
299	05C9aUWg2-q1	15.35	0.17	9.768	0.145				
300	05C9aUWg2-q2	15.25	0.17	9.676	0.158				
301	05C9aUWg2-q3	15.22	0.17	9.642	0.121				
302	05C9aUWg2-q4	13.75	0.17	8.178	0.144				
303	05C9aUWg1-q1	13.81	0.17	8.242	0.190				
304	05C9aUWg1-q2	15.54	0.17	9.958	0.161				
305	05C9aUWg1-q3	16.22	0.17	10.639	0.120				
306	05C9aUWg1-q4	15.68	0.17	10.100	0.223				
307	05C9aUWg1-q5	14.43	0.17	8.856	0.221				
308	05C9aUWg1-q6	14.15	0.17	8.582	0.151				
309	05C9aUWg1-q7	14.37	0.17	8.801	0.219				
310	05C9aUW-mtx q S	13.52	0.17	7.951	0.239				
311	05C9aUW-UWQ-1			6.845	0.154				
312	05C9aUW-UWQ-1			6.843	0.158				
313	05C9aUW-UWQ-1			6.902	0.138				
314	05C9aUW-UWQ-1			6.678	0.139				
	average		0.19	**6.817**					
	bracket 295-298, 311-314		0.17	**6.768**					

Fig. DR–3 Time series garnet analyses by SIMS

corrected to VSMOW, error bars are 2 S.D. from bracketing standards

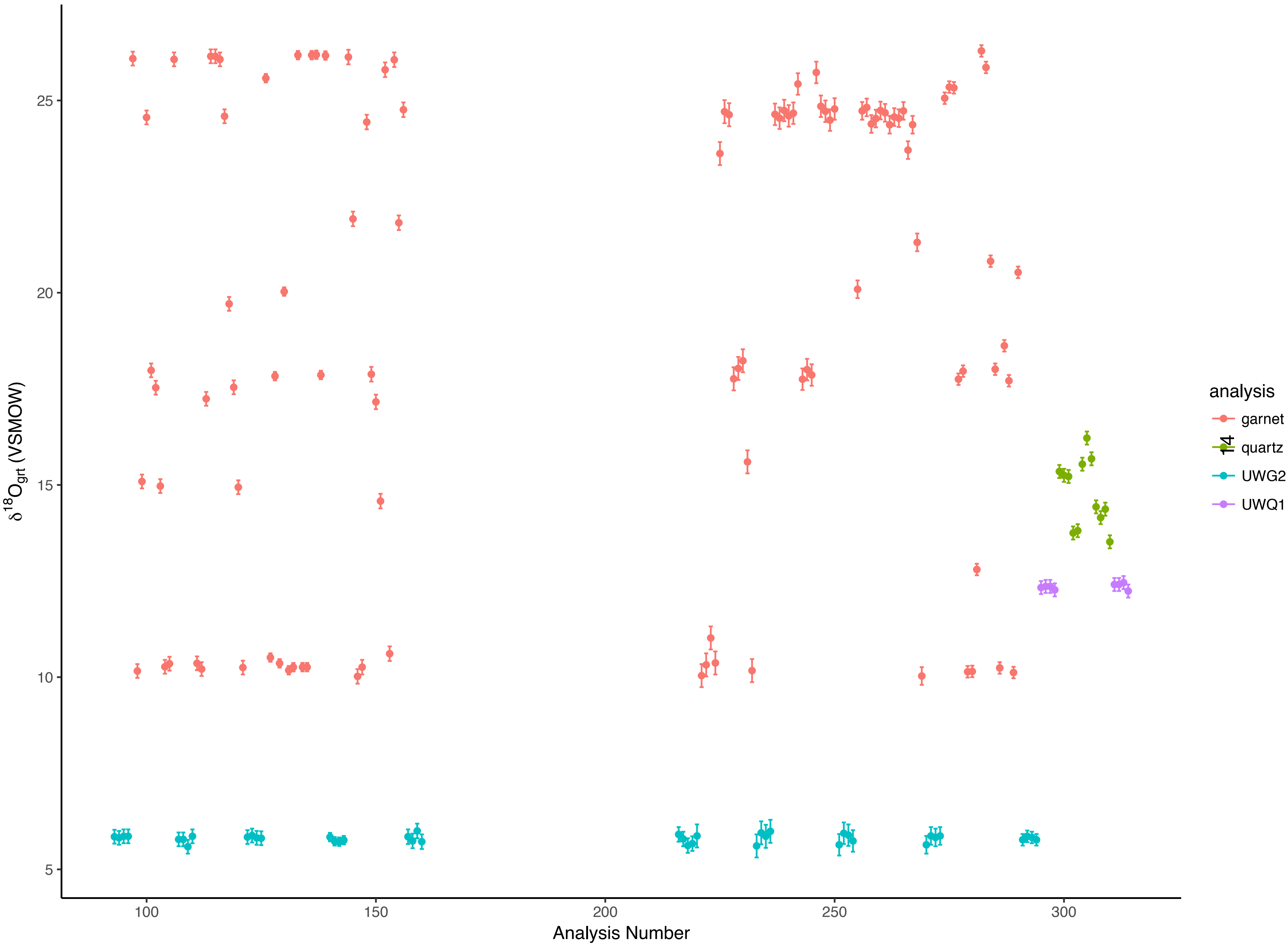

TABLE DR-3 EMPA ANALYSES OF CATALINA GARNET FOR COMPOSITIONAL BIAS CORRECTION

traverse distance (microns)	SIMS spot	eProbe #	SiO2	TiO2	Al2O3	Cr2O3	FeO	MnO	MgO	CaO	Total	Si	Al VI	Ti	Fe3+	Fe 2+	Cr	Mn	Mg	Ca	% Alm	% Pyp	% Sps	% Grs	% And	% Uvar	% CaTi grt
Sample: 05C-09aUW																											
g2																											
13	221	1	37.62	0.02	21.56	0.00	25.18	3.65	7.46	3.91	99.40	2.94	1.98	0.00	0.14	1.50	0.00	0.24	0.87	0.33	51.12	29.55	8.21	10.37	0.74	0.00	0.01
841	222	2	38.08	0.00	21.85	0.00	25.25	3.77	7.47	3.90	100.32	2.94	1.99	0.00	0.12	1.51	0.00	0.25	0.86	0.32	51.39	29.24	8.39	10.36	0.62	0.00	0.00
452	274	3	37.48	0.10	21.17	0.00	25.20	4.03	6.80	4.21	99.01	2.95	1.96	0.01	0.13	1.53	0.00	0.27	0.80	0.36	51.88	27.01	9.09	11.27	0.72	0.00	0.03
383	275	4	37.92	0.04	20.92	0.00	25.21	3.93	6.92	4.48	99.42	2.97	1.93	0.00	0.12	1.53	0.00	0.26	0.81	0.38	51.41	27.18	8.78	11.86	0.76	0.00	0.01
275	276	5	37.66	0.04	21.06	0.00	24.40	4.12	7.06	4.28	98.62	2.97	1.96	0.00	0.10	1.50	0.00	0.27	0.83	0.36	50.65	27.92	9.25	11.55	0.61	0.00	0.01
135	277	6	37.82	0.10	21.21	0.00	25.21	3.87	7.10	4.43	99.74	2.95	1.95	0.01	0.14	1.50	0.00	0.26	0.83	0.37	50.90	27.95	8.64	11.64	0.83	0.00	0.04
71	278	7	37.99	0.03	21.43	0.00	25.73	3.64	7.62	3.77	100.22	2.94	1.96	0.00	0.15	1.51	0.00	0.24	0.88	0.31	51.40	29.88	8.11	9.84	0.77	0.00	0.01
13	279	8	38.31	-0.03	21.83	0.00	25.17	3.73	7.53	3.95	100.50	2.96	1.99	0.00	0.11	1.52	0.00	0.24	0.87	0.33	51.34	29.34	8.25	10.51	0.57	0.00	-0.01
35	280	9	38.08	0.04	21.78	0.00	25.62	3.67	7.58	3.73	100.49	2.94	1.98	0.00	0.13	1.52	0.00	0.24	0.87	0.31	51.73	29.64	8.15	9.82	0.65	0.00	0.01
54	281	10	38.21	0.04	21.71	0.00	25.06	3.83	7.45	4.00	100.30	2.96	1.98	0.00	0.10	1.52	0.00	0.25	0.86	0.33	51.25	29.06	8.49	10.62	0.56	0.00	0.01
179	282	11	38.17	0.11	21.50	0.00	24.59	3.95	6.99	4.60	99.91	2.97	1.97	0.01	0.08	1.52	0.00	0.26	0.81	0.38	51.11	27.25	8.74	12.36	0.50	0.00	0.04
652	283	12	38.09	0.08	21.53	0.00	25.05	4.11	6.92	4.56	100.34	2.95	1.97	0.00	0.12	1.51	0.00	0.27	0.80	0.38	51.01	27.05	9.13	12.08	0.71	0.00	0.03
759	284	13	38.13	0.05	21.41	0.00	25.50	3.90	7.52	3.48	99.99	2.96	1.96	0.00	0.11	1.55	0.00	0.26	0.87	0.29	52.20	29.38	8.65	9.25	0.51	0.00	0.01
800	285	14	38.20	0.05	21.41	0.00	25.95	3.57	7.65	3.39	100.22	2.96	1.96	0.00	0.12	1.56	0.00	0.23	0.88	0.28	52.76	29.84	7.91	8.93	0.54	0.00	0.01
820	286	15	38.36	0.05	21.81	0.00	25.03	3.66	7.51	3.74	100.17	2.97	1.99	0.00	0.06	1.56	0.00	0.24	0.87	0.31	52.33	29.16	8.07	10.10	0.33	0.00	0.02
g1																											
17	223	16	38.19	0.06	21.58	0.00	25.41	3.62	6.98	3.76	99.60	2.98	1.99	0.00	0.04	1.62	0.00	0.24	0.81	0.31	54.26	27.21	8.01	10.30	0.20	0.00	0.02
2662	224	17	38.19	0.06	21.36	0.00	25.28	3.72	7.30	4.01	99.91	2.97	1.96	0.00	0.10	1.55	0.00	0.24	0.85	0.33	52.06	28.46	8.24	10.70	0.53	0.00	0.02
1429	225	18	36.82	0.12	20.17	0.00	26.00	8.21	4.16	3.73	99.21	2.96	1.91	0.01	0.16	1.59	0.00	0.56	0.50	0.32	53.53	16.79	18.84	9.97	0.83	0.00	0.04
1957	226	19	37.25	0.15	20.68	0.00	26.88	5.43	5.52	3.42	99.33	2.96	1.94	0.01	0.13	1.66	0.00	0.37	0.65	0.29	55.89	22.01	12.30	9.17	0.60	0.00	0.04
2324	227	20	37.57	0.02	21.03	0.00	26.81	4.99	6.12	3.24	99.78	2.96	1.95	0.00	0.13	1.63	0.00	0.33	0.72	0.27	55.22	24.29	11.25	8.66	0.58	0.00	0.00
2503	228	21	37.81	0.10	20.96	0.00	25.87	4.35	6.74	4.17	100.00	2.95	1.93	0.01	0.15	1.54	0.00	0.29	0.78	0.35	51.96	26.52	9.73	10.89	0.86	0.00	0.03
2586	229	22	37.60	0.12	21.20	0.00	25.75	4.25	7.03	4.04	100.00	2.93	1.95	0.01	0.18	1.50	0.00	0.28	0.82	0.34	51.11	27.83	9.56	10.51	0.95	0.00	0.04
2625	230	23	37.91	0.05	21.17	0.00	25.38	4.06	7.24	3.86	99.68	2.96	1.95	0.00	0.13	1.53	0.00	0.27	0.84	0.32	51.58	28.45	9.07	10.22	0.68	0.00	0.02
2641	231	24	38.41	0.01	21.53	0.00	25.75	3.94	7.24	3.88	100.76	2.97	1.96	0.00	0.11	1.55	0.00	0.26	0.83	0.32	52.41	28.08	8.69	10.25	0.56	0.00	0.00
2675	232	25	38.20	0.03	21.69	0.00	25.33	3.55	7.10	3.87	99.77	2.98	1.99	0.00	0.05	1.59	0.00	0.23	0.82	0.32	53.57	27.70	7.87	10.56	0.29	0.00	0.01
1684	237	26	37.23	0.10	20.50	0.00	26.48	6.27	5.05	3.94	99.58	2.96	1.92	0.01	0.15	1.61	0.00	0.42	0.60	0.34	54.25	20.20	14.22	10.47	0.82	0.00	0.03
1527	238	27	37.48	0.04	20.59	0.00	25.85	7.58	4.25	3.85	99.64	2.99	1.94	0.00	0.08	1.65	0.00	0.51	0.51	0.33	55.00	16.89	17.11	10.56	0.43	0.00	0.01
	239	28	37.81	0.06	21.05	0.00	26.82	5.09	5.82	3.54	100.19	2.97	1.95	0.00	0.11	1.65	0.00	0.34	0.68	0.30	55.66	22.94	11.38	9.49	0.52	0.00	0.02
	240	29	37.67	0.02	21.00	0.00	27.11	5.02	5.88	3.24	99.95	2.97	1.95	0.00	0.12	1.67	0.00	0.33	0.69	0.27	56.23	23.27	11.28	8.69	0.52	0.00	0.00
2194	241	30	37.52	0.10	21.03	0.00	27.40	5.09	5.78	3.12	100.05	2.96	1.95	0.01	0.13	1.68	0.00	0.34	0.68	0.26	56.71	22.93	11.48	8.33	0.54	0.00	0.02
2412	242	31	37.61	-0.02	21.04	0.00	26.53	4.72	6.29	3.36	99.53	2.96	1.95	0.00	0.12	1.62	0.00	0.32	0.74	0.28	54.85	24.94	10.64	9.01	0.57	0.00	-0.01
2544	243	32	38.25	0.05	21.26	0.00	25.59	4.14	6.73	4.11	100.12	2.98	1.95	0.00	0.08	1.59	0.00	0.27	0.78	0.34	53.17	26.19	9.16	11.02	0.46	0.00	0.02
2603	244	33	37.72	0.12	21.19	0.00	25.37	4.28	6.75	4.18	99.61	2.95	1.96	0.01	0.12	1.54	0.00	0.28	0.79	0.35	51.95	26.61	9.59	11.11	0.70	0.00	0.04
2563	245	34	38.09	0.16	21.14	0.00	25.93	4.10	6.80	3.94	100.17	2.97	1.94	0.01	0.10	1.59	0.00	0.27	0.79	0.33	53.31	26.53	9.10	10.46	0.55	0.00	0.05
2461	246	35	37.69	0.11	21.18	0.00	26.76	4.53	6.76	3.24	100.26	2.94	1.95	0.01	0.16	1.59	0.00	0.30	0.79	0.27	53.97	26.70	10.16	8.48	0.68	0.00	0.03
2485	247	36	37.67	0.08	21.02	0.00	25.61	4.45	6.55	3.74	99.11	2.97	1.95	0.00	0.10	1.59	0.00	0.30	0.77	0.32	53.50	25.89	10.00	10.09	0.50	0.00	0.02
	248	37	37.80	0.06	21.32	0.00	26.55	5.61	5.63	3.55	100.52	2.96	1.97	0.00	0.10	1.64	0.00	0.37	0.66	0.30	55.21	22.19	12.56	9.53	0.50	0.00	0.02
	249	38	37.90	0.08	20.67	0.00	27.03	5.58	5.40	3.24	99.89	3.00	1.93	0.00	0.07	1.72	0.00	0.37	0.64	0.27	57.22	21.21	12.44	8.79	0.32	0.00	0.02
	250	39	37.63	0.02	21.10	0.00	27.34	5.57	5.66	2.83	100.17	2.96	1.96	0.00	0.11	1.69	0.00	0.37	0.66	0.24	56.97	22.42	12.54	7.63	0.43	0.00	0.01
1802	255	40	37.30	0.05	21.14	0.00	26.63	5.99	5.38	3.51	100.01	2.94	1.97	0.00	0.14	1.62	0.00	0.40	0.63	0.30	54.86	21.48	13.58	9.39	0.67	0.00	0.02
	256	41	37.41	0.11	20.63	0.00	27.99	5.66	4.75	3.59	100.14	2.97	1.93	0.01	0.13	1.73	0.00	0.38	0.56	0.30	58.08	18.89	12.78	9.58	0.64	0.00	0.03
	257	42	37.48	0.18	20.85	0.00	27.99	6.05	5.20	3.08	100.83	2.95	1.93	0.01	0.16	1.68	0.00	0.40	0.61	0.26	56.98	20.62	13.61	8.09	0.65	0.00	0.04
	258	43	37.18	-0.01	20.90	0.00	27.44	5.54	4.94	3.32	99.30	2.96	1.96	0.00	0.11	1.72	0.00	0.37	0.59	0.28	57.99	19.83	12.62	9.05	0.51	0.00	0.00
	259	44	38.02	0.01	21.21	0.00	26.89	5.54	5.69	3.31	100.67	2.98	1.96	0.00	0.09	1.67	0.00	0.37	0.66	0.28	56.04	22.30	12.35	8.89	0.42	0.00	0.00
	260	45	37.49	0.06	21.33	0.00	27.35	5.63	5.08	3.25	100.19	2.96	1.98	0.00	0.09	1.71	0.00	0.38	0.60	0.27	57.83	20.19	12.70	8.85	0.41	0.00	0.02
	261	46	37.66	0.05	21.09	0.00	28.16	5.63	5.15	2.63	100.38	2.97	1.96	0.00	0.09	1.77	0.00	0.38	0.61	0.22	59.52	20.35	12.65	7.15	0.32	0.00	0.01
	262	47	37.10	0.04	20.71	0.00	27.75	5.78	5.01	3.47	99.86	2.94	1.94	0.00	0.17	1.67	0.00	0.39	0.59	0.29	56.69	20.13	13.17	9.19	0.81	0.00	0.01
1772	263	48	37.77	0.14	20.75	0.00	26.65	5.75	5.23	4.01	100.30	2.97	1.93	0.01	0.11	1.65	0.00	0.38	0.61	0.34	55.19	20.60	12.86	10.71	0.60	0.00	0.04
1079	264	49	36.61	0.07	20.37	0.00	27.21	6.88	4.08	3.41	98.61	2.96	1.94	0.00	0.13	1.71	0.00	0.47	0.49	0.30	57.57	16.58	15.88	9.31	0.64	0.00	0.02
784	265	50	37.38	0.04	20.91	0.00	28.01	5.72	4.75	3.21	100.02	2.97	1.96	0.00	0.11	1.75	0.00	0.38	0.56	0.27	58.94	18.92	12.95	8.69	0.48	0.00	0.01
644	266	51	37.03	0.06	20.43	0.00	27.68	5.50	4.96	3.25	98.90	2.97	1.93	0.00	0.13	1.73	0.00	0.37	0.59	0.28	58.10	19.94	12.57	8.79	0.59	0.00	0.02
499	267	52	37.26	0.02	21.02	0.00	27.87	5.42	5.23	3.23	100.05	2.95	1.96	0.00	0.15	1.69	0.00	0.36	0.62	0.27	57.50	20.91	12.31	8.61	0.65	0.00	0.01
327	268	53	37.05	0.08	21.05	0.00	26.82	5.61	5.58	3.25	99.45	2.94	1.97	0.00	0.15	1.63	0.00	0.38	0.66	0.28	55.41	22.41	12.80	8.71	0.65	0.00	0.02
13	269	54	37.82	0.00	21.46	0.00	24.91	3.52	7.23	3.87	98.80	2.97	1.99	0.00	0.07	1.57	0.00	0.23	0.85	0.33	52.69	28.48	7.88	10.58	0.38	0.00	0.00
151	287	55	38.45	0.07	21.33	0.00	25.43	4.75	6.90	3.75	100.69	2.98	1.95	0.00	0.08	1.56	0.00	0.31	0.80	0.31	52.38	26.72	10.45	9.99	0.44	0.00	0.02
93	288	56	38.08	0.02	21.28	0.00	25.32	4.20	7.08	3.83	99.82	2.97	1.96	0.00	0.10	1.55	0.00	0.28	0.82	0.32	52.20	27.68	9.34	10.25	0.53	0.00	0.01
54	289	57	38.48	0.03	21.80	0.00	25.08	3.84	7.45	4.04	100.72	2.96	1.98	0.00	0.09	1.53	0.00	0.25	0.86	0.33	51.48	28.83	8.45	10.75	0.48	0.00	0.01
255	290	58	37.89	0.09	21.07	0.00	26.34	6.02	5.97	2.90	100.27	2.97	1.95	0.01	0.09	1.64	0.00	0.40	0.70	0.24	54.93	23.45	13.44	7.78	0.37	0.00	0.02
Sample: 05C-09aOB																											
g1Baby																											
	127	59	37.42	0.04	21.61	0.00	25.47	3.57	7.60	3.79	99.50	2.92	1.99	0.00	0.18	1.48	0.00	0.24	0.88	0.32	50.82	30.26	8.07	9.95	0.89	0.00	0.01
	130	60	37.68	0.13	20.97	0.00	25.41	3.56	7.44	4.10	99.28	2.95	1.93	0.01	0.16	1.51	0.00	0.24	0.87	0.34	51.01	29.38	7.99	10.72	0.86	0.00	0.04
	126	61	37.44	0.01	21.23	0.00	26.25	3.52	7.28	3.86	99.58	2.93	1.95	0.00	0.19	1.52	0.00	0.23	0.85	0.32	52.02	28.98	7.97	10.04	0.99	0.00	0.00
	128 & 129	62	37.61	0.04	21.41	0.00	25.08	3.37	7.38	3.84	98.72	2.96	1.98	0.00	0.10	1.55	0.00	0.22	0.86	0.32	52.28	29.22	7.58	10.38	0.53	0.00	0.01
	131	63	37.99	0.06	21.44	0.00	25.16	3.37	7.36	4.10	99.47	2.96	1.97	0.00	0.10	1.55	0.00	0.22	0.86	0.34	52.08	28.87	7.50	10.99	0.54	0.00	0.02
g1																											
1099	97 & 98	64	37.35	0.10	20.99	0.00	25.63	4.00	6.51	4.47	99.04	2.94	1.95	0.01	0.15	1.54	0.00	0.27	0.76	0.38	52.23	25.92	9.06	11.86	0.90	0.00	0.03
1017	99	65	37.13	0.02	21.51	0.00	25.31	3.38	7.41	4.13	98.90	2.91	1.99	0.00	0.18	1.48	0.00	0.22	0.87	0.35	50.67	29.72	7.70	10.90	1.01	0.00	0.01
889	100	66	37.37	0.04	21.08	0.00	25.34	3.64	7.34	3.87	98.69	2.94	1.96	0.00	0.16	1.51	0.00	0.24	0.86	0.33	51.38	29.28	8.25	10.26	0.82	0.00	0.01
973	101	67	36.95	0.07	21.23	0.00	25.31	3.82	7.00	4.35	98.73	2.91	1.97	0.00	0.20	1.47	0.00	0.26	0.82	0.37	50.46	28.19	8.75	11.43	1.14	0.00	0.03
994	102	68	36.96	0.06	20.93	0.00	25.53	3.69	7.11	4.18	98.45	2.92	1.95	0.00	0.20	1.49	0.00	0.25	0.84	0.35	50.82	28.63	8.45	10.95	1.13	0.00	0.02
1007	103	69	37.21	0.04	21.31	0.00	25.76	3.77	7.60	3.52	99.21	2.91	1.97	0.00	0.20	1.48	0.00	0.25	0.89	0.30	50.90	30.40	8.57	9.17	0.94	0.00	0.01
1063	104	70	37.26	-0.01	21.24	0.00	25.30	3.40	7.18	4.06	98.43	2.94	1.98	0.00	0.14	1.53	0.00	0.23	0.84	0.34	51.87	28.72	7.73	10.88	0.79	0.00	0.00
1037	105	71	37.02	-0.03	21.42	0.00	25.61	3.61	7.43	3.78	98.86	2.91	1.98	0.00	0.20	1.48	0.00	0.24	0.87	0.32	50.84	29.95	8.27	9.92	1.03	0.00	-0.01
766	106	72	37.26	0.00	21.47	0.00	25.81	3.54	7.50	3.84	99.41	2.91	1.98	0.00	0.20	1.48	0.00	0.23	0.87	0.32	50.93	29.99	8.04	10.01	1.03	0.00	0.00
1080	111	73	37.24	0.08	21.00	0.00	25.88	4.02	6.49	4.33	99.04	2.94	1.95	0.00	0.16	1.54	0.00	0.27	0.76	0.37	52.49	25.94	9.13	11.45	0.96	0.00	0.03
20	112	74	37.22	0.02	21.37	0.00	25.01	3.56	7.51	3.80	98.48	2.93	1.98	0.00	0.15	1.49	0.00	0.24	0.88	0.32	50.91	30.07	8.09	10.13	0.79	0.00	0.00
150	113	75	37.12	0.03	21.46	0.00	25.34	3.39	7.46	3.80	98.60	2.92	1.99	0.00	0.17	1.50	0.00	0.23	0.88	0.32	51.36	29.95	7.73	10.10	0.85	0.00	0.01
376	114	76	36.86	0.03	21.00	0.00	25.89	3.59	7.34	3.99	98.70	2.90	1.95	0.00	0.24	1.47	0.00	0.24	0.86	0.34	50.47	29.69	8.24	10.32	1.27	0.00	0.01
542	115	77	36.89	0.12	20.93	0.00	25.42	3.75	6.89	4.59	98.58	2.91	1.95	0.01	0.21	1.47	0.00	0.25	0.81	0.39	50.31	27.80	8.58	11.98	1.29	0.00	0.04
327	116	78	36.94	0.12	21.15	0.00	26.13	3.80	6.54	4.54	99.22	2.91	1.96	0.01	0.21	1.51	0.00	0.25	0.77	0.38	51.85	26.31	8.69	11.85	1.26	0.00	0.04
220	117	79	36.97	0.16	20.92	0.00	25.43	3.80	6.65	4.40	98.32	2.93	1.96	0.01	0.16	1.53	0.00	0.26	0.79	0.37	51.90	26.71	8.67	11.70	0.96	0.00	0.06
192	118	80	37.36	0.08	21.08	0.00	25.09	3.83	7.03	4.42	98.89	2.94	1.95	0.00	0.16	1.49	0.00	0.26	0.82	0.37	50.69	28.00	8.67	11.67	0.94	0.00	0.03
175	119	81	36.88	0.08	20.95	0.00	25.47	3.79	7.25	4.02	98.43	2.91	1.95	0.00	0.21	1.47	0.00	0.25	0.85	0.34	50.39	29.28	8.69	10.48	1.14	0.00	0.03
86	120	82	37.25	0.09	20.74	0.00	25.51	3.72	6.97	4.45	98.74	2.94	1.93	0.01	0.18	1.50	0.00	0.25	0.82	0.38	50.93	27.84	8.44	11.64	1.11	0.00	0.03
51	121	83	37.36	0.06	21.30	0.00	25.87	3.51	7.47	3.66	99.23	2.93	1.97	0.00	0.18	1.52	0.00	0.23	0.87	0.31	51.79	29.77	7.95	9.61	0.87	0.00	0.02
16	132	84	37.35	-0.01	21.41	0.00	25.76	3.42	7.48	3.80	99.20	2.92	1.97	0.00	0.18	1.50	0.00	0.23	0.87	0.32	51.49	29.86	7.75	9.99	0.91	0.00	0.00
187	133	85	37.00	0.05	21.13	0.00	25.31	3.46	7.32	3.87	98.13	2.93	1.97	0.00	0.17	1.51	0.00	0.23	0.86	0.33	51.45	29.46	7.91	10.29	0.87	0.00	0.01

TABLE DR-3 (CONTINUED). EMPA ANALYSES OF CATALINA GARNET FOR COMPOSITIONAL BIAS CORRECTION

traverse distance (microns)	SIMS spot	eProbe #	SiO2	TiO2	Al2O3	Cr2O3	FeO	MnO	MgO	CaO	Total	Si	Al VI	Ti	Fe3+	Fe 2+	Cr	Mn	Mg	Ca	% Alm	% Pyp	% Sps	% Grs	% And	% Uvar	% CaTi grt
809	134	86	37.21	0.10	20.94	0.00	25.16	3.98	6.90	4.49	98.78	2.93	1.95	0.01	0.18	1.48	0.00	0.27	0.81	0.38	50.47	27.59	9.03	11.81	1.07	0.00	0.04
	135	87	37.77	0.02	21.05	0.00	25.00	3.47	7.48	3.64	98.43	2.98	1.96	0.00	0.09	1.56	0.00	0.23	0.88	0.31	52.38	29.52	7.77	9.88	0.44	0.00	0.01
302	136	88	37.70	0.01	21.33	0.00	25.16	3.57	7.51	4.00	99.28	2.95	1.96	0.00	0.14	1.50	0.00	0.24	0.87	0.33	50.94	29.67	8.02	10.59	0.77	0.00	0.00
157	137	89	37.12	0.07	20.98	0.00	25.83	4.15	6.62	4.38	99.14	2.92	1.95	0.00	0.20	1.51	0.00	0.28	0.78	0.37	51.40	26.53	9.46	11.44	1.15	0.00	0.03
102	138	90	37.41	0.12	20.87	0.00	25.33	4.00	6.88	4.31	98.94	2.95	1.94	0.01	0.15	1.51	0.00	0.27	0.81	0.36	51.27	27.37	9.04	11.38	0.90	0.00	0.04
672	139	91	37.11	0.09	21.21	0.00	25.83	3.93	7.45	3.73	99.35	2.91	1.96	0.01	0.22	1.47	0.00	0.26	0.87	0.31	50.42	29.88	8.96	9.62	1.10	0.00	0.03
g2																											
	144	92	37.36	0.07	21.10	0.00	26.01	4.18	6.58	4.33	99.65	2.93	1.95	0.00	0.18	1.52	0.00	0.28	0.77	0.36	51.90	26.23	9.47	11.32	1.06	0.00	0.03
	145	93	38.00	0.06	21.24	0.00	26.18	4.14	6.52	4.29	100.43	2.96	1.95	0.00	0.13	1.57	0.00	0.27	0.76	0.36	53.15	25.56	9.21	11.30	0.75	0.00	0.02
	146	94	37.95	0.03	21.37	0.00	24.94	3.39	7.45	3.81	98.94	2.97	1.97	0.00	0.07	1.56	0.00	0.23	0.87	0.32	52.45	29.24	7.56	10.35	0.38	0.00	0.01
	147	95	37.89	0.04	21.60	0.00	25.04	3.60	7.59	3.92	99.69	2.95	1.98	0.00	0.12	1.51	0.00	0.24	0.88	0.33	51.05	29.84	8.05	10.41	0.65	0.00	0.01
	148	96	37.65	0.05	21.46	0.00	25.91	3.75	6.64	4.42	99.89	2.94	1.97	0.00	0.14	1.55	0.00	0.25	0.77	0.37	52.71	26.28	8.43	11.72	0.83	0.00	0.02
	149	97	37.41	0.15	21.00	0.00	25.60	3.70	7.01	4.03	98.87	2.95	1.95	0.01	0.14	1.55	0.00	0.25	0.82	0.34	52.31	27.85	8.34	10.68	0.77	0.00	0.05
	150	98	37.49	0.14	20.77	0.00	25.98	3.65	6.82	4.44	99.30	2.95	1.92	0.01	0.17	1.54	0.00	0.24	0.80	0.37	52.08	27.04	8.23	11.59	1.02	0.00	0.05
	151	99	37.92	0.07	21.31	0.00	26.07	3.61	7.56	3.74	100.29	2.94	1.95	0.00	0.17	1.52	0.00	0.24	0.87	0.31	51.70	29.70	8.06	9.69	0.84	0.00	0.02
	152	100	37.95	0.04	21.48	0.00	25.89	4.14	6.77	4.48	100.75	2.94	1.96	0.00	0.16	1.52	0.00	0.27	0.78	0.37	51.57	26.57	9.24	11.66	0.95	0.00	0.01
	153	101	37.76	0.03	21.50	0.00	25.30	3.60	7.31	4.00	99.50	2.95	1.98	0.00	0.13	1.53	0.00	0.24	0.85	0.33	51.74	28.84	8.07	10.66	0.67	0.00	0.01
	154	102	37.57	0.08	21.10	0.00	25.70	4.06	6.82	4.31	99.64	2.94	1.95	0.00	0.16	1.52	0.00	0.27	0.80	0.36	51.58	27.00	9.13	11.31	0.95	0.00	0.03
	155	103	37.60	0.07	21.14	0.00	25.36	3.92	7.06	3.70	98.86	2.96	1.96	0.00	0.11	1.56	0.00	0.26	0.83	0.31	52.69	27.96	8.81	9.97	0.55	0.00	0.02
	156	104	37.99	0.06	21.50	0.00	25.85	3.82	6.84	4.41	100.46	2.95	1.97	0.00	0.13	1.54	0.00	0.25	0.79	0.37	52.29	26.80	8.50	11.60	0.79	0.00	0.02

TABLE DR-4. $\delta^{18}O$ ANALYSES OF ZIRCON IN CATALINA QUARTZITE BY ION MICROPROBE

Analysis #	Comment	$\delta^{18}O$ VSMOW	2 S.D. KIM-5 bracket	$\alpha^{18}O$	$\delta^{18}O$ Raw	2 S.E. measurement	^{16}O cps x10-9	Prim. Intensity nA	Yield GHz/nA
Session #1 Date: 4/24-4/25/2007									
Sample: 05C-09									
Analysis numbers not reported are from other samples									
99	ZP-12_KIM5				6.18	0.35	2.91	2.91	1.000
100	ZP-12_KIM5				6.54	0.53	2.90	2.93	0.990
101	ZP-12_KIM5				6.24	0.35	2.89	2.92	0.989
102	ZP-12_KIM5				6.00	0.48	2.89	2.91	0.994
	average		0.45		6.24				
	bracket (60-62,64,78-81)		0.44	1.001037	6.13				
103	ZP-12_C-9-40r	17.82	0.31		19.02	0.50	2.78	2.85	0.976
104	ZP-12_C-9-39r?	23.54	0.31		24.74	0.40	2.75	2.86	0.962
~~105~~	~~ZP-12_C-9-39c~~	~~8.00~~	~~0.31~~		~~9.19~~	~~0.49~~	~~2.75~~	~~2.86~~	~~0.964~~
106	ZP-12_C-9-38r	15.45	0.31		16.65	0.48	2.63	2.83	0.931
~~107~~	~~ZP-12_C-9-38c inclusion~~	~~14.43~~	~~0.31~~		~~15.63~~	~~0.47~~	~~2.78~~	~~2.84~~	~~0.977~~
108	ZP-12_C-9-37r	18.42	0.31		19.62	0.37	2.64	2.83	0.934
109	ZP-12_C-9-36?r	12.63	0.31		13.83	0.52	2.73	2.82	0.967
~~110~~	~~ZP-12_C-9-33c inclusion~~	~~12.08~~	~~0.31~~		~~13.27~~	~~0.41~~	~~2.70~~	~~2.82~~	~~0.956~~
111	ZP-12_C-9-33r	15.41	0.31		16.61	0.44	2.75	2.83	0.970
112	ZP-12_C-9-34r	24.00	0.31		25.20	0.43	2.73	2.82	0.970
113	ZP-12_C-9-34r	24.57	0.31		25.78	0.41	2.72	2.82	0.964
~~114~~	~~ZP-12_C-9-30c inclusion~~	~~11.33~~	~~0.31~~		~~12.53~~	~~0.16~~	~~2.88~~	~~2.81~~	~~1.025~~
115	ZP-12_C-9-27r	11.48	0.31		12.67	0.47	2.79	2.80	0.997
116	ZP-12_C-9-27c	16.69	0.31		17.89	0.37	2.77	2.81	0.985
117	ZP-12_C-9-28c	22.28	0.31		23.49	0.35	2.79	2.81	0.992
~~118~~	~~ZP-12_C-9-25c inclusion~~	~~9.17~~	~~0.31~~		~~10.36~~	~~0.45~~	~~2.59~~	~~2.83~~	~~0.916~~
119	ZP-12_C-9-25r	15.23	0.31		16.43	0.45	2.65	2.84	0.931
120	ZP-12_KIM5				6.38	0.32	2.79	2.81	0.991
121	ZP-12_KIM5				6.33	0.48	2.75	2.82	0.974
122	ZP-12_KIM5				6.32	0.42	2.76	2.81	0.984
123	ZP-12_KIM5				6.22	0.39	2.72	2.77	0.982
	average		0.13		6.31				
	bracket (78-81,120-123)		0.31	1.001180	6.28				
128	ZP-12_C-9-23r	19.06	0.17		20.32	0.38	2.66	2.68	0.992
129	ZP-12_C-9-22r	17.74	0.17		19.00	0.44	2.68	2.69	0.997
~~130~~	ZP-12_C-9-26r	19.22	0.17		20.48	0.42	2.56	2.70	0.948
~~131~~	~~ZP-12_C-9-26c~~	~~11.27~~	~~0.17~~		~~12.52~~	~~0.44~~	~~2.62~~	~~2.68~~	~~0.976~~
132	ZP-12_C-9-21c	4.74	0.17		5.98	0.49	2.64	2.68	0.985
~~133~~	~~ZP-12_C-9-21m inclusion~~	~~18.56~~	~~0.17~~		~~19.82~~	~~0.60~~	~~2.54~~	~~2.69~~	~~0.941~~
134	ZP-12_C-9-17r	18.26	0.17		19.52	0.37	2.70	2.69	1.002
135	ZP-12_C-9-16r	19.80	0.17		21.06	0.36	2.66	2.70	0.986
~~136~~	~~ZP-12_C-9-16ccrack~~	~~14.24~~	~~0.17~~		~~15.49~~	~~0.53~~	~~2.71~~	~~2.67~~	~~1.017~~
137	ZP-12_C-9-18r	13.59	0.17		14.85	0.42	2.59	2.69	0.963
138	ZP-12_C-9-15r	17.56	0.17		18.82	0.32	2.67	2.68	0.997
~~139~~	~~ZP-12_C-9-15c inclusion~~	~~15.50~~	~~0.17~~		~~16.76~~	~~0.57~~	~~2.68~~	~~2.69~~	~~0.997~~
140	ZP-12_KIM-5				6.35	0.46	2.60	2.69	0.967
141	ZP-12_KIM-5				6.22	0.51	2.63	2.71	0.969
142	ZP-12_KIM-5				6.47	0.48	2.65	2.70	0.981
143	ZP-12_KIM-5				6.38	0.45	2.63	2.69	0.977
	average		0.21		6.35				
	bracket (120-123,140-143)		0.17	1.001237	6.33				
221	ZP-12-KIM5				6.93	0.42	2.52	2.62	0.962
222	ZP-12-KIM5				6.45	0.42	2.55	2.62	0.974
223	ZP-12-KIM5				6.38	0.48	2.54	2.61	0.973
224	ZP-12-KIM5				6.64	0.32	2.51	2.62	0.960
	average		0.49		6.60				
	bracket (195-198,221-224)		0.39	1.001599	6.70				
231	ZP-12C-9-1c	16.62	0.45		18.17	0.43	2.57	2.56	1.006
232	ZP-12C-9-1r	11.49	0.45		13.03	0.57	2.52	2.58	0.977
233	ZP-12KIM5				6.66	0.44	2.56	2.58	0.990
234	ZP-12KIM5				6.60	0.51	2.52	2.58	0.977
235	ZP-12KIM5				6.37	0.35	2.51	2.59	0.969
236	ZP-12KIM5				6.94	0.46	2.42	2.59	0.934
	average		0.47		6.64				
	bracket (221-224,233-236)		0.45	1.001524	6.62				

Analysis #	Comment	$\delta^{18}O$ VSMOW	2 S.D. KIM-5 bracket	$\alpha^{18}O$	$\delta^{18}O$ Raw	2 S.E. measurement	^{16}O cps x10-9	Prim. Intensity nA	Yield GHz/nA
237	ZP-12-C-9-2r	12.43	0.37		14.05	0.61	2.50	2.56	0.974
~~238~~	~~ZP-12-C-9-2c inclusion~~	~~6.92~~	~~0.37~~		~~8.53~~	~~0.56~~	~~2.46~~	~~2.58~~	~~0.952~~
239	ZP-12-C-9-3c	8.40	0.37		10.01	0.52	2.41	2.55	0.941
240	ZP-12-C-9-3r	19.60	0.37		21.23	0.41	2.39	2.57	0.931
241	ZP-12-C-9-5c	6.14	0.37		7.75	0.52	2.46	2.58	0.953
242	ZP-12-C-9-5m	21.74	0.37		23.38	0.58	2.48	2.58	0.962
243	ZP-12-C-9-5r	17.49	0.37		19.12	0.55	2.52	2.57	0.979
244	ZP-12-C-9-6c	5.52	0.37		7.13	0.55	2.29	2.56	0.896
~~245~~	~~ZP-12-C-9-6m inclusion~~	~~20.90~~	~~0.37~~		~~22.53~~	~~0.49~~	~~2.36~~	~~2.57~~	~~0.919~~
246	ZP-12-C-9-4c	6.40	0.37		8.01	0.44	2.35	2.53	0.931
247	ZP-12-C-9-4r	23.50	0.37		25.13	0.45	2.41	2.55	0.944
248	ZP-12-C-9-9m	23.89	0.37		25.52	0.47	2.49	2.52	0.987
249	ZP-12-C-9-9r	20.14	0.37		21.77	0.36	2.45	2.53	0.968
250	ZP-12-C-9-9c?	20.94	0.37		22.58	0.43	2.48	2.54	0.978
~~251~~	~~ZP-12-C-9-11r~~	~~20.16~~	~~0.37~~		~~21.79~~	~~0.64~~	~~2.49~~	~~2.50~~	~~0.994~~
252	ZP-12-C-9-12c	16.64	0.37		18.27	0.41	2.44	2.51	0.974
253	ZP-12-C-9-12m	22.84	0.37		24.48	0.41	2.42	2.50	0.964
254	ZP-12-C-9-12r	13.73	0.37		15.35	0.58	2.26	2.53	0.896
255	ZP-12-C-9-14r	16.10	0.37		17.72	0.38	2.34	2.51	0.931
256	ZP-12-C-9-14c?	5.81	0.37		7.42	0.41	2.42	2.48	0.976
257	ZP-12-C-9-13c/m?	19.68	0.37		21.32	0.58	2.28	2.49	0.915
258	ZP-12-C-9-19c/m?	4.78	0.37		6.39	0.56	2.28	2.48	0.920
259	ZP-12-C-9-19r	23.25	0.37		24.89	0.37	2.40	2.48	0.967
260	ZP-12-C-9-20r	18.31	0.37		19.94	0.50	2.37	2.47	0.957
261	ZP-12-C-9-20c/m	24.11	0.37		25.74	0.44	2.39	2.48	0.962
262	ZP-12-C-9-24c	19.60	0.37		21.23	0.69	2.25	2.47	0.913
263	ZP-12-C-9-24r	18.72	0.37		20.35	0.44	2.45	2.48	0.988
264	ZP-12-C-9-29c	10.47	0.37		12.09	0.48	2.37	2.46	0.961
~~265~~	~~ZP-12-C-9-ac? Inclusion~~	~~9.06~~	~~0.37~~		~~10.67~~	~~0.73~~	~~2.42~~	~~2.46~~	~~0.983~~
~~266~~	~~ZP-12-C-9-31c inclusion~~	~~7.35~~	~~0.37~~		~~8.96~~	~~0.51~~	~~2.39~~	~~2.44~~	~~0.976~~
267	ZP-12-C-9-31m	23.46	0.37		25.10	0.42	2.32	2.45	0.945
268	ZP-12-C-9-31r	18.09	0.37		19.72	0.39	2.29	2.46	0.934
269	ZP-12-C-9-35m	23.94	0.37		25.57	0.47	2.25	2.48	0.905
270	ZP-12-KIM5				6.78	0.47	2.33	2.48	0.943
271	ZP-12-KIM5				6.65	0.24	2.34	2.46	0.950
272	ZP-12-KIM5				6.65	0.42	2.33	2.46	0.946
273	ZP-12-KIM5				6.94	0.22	2.35	2.45	0.957
	average		0.28		6.75				
	bracket (221-224,233-236)		0.37	1.001599	6.70				
			2 S.D.						

Fig. DR–4 Time series zircon analyses by SIMS (15 μm spots)

corrected to VSMOW, error bars are 2 S.D. from bracketing standards

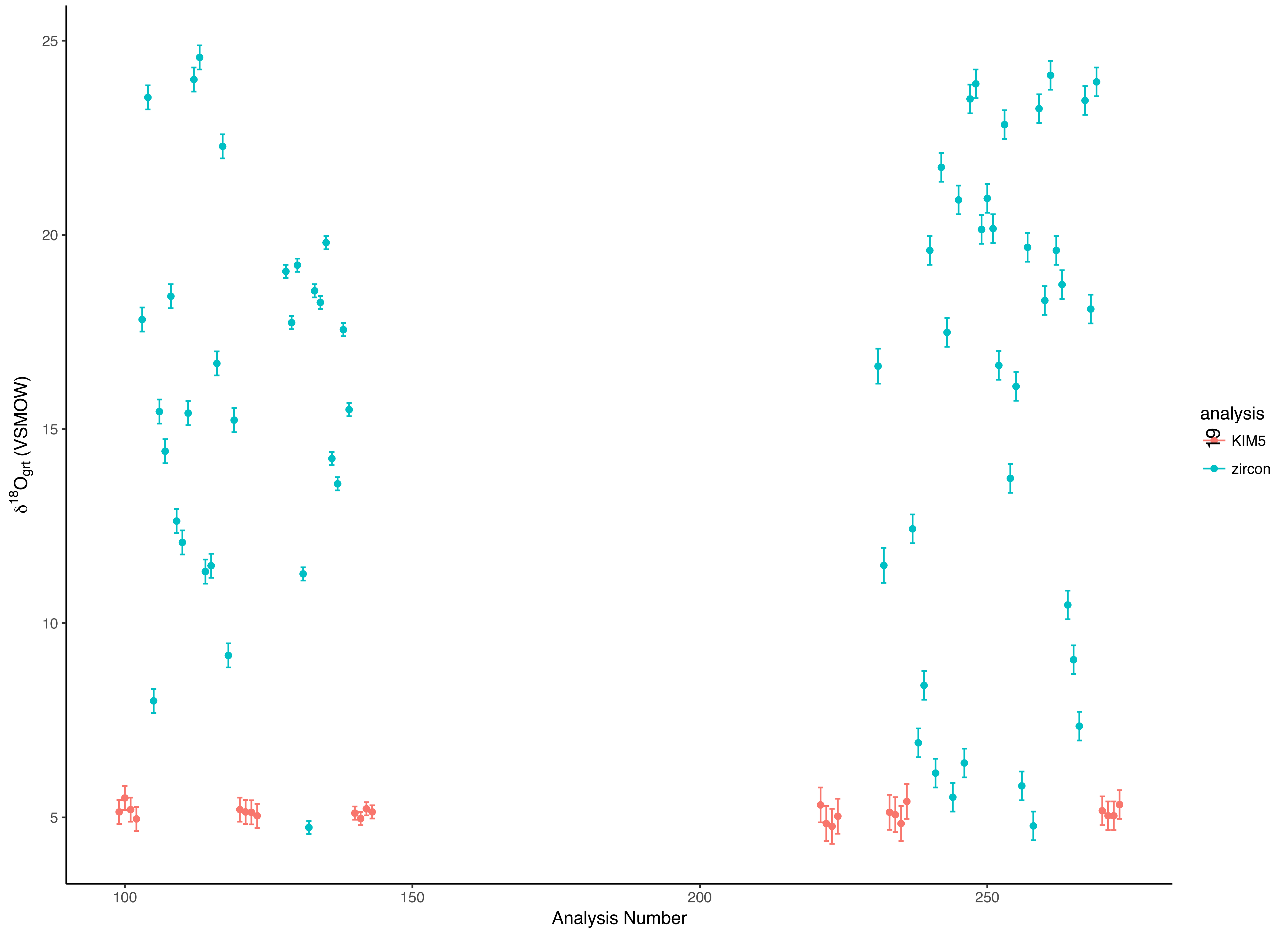

TABLE DR-5. SUB-MICRON PIT $\delta^{18}O$ ANALYSES OF ZIRCON FROM CATALINA QUARTZITE BY ION MICROPROBE

Analysis #	Comment	$\delta^{18}O$ VSMOW	2 S.D. KIM-5 bracket	$\alpha^{18}O$	$\delta^{18}O$ Raw	2 S.E. measurement	^{16}O cps x10-9
Session #1 Date: 5/9/2007							
Sample: 05C-09 zircon 34							
20070509@1.asc	ZP-12_KIM5				-2.6	0.982	0.00219
20070509@2.asc	ZP-12_KIM5				-2.8	1.048	0.00215
20070509@3.asc	ZP-12_KIM5				-2.1	1.023	0.00208
20070509@4.asc	ZP-12_KIM5				-2.8	0.941	0.00205
	average KIM 5		0.6		-2.6		
~~20070509@5.asc~~	~~ZP-12 KIM-5 1 um step pits overlap~~	~~5.0~~	~~1.7~~		~~-2.0~~	~~1.077~~	~~0.00200~~
~~20070509@6.asc~~	~~ZP-12 KIM-5 1 um step pits overlap~~	~~5.0~~	~~1.7~~		~~-2.0~~	~~0.945~~	~~0.00204~~
~~20070509@7.asc~~	~~ZP-12 KIM-5 1 um step pits overlap~~	~~2.0~~	~~1.7~~		~~-5.0~~	~~1.125~~	~~0.00237~~
~~20070509@8.asc~~	~~ZP-12 KIM-5 1 um step pits overlap~~	~~6.1~~	~~1.7~~		~~-1.0~~	~~0.837~~	~~0.00199~~
20070509@9.asc	ZP-12_C-9_34 core	6.5	1.7		-0.5	1.079	0.00199
20070509@10.asc	ZP-12 C-9 z34 Trav1 rim-core 2 um step 10 analyses	17.9	1.7		10.8	1.046	0.00196
20070509@11.asc	ZP-12 C-9 z34 Trav1 rim-core 2 um step 10 analyses	15.9	1.7		8.8	0.985	0.00194
20070509@12.asc	ZP-12 C-9 z34 Trav1 rim-core 2 um step 10 analyses	18.6	1.7		11.5	0.956	0.00190
20070509@13.asc	ZP-12 C-9 z34 Trav1 rim-core 2 um step 10 analyses	23.4	1.7		16.3	1.090	0.00189
20070509@14.asc	ZP-12 C-9 z34 Trav1 rim-core 2 um step 10 analyses	23.1	1.7		16.0	0.995	0.00189
20070509@15.asc	ZP-12 C-9 z34 Trav1 rim-core 2 um step 10 analyses	22.7	1.7		15.5	1.055	0.00190
20070509@16.asc	ZP-12 C-9 z34 Trav1 rim-core 2 um step 10 analyses	23.1	1.7		15.9	1.011	0.00185
20070509@17.asc	ZP-12 C-9 z34 Trav1 rim-core 2 um step 10 analyses	23.5	1.7		16.3	1.027	0.00184
20070509@18.asc	ZP-12 C-9 z34 Trav1 rim-core 2 um step 10 analyses	19.9	1.7		12.8	1.079	0.00181
20070509@19.asc	ZP-12 C-9 z34 Trav1 rim-core 2 um step 10 analyses	5.4	1.7		-1.6	0.947	0.00181
20070509@20.asc	ZP-12_KIM5				-1.8	1.000	0.00174
20070509@21.asc	ZP-12_KIM5				-0.7	1.008	0.00173
20070509@22.asc	ZP-12_KIM5				-0.7	1.049	0.00176
20070509@23.asc	ZP-12_KIM5				-2.0	1.102	0.00171
	average KIM 5		1.4		-1.3	1.040	
	bracket KIM 5		1.7	0.9930251	-1.9		
20070509@24.asc	ZP-12 KIM-5 after Reservoir increase				-1.9	0.945	0.00181
20070509@25.asc	ZP-12 KIM-5 after Reservoir increase				-1.6	1.020	0.00179
20070509@26.asc	ZP-12 KIM-5 after Reservoir increase				-2.2	1.002	0.00177
20070509@27.asc	ZP-12 KIM-5 after Reservoir increase				-2.3	1.090	0.00177
	average KIM 5		0.7		-2.0		
20070509@28.asc	ZP-12 C-9 z34 Trav2 rim-core 2 um step 13 analyses	16.1	0.9		9.3	1.158	0.00177
20070509@29.asc	ZP-12 C-9 z34 Trav2 rim-core 2 um step 13 analyses	16.0	0.9		9.1	1.166	0.00178
20070509@30.asc	ZP-12 C-9 z34 Trav2 rim-core 2 um step 13 analyses	15.7	0.9		8.8	1.074	0.00173
20070509@31.asc	ZP-12 C-9 z34 Trav2 rim-core 2 um step 13 analyses	17.7	0.9		10.9	1.143	0.00177
20070509@32.asc	ZP-12 C-9 z34 Trav2 rim-core 2 um step 13 analyses	18.4	0.9		11.5	1.083	0.00177
20070509@33.asc	ZP-12 C-9 z34 Trav2 rim-core 2 um step 13 analyses	22.3	0.9		15.4	1.038	0.00172
20070509@34.asc	ZP-12 C-9 z34 Trav2 rim-core 2 um step 13 analyses	22.9	0.9		16.0	1.013	0.00173
20070509@35.asc	ZP-12 C-9 z34 Trav2 rim-core 2 um step 13 analyses	22.3	0.9		15.5	1.063	0.00171
20070509@36.asc	ZP-12 C-9 z34 Trav2 rim-core 2 um step 13 analyses	23.5	0.9		16.6	1.091	0.00171
20070509@37.asc	ZP-12 C-9 z34 Trav2 rim-core 2 um step 13 analyses	21.8	0.9		14.9	1.125	0.00172
20070509@38.asc	ZP-12 C-9 z34 Trav2 rim-core 2 um step 13 analyses	24.1	0.9		17.2	1.027	0.00169
20070509@39.asc	ZP-12 C-9 z34 Trav2 rim-core 2 um step 13 analyses	24.2	0.9		17.4	1.126	0.00173
20070509@40.asc	ZP-12 C-9 z34 Trav2 rim-core 2 um step 13 analyses	7.0	0.9		0.2	0.990	0.00168
20070509@41.asc	ZP-12 KIM-5				-1.2	1.024	0.00165
20070509@42.asc	ZP-12 KIM-5				-1.5	1.232	0.00158
20070509@43.asc	ZP-12 KIM-5				-1.6	1.176	0.00164
20070509@44.asc	ZP-12 KIM-5				-1.1	1.308	0.00149
	average KIM 5		0.5		-1.4		
	bracket KIM 5		0.9	0.9932706	-1.7		
20070509@45.asc	ZP-12 KIM-5 after Reservoir increase				-2.5	0.990	0.00164
20070509@46.asc	ZP-12 KIM-5 after Reservoir increase				-2.2	1.163	0.00164
20070509@47.asc	ZP-12 KIM-5 after Reservoir increase				-1.3	1.011	0.00160
20070509@48.asc	ZP-12 KIM-5 after Reservoir increase				-1.2	1.306	0.00163
	average KIM 5		1.4		-1.8		
20070509@49.asc	ZP-12 C-9 z34 Trav3 rcore-rim 2 um step 1 analysis	22.1	1.3		15.7	1.100	0.00169
20070509@50.asc	ZP-12 C-9 z34 Trav4 core-rim 2 um step 6 analyses;	6.8	1.3		0.6	1.071	0.00164
20070509@51.asc	ZP-12 C-9 z34 Trav4 core-rim 2 um step	6.0	1.3		-0.3	1.185	0.00158
20070509@52.asc	ZP-12 C-9 z34 Trav4 core-rim 2 um step	6.2	1.3		0.0	1.286	0.00156
~~20070509@53.asc~~	~~ZP-12 C-9 z34 Trav4 core-rim 2 um step; overlaps @49~~	~~10.0~~	~~1.3~~		~~3.7~~	~~1.171~~	~~0.00154~~
~~20070509@54.asc~~	~~ZP-12 C-9 z34 Trav4 core-rim 2 um step; overlaps @49~~	~~17.8~~	~~1.3~~		~~11.5~~	~~1.223~~	~~0.00164~~
20070509@55.asc	ZP-12 C-9 z34 Trav4 core-rim 2 um step	20.8	1.3		14.4	1.022	0.00158
20070509@56.asc	ZP-12 KIM-5				-0.3	1.151	0.00154
20070509@57.asc	ZP-12 KIM-5				-1.5	1.188	0.00156
20070509@58.asc	ZP-12 KIM-5				-0.1	1.233	0.00154
20070509@59.asc	ZP-12 KIM-5				-2.0	1.147	0.00151
	average KIM 5		1.9		-1.0		
	bracket KIM 5		1.3	0.9937728	-1.2		

Fig. DR–5 Time series zircon analyses by SIMS (sub μm spots)

corrected to VSMOW, error bars are 2 S.D. from bracketing standards

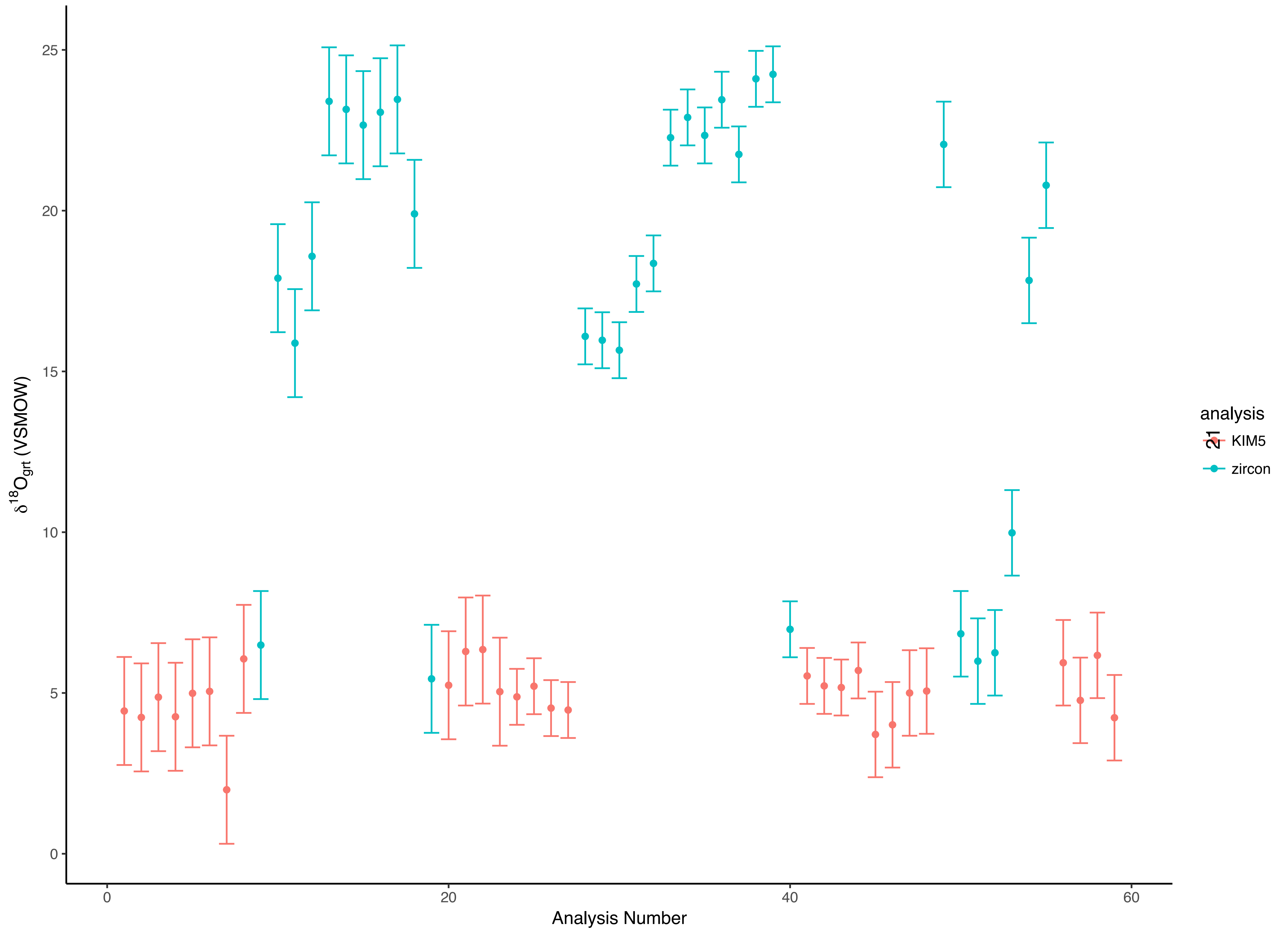

TABLE DR-6.SHRIMP U-Pb ISOTOPE DATA FROM CATALINA QUARTZITE ZIRCON

Analysis	Common ^{206}Pb (%)	U (ppm)	Th (ppm)	U/Th	^{207}Pb*/^{235}U	± 1s (%)	^{206}Pb*/^{238}U	± 1s (%)	error corr.	^{206}Pb/^{207}Pb	± 1s (%)	^{206}Pb*/^{238}U (Ma)	± 1s (Ma)
C9-11.1C	0.02	1686	1486	0.88	0.13	2.2	0.02	1	0.45	0.0475	2	125.1	1.2
C9-14.1C	1.03	148	121	0.82	0.15	5.2	0.02	1.6	0.31	0.0567	4.9	124.9	2
C9-15.1R	0.29	208	9	0.04	0.12	4.9	0.017	1.5	0.31	0.0505	4.7	111.4	1.7
C9-16.1R	-0.37	394	15	0.04	0.11	6.9	0.018	1.3	0.19	0.0423	6.7	116	1.5
C9-17.1C	0.45	186	67	0.36	0.13	7	0.02	1.5	0.22	0.0486	6.9	126.5	1.9
C9-18.1R	2.09	184	12	0.07	0.11	21	0.018	1.9	0.09	0.0431	20.8	113.2	2.1
C9-21.1M	1.14	592	78	0.13	0.13	5.3	0.018	1.2	0.22	0.0533	5.2	112.6	1.3
~~C9-22.1C~~	~~1.77~~	~~1950~~	~~80~~	~~0.04~~	~~0.20~~	~~1.6~~	~~0.023~~	~~1~~	~~0.6~~	~~0.0626~~	~~1.3~~	~~146.4~~	~~1.4~~
C9-23.1C	0.39	1224	466	0.38	0.13	2.6	0.019	1	0.4	0.0504	2.4	121.7	1.2
C9-25.1R	2.49	156	10	0.06	0.14	15	0.019	1.9	0.13	0.0542	14.4	118.2	2.2
C9-27	0.06	540	9	0.02	0.11	6.1	0.018	1.2	0.2	0.0446	6	117.4	1.4
C9-28.1C	0.19	1445	21	0.01	0.13	1.9	0.019	1	0.52	0.0499	1.7	120.1	1.2
C9-30.1	1.9	300	253	0.84	0.15	4.7	0.018	1.4	0.29	0.0609	4.5	117.6	1.6
C9-32.1C	0.27	425	160	0.38	0.13	3.4	0.019	1.2	0.36	0.0506	3.2	121.4	1.5
C9-33.1R	4.35	182	9	0.05	0.08	58	0.018	2.5	0.04	0.0299	57.4	117.1	2.9
C9-34.1C	0.88	442	224	0.51	0.13	8.5	0.02	1.3	0.15	0.0476	8.4	124.3	1.6
C9-35.1C	-0.16	1331	1189	0.89	0.13	2.4	0.02	1	0.43	0.0463	2.2	126	1.3
C9-36.1R	1.44	149	9	0.06	0.10	24	0.018	2	0.08	0.0402	23.6	112.4	2.2
C9-37.1C	0.44	327	224	0.69	0.13	6.4	0.019	1.3	0.21	0.0486	6.3	123.6	1.6
C9-38.1R	4.04	182	8	0.04	0.12	25	0.018	2.1	0.09	0.048	24.6	113.4	2.4
C9-39.1R	0.25	353	10	0.03	0.12	3.9	0.018	1.3	0.34	0.0503	3.7	115.1	1.5
~~C9-40.1~~	~~0.88~~	~~1653~~	~~42~~	~~0.03~~	~~0.13~~	~~4.1~~	~~0.019~~	~~1~~	~~0.25~~	~~0.0498~~	4	~~123.3~~	~~1.3~~

Analyses 22 and 40 were found to contain inclusions and were discarded

TABLE DR-7.SHRIMP REE DATA FROM CATALINA QUARTZITE ZIRCON

Analysis	La (ppm)	Ce (ppm)	Nd (ppm)	Sm (ppm)	Eu (ppm)	Gd (ppm)	Dy (ppm)	Er (ppm)	Yb (ppm)	Hf (ppm)	Yb/Gd	U/Yb	Th/Yb	Ce/Sm	Yb/Dy	Gd/Nd	Gd/Sm	Sm/Nd	Ce/Ce*	Eu/Eu*
C9-11.1C	0.198	119.3	5.1	12.8	2.6	121.4	532	824	1214	10457	10.0	1.5	1.30	9.3	2.3	23.6	9.5	2.5	99	0.20
C9-14.1C	0.114	252.5	0.9	1.6	0.6	11.1	61	134	325	12043	29.2	0.5	0.40	155.8	5.3	11.8	6.9	1.7	530	0.44
C9-15.1R	0.040	2.2	0.0	0.2	0.2	2.7	12	14	22	12202	8.3	9.6	0.43	12.5	1.9	54.9	15.2	3.6	25	0.86
C9-16.1R	0.031	3.4	0.1	0.3	0.3	6.1	32	34	44	11663	7.2	9.0	0.36	10.8	1.4	111.0	19.6	5.7	43	0.71
C9-17.1C	0.035	54.6	0.7	2.0	0.4	21.7	115	217	368	11010	17.0	0.5	0.19	27.1	3.2	29.5	10.8	2.7	273	0.20
C9-18.1R	2.211	3.4	0.5	0.5	0.3	3.4	12	19	35	11063	10.4	5.4	0.37	7.2	3.0	6.5	7.1	0.9	1	0.73
C9-21.1M	0.225	85.1	0.0	0.3	0.3	8.7	80	101	142	17218	16.4	4.3	0.58	321.3	1.8	199.1	32.8	6.1	316	0.69
C9-22.1C	0.680	7.4	0.4	1.2	0.7	12.6	34	50	118	12703	9.4	17.1	0.72	6.0	3.5	28.3	10.2	2.8	6	0.50
C9-23.1C	4.270	72.7	1.6	2.7	0.6	26.2	168	340	703	13093	26.8	1.8	0.70	27.1	4.2	16.0	9.8	1.6	11	0.23
C9-25.1R	2.335	3.3	0.1	0.2	0.2	1.8	8	11	21	10118	11.7	7.7	0.50	19.3	2.8	18.6	10.6	1.8	2	0.86
C9-27.1C	1.278	2.8	0.5	0.7	0.4	7.5	31	42	59	12057	7.8	9.8	0.17	4.1	1.9	14.9	11.1	1.3	1	0.56
C9-28.1C	0.128	3.9	0.2	0.8	0.6	6.8	10	10	21	12655	3.1	71.8	1.05	5.0	2.2	41.8	8.7	4.8	14	0.75
C9-30.1C	0.631	14.4	0.2	0.4	0.3	6.8	53	117	310	15720	45.8	1.0	0.85	36.3	5.8	31.8	17.1	1.9	16	0.54
C9-32.1C	0.141	60.6	0.5	1.7	0.2	19.6	125	241	407	12985	20.7	1.1	0.42	36.2	3.3	38.6	11.7	3.3	136	0.12
C9-33.1R	3.841	2.6	0.1	0.2	0.2	1.8	9	14	26	9922	14.2	7.0	0.36	14.2	2.9	21.0	10.2	2.1	1	0.84
C9-34.1C	3.126	32.4	2.8	5.8	0.7	61.1	332	584	903	11228	14.8	0.5	0.27	5.6	2.7	21.7	10.6	2.0	5	0.12
C9-35.1C	9.396	99.8	4.3	7.8	1.7	71.0	324	508	773	10909	10.9	1.8	1.63	12.8	2.4	16.6	9.1	1.8	7	0.23
C9-36.1R	1.521	6.2	0.3	0.3	0.3	3.1	13	17	27	10357	8.8	5.6	0.36	17.7	2.1	9.5	8.8	1.1	3	0.74
C9-37.1C	0.044	536.8	0.4	1.3	0.3	12.4	74	151	301	13790	24.2	1.1	0.78	422.3	4.1	27.7	9.8	2.8	2707	0.21
C9-38.1R	3.978	9.6	0.6	0.6	0.3	4.2	15	19	29	12270	7.0	6.4	0.31	16.9	1.9	7.4	7.3	1.0	2	0.59
C9-39.1R	0.046	3.2	0.1	0.9	0.8	8.2	11	5	5	13310	0.6	72.2	2.08	3.5	0.4	72.7	8.9	8.1	25	0.84
C9-40.1	1.645	15.9	0.9	1.1	0.5	6.9	47	151	525	10524	76.1	3.3	0.09	14.9	11.1	7.4	6.5	1.1	6	0.54

Appendix DR-8 Catalina Metachert zircon CL, pit locations and $\delta^{18}O$

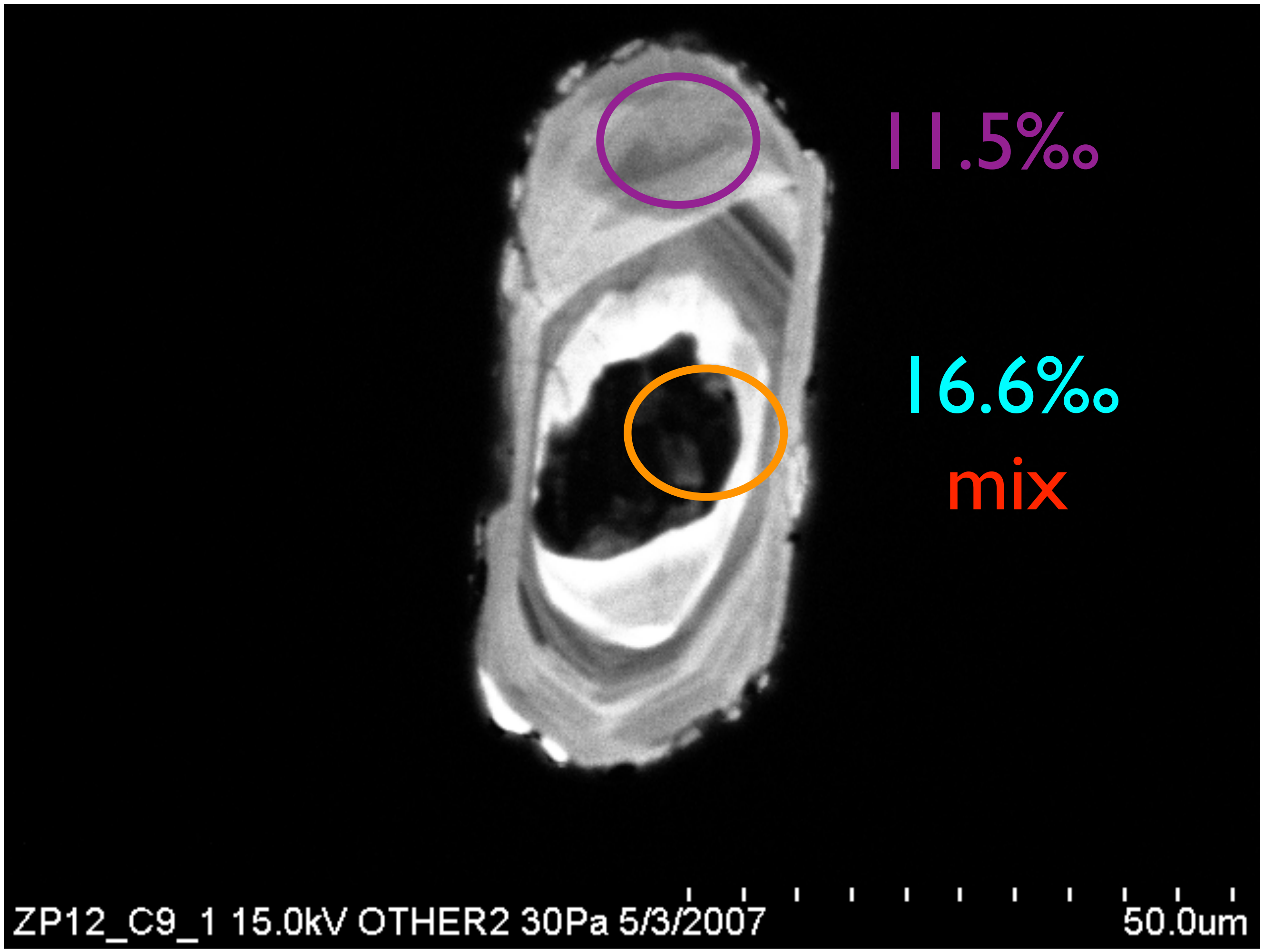

CL zones:
detrital core
mottled/bright
inner rim
oscillatory
intermediate rim
rare bright outer rim

ZP-12 05C-9z1

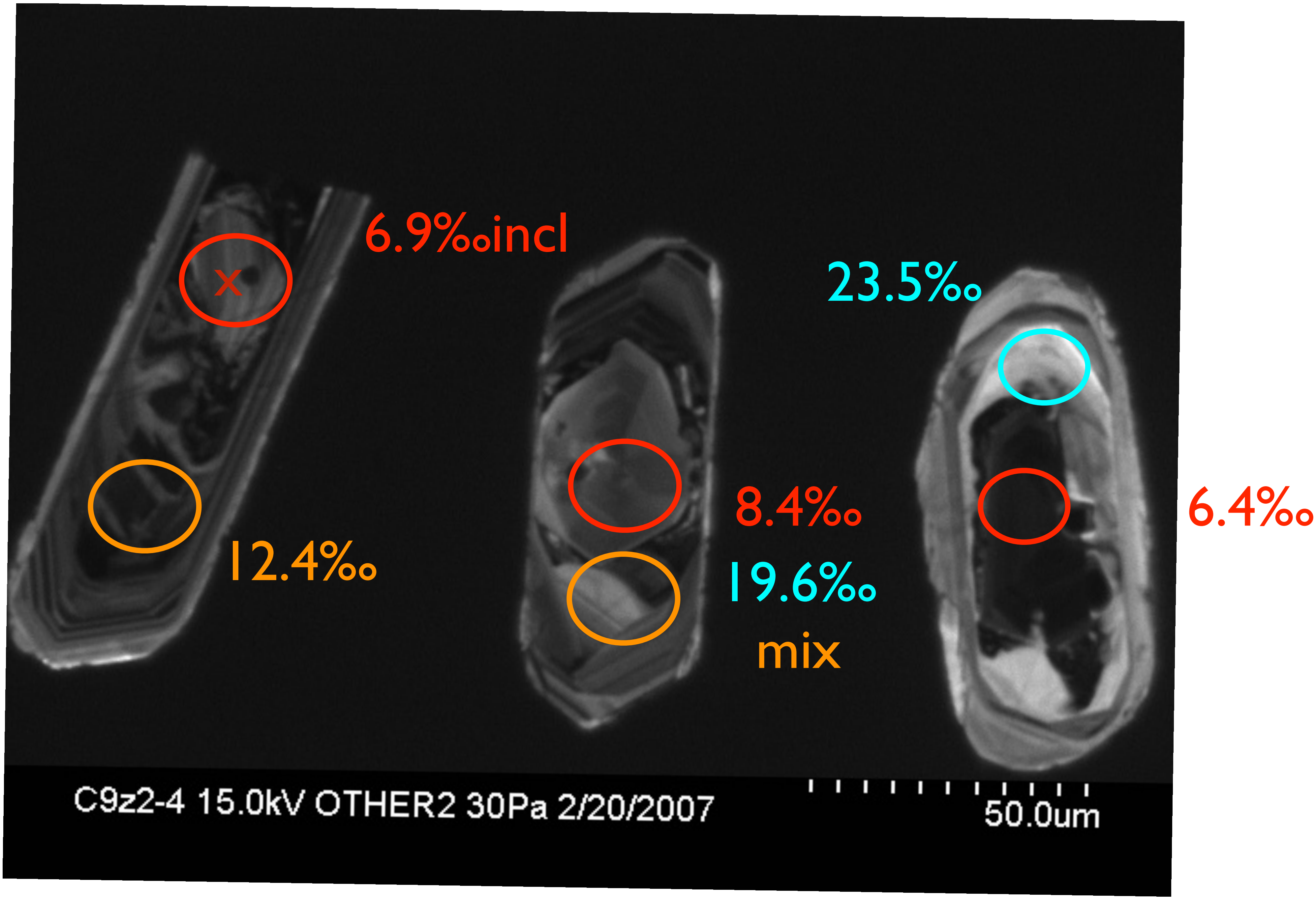

ZP-12 05C-9z2,3,4

ZP-12 05C-9z5

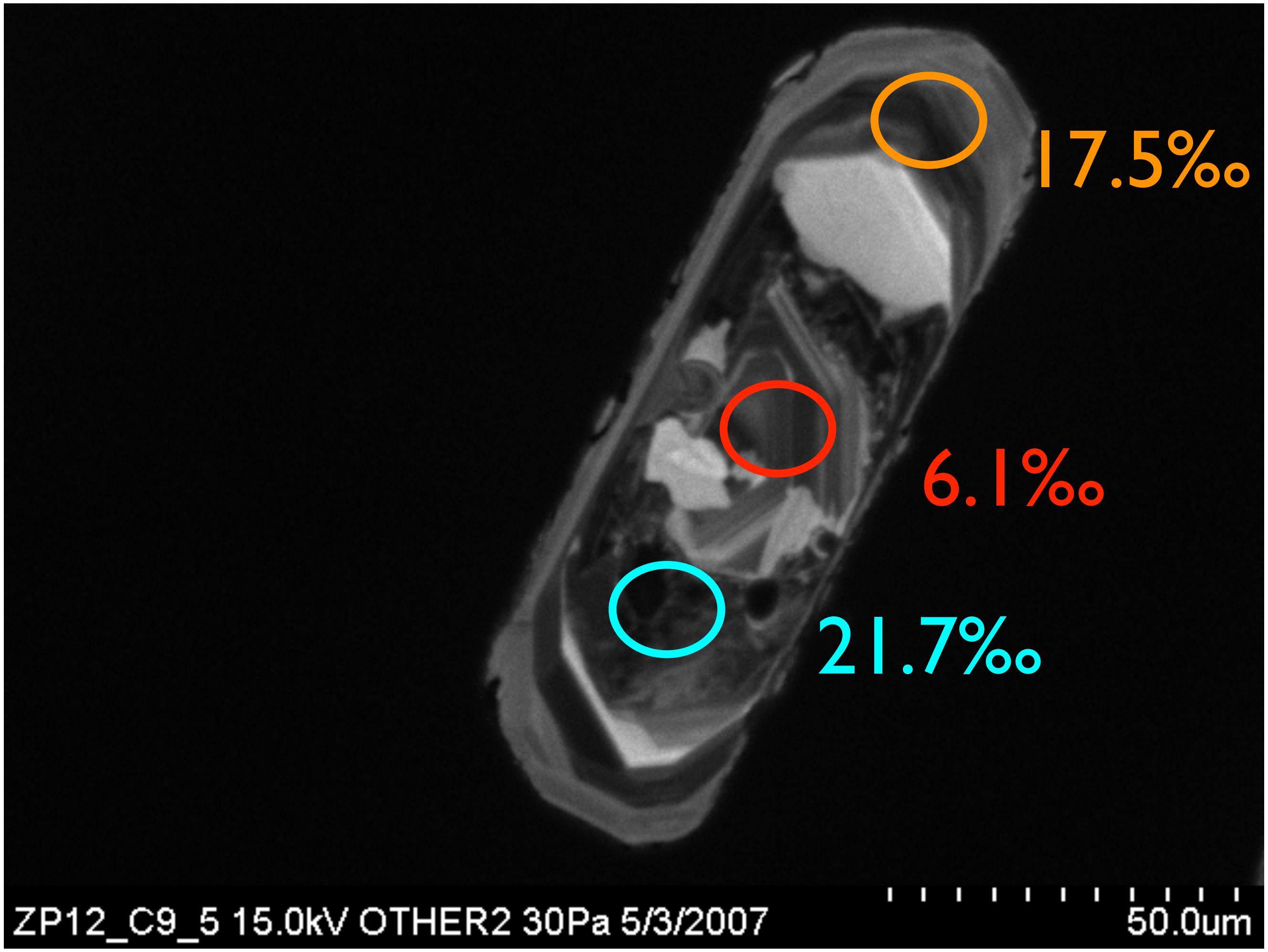

ZP-12 05C-9z6

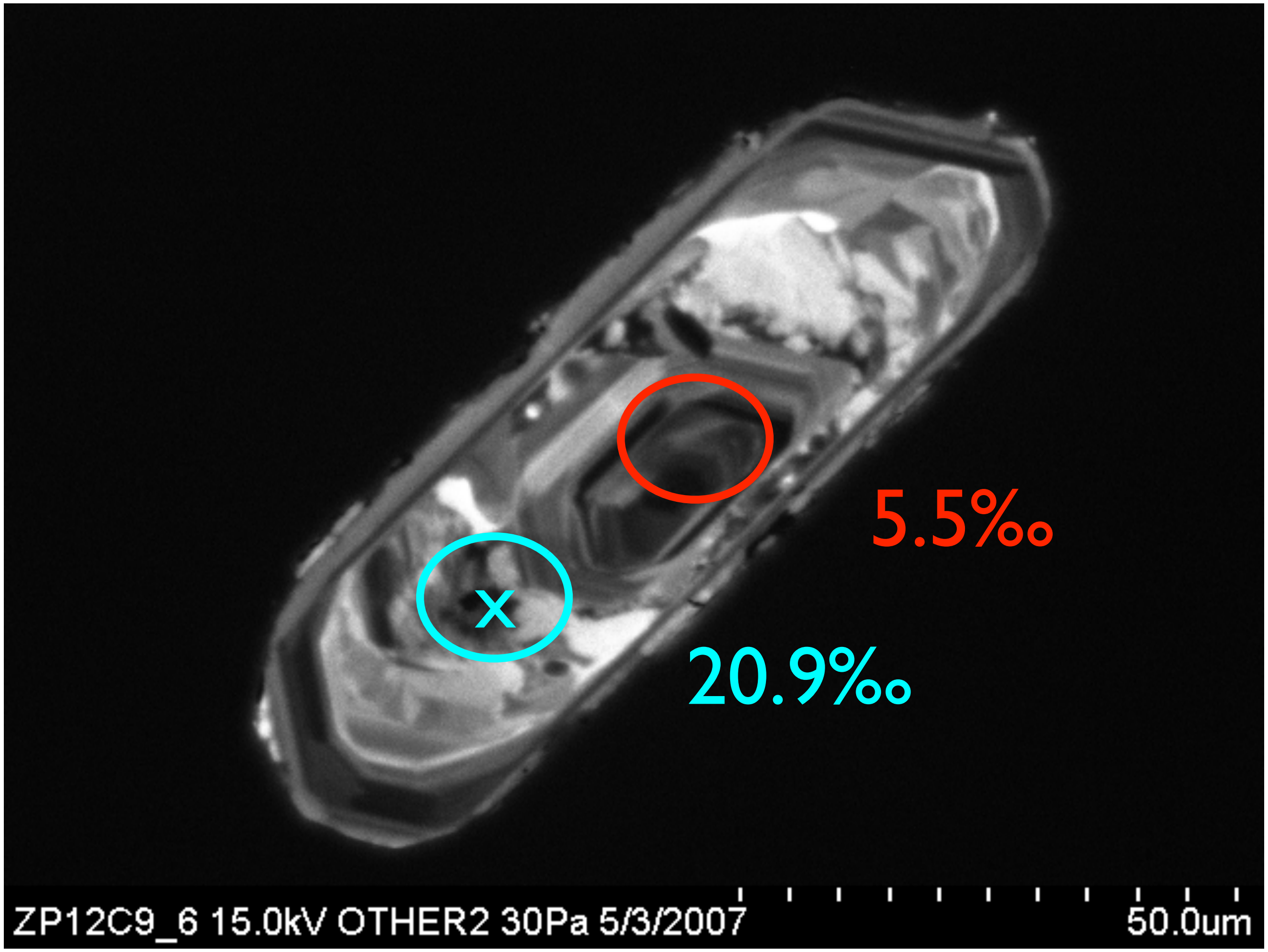

ZP-12 05C-9z9

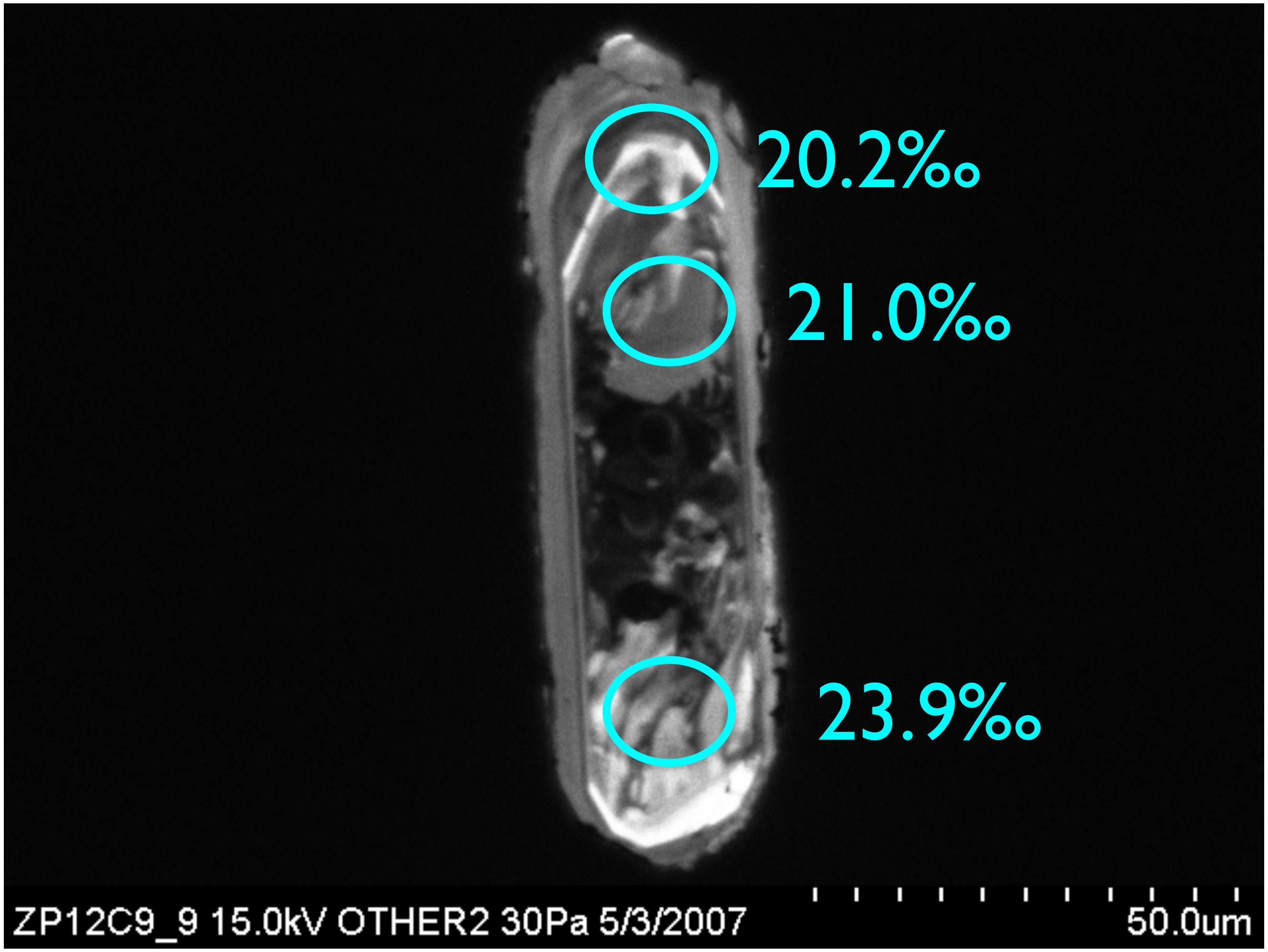

ZP-12 05C-9z11&14

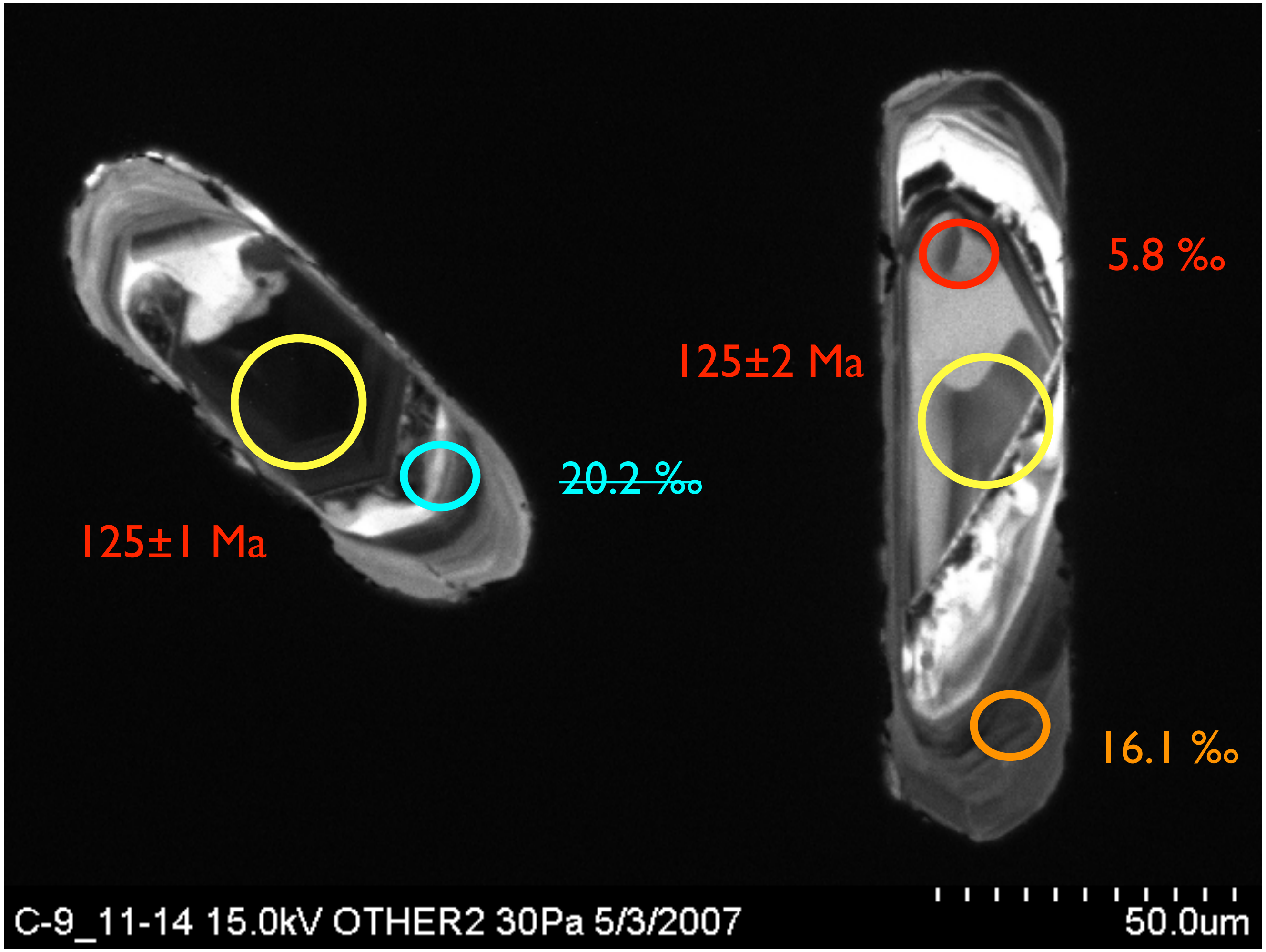

ZP-12 05C-9z12-13

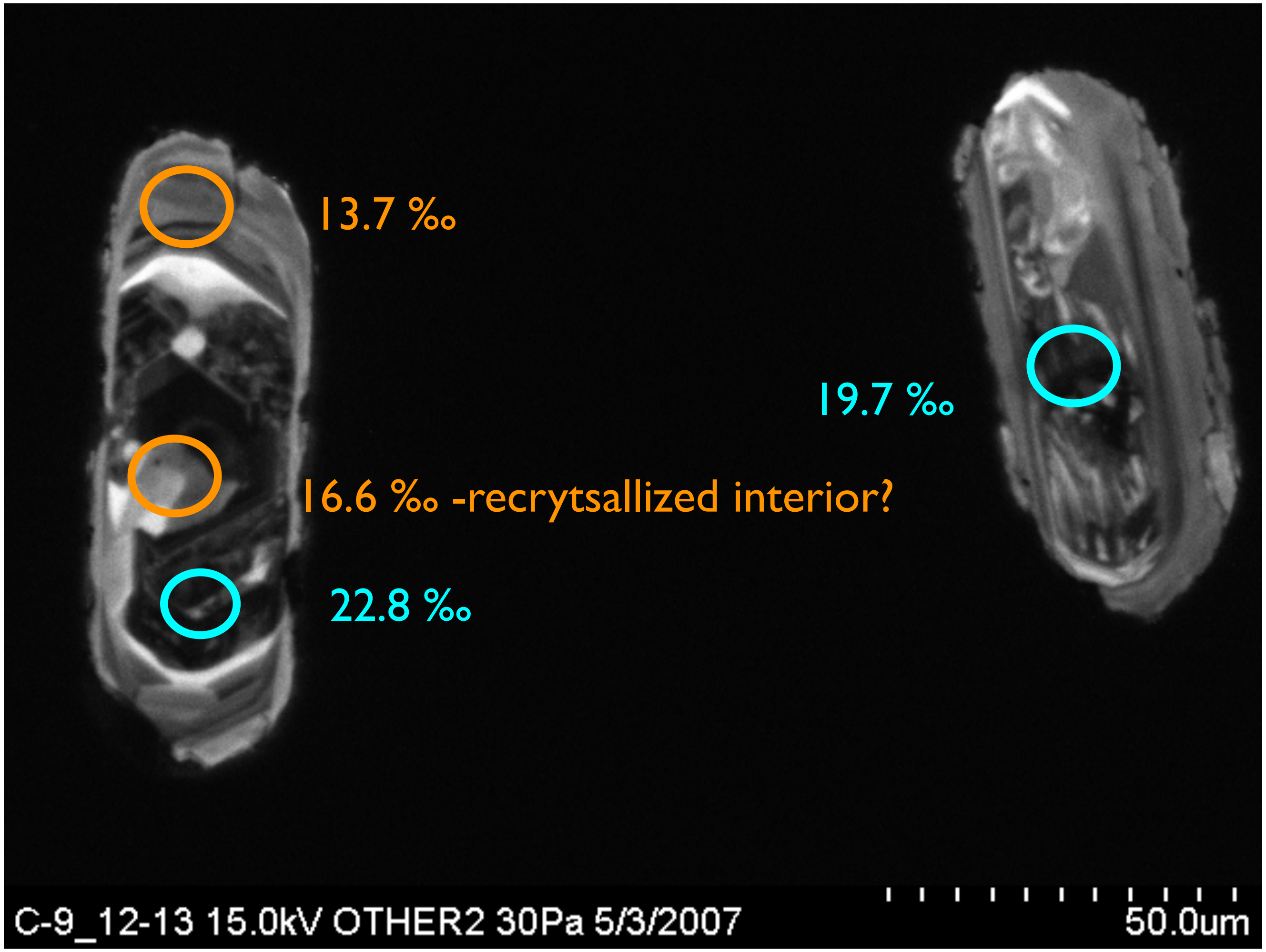

ZP-12 05C-9z16-17

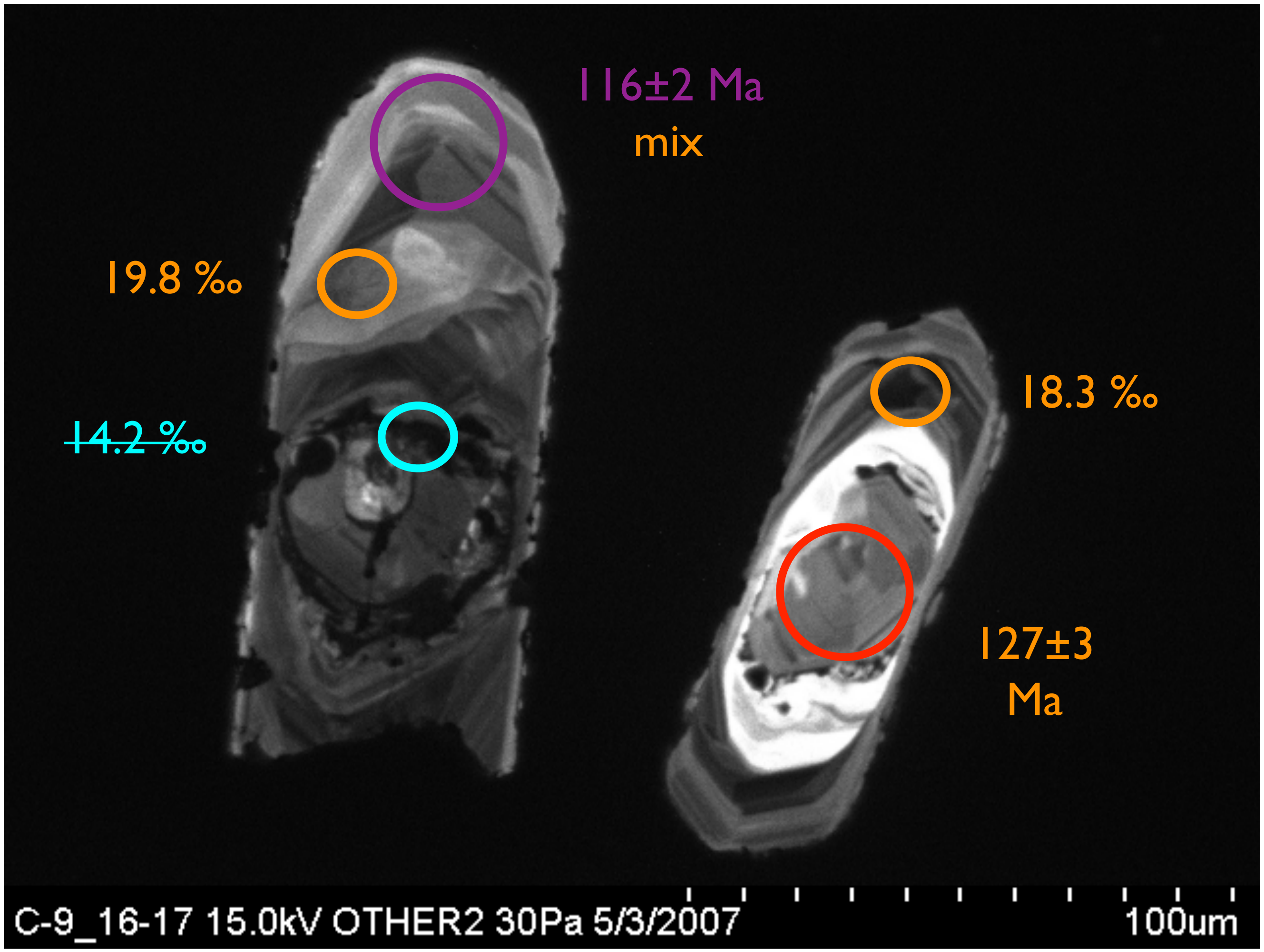

ZP-12 05C-9z15&18

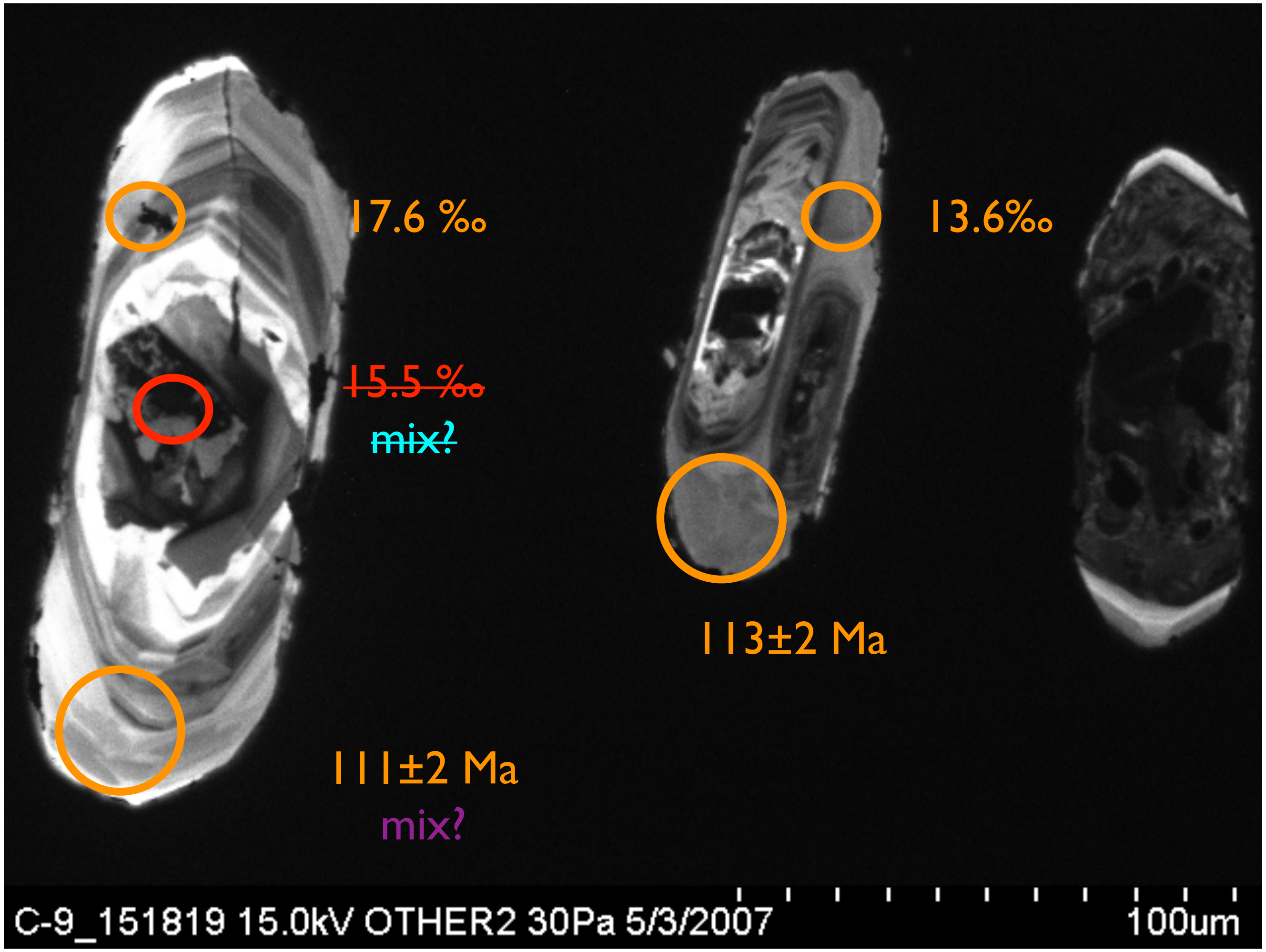

ZP-12 05C-9z19&22

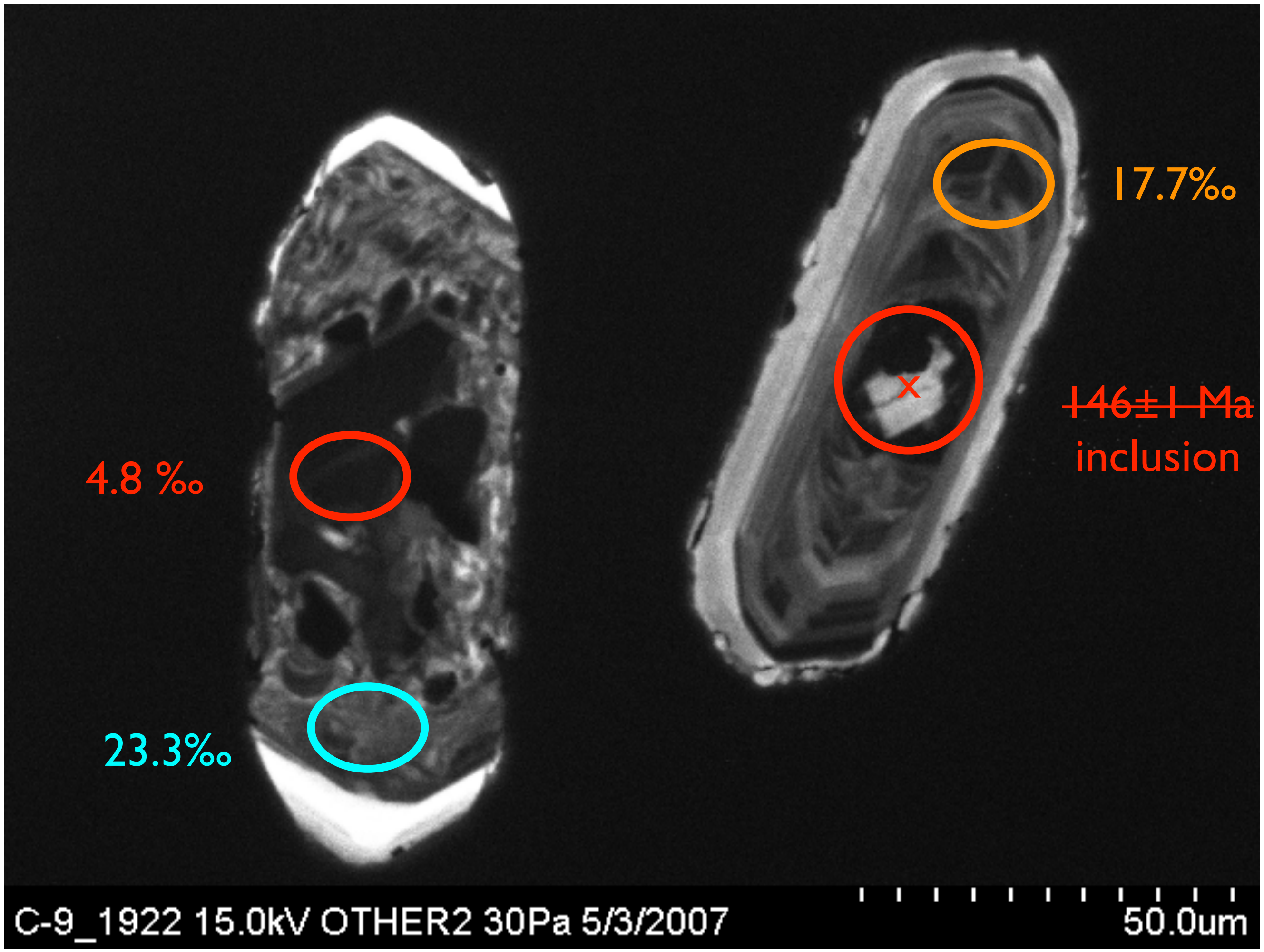

ZP-12 05C-9z20-21

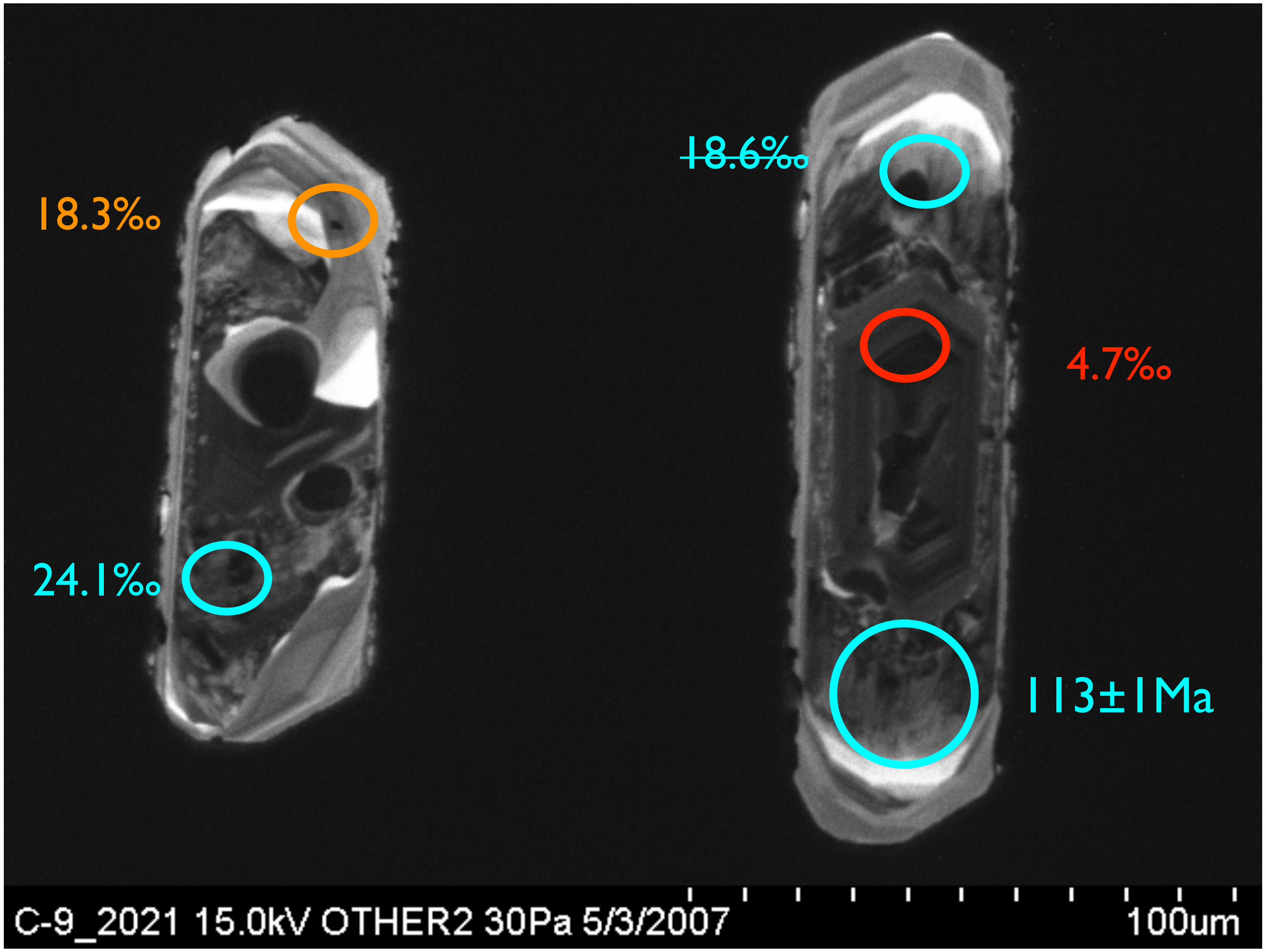

ZP-12 05C-9z23-24

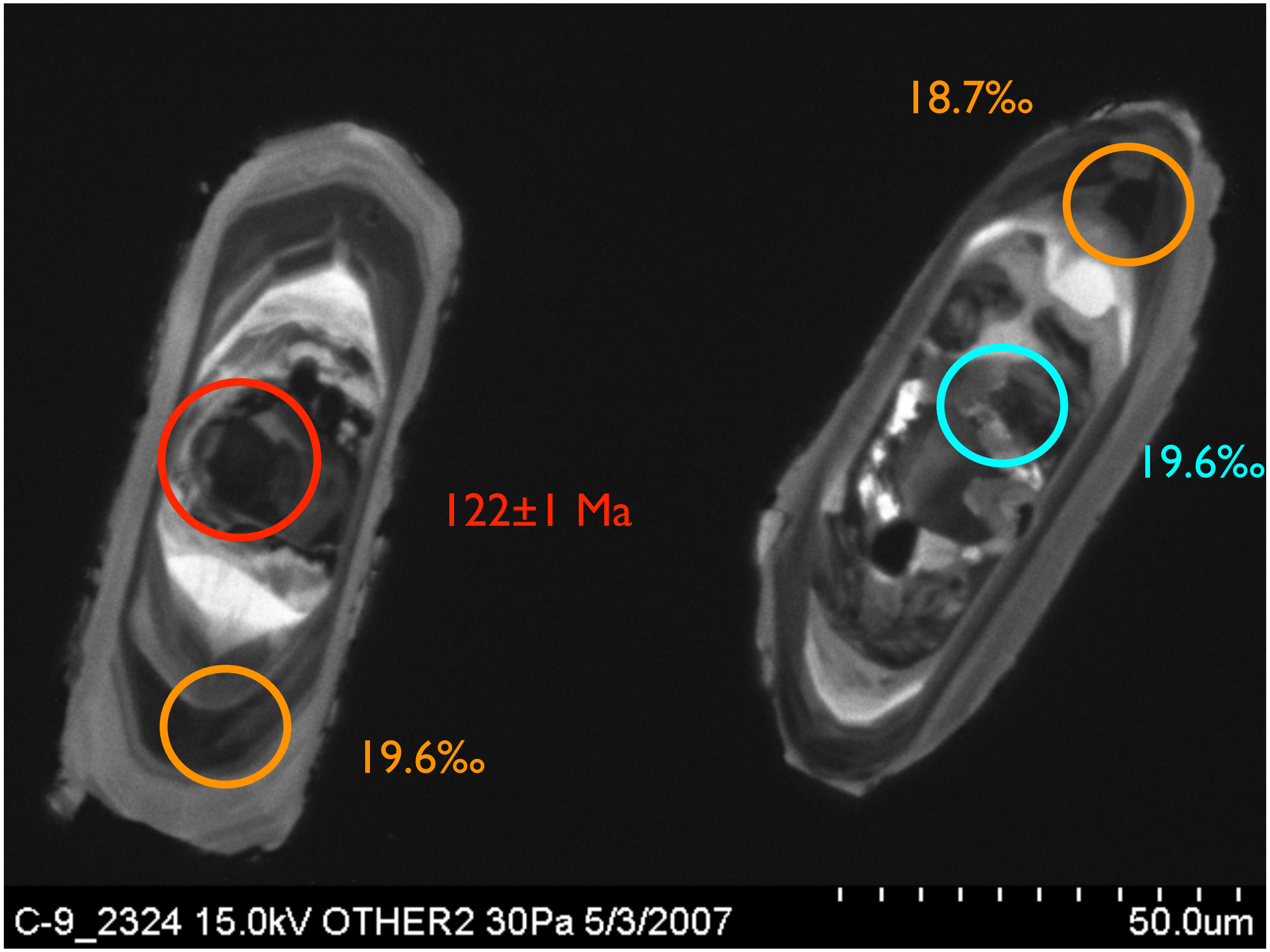

ZP-12 05C-9z25

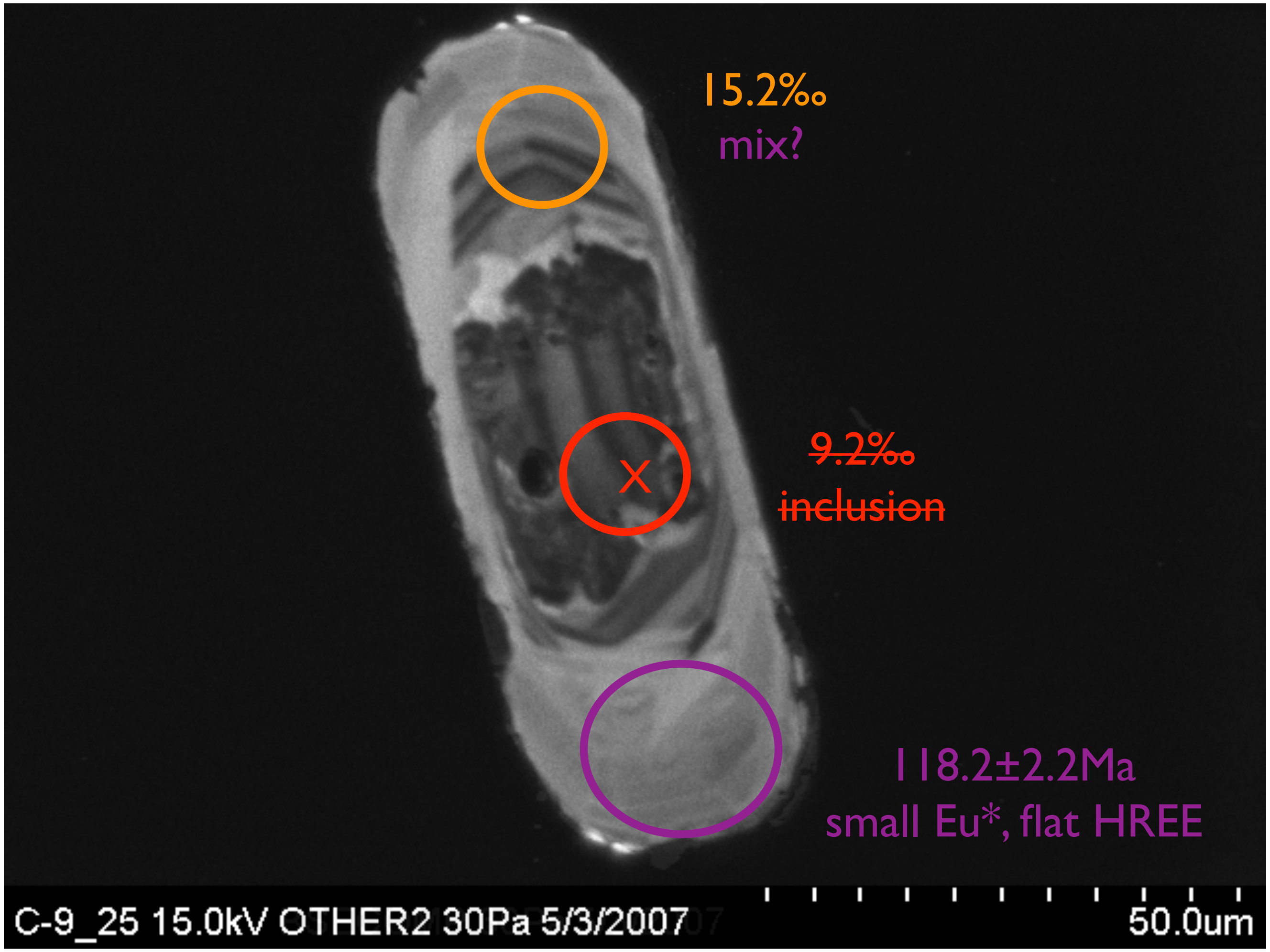

ZP-12 05C-9z26

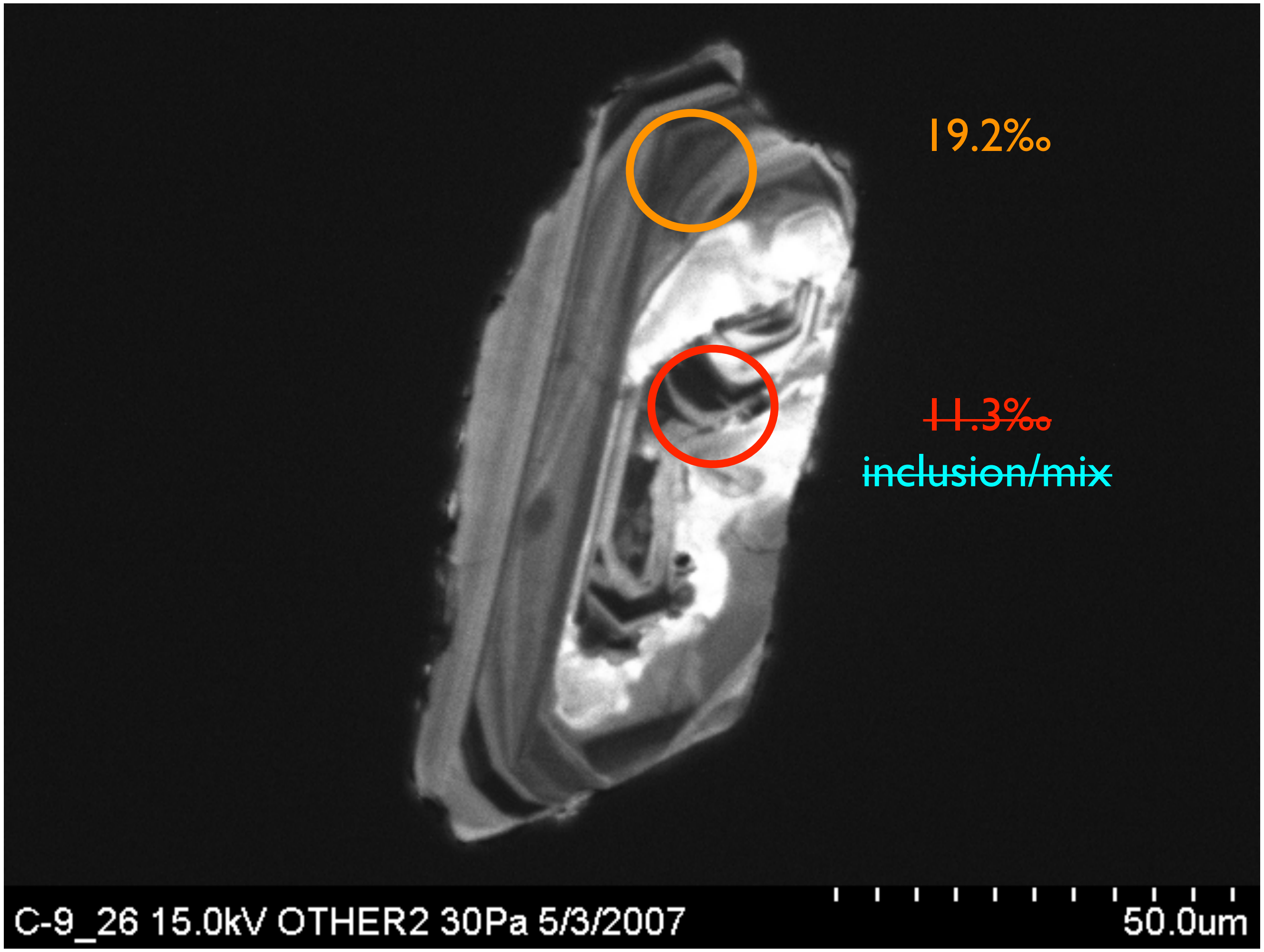

ZP-12 05C-9z27-28

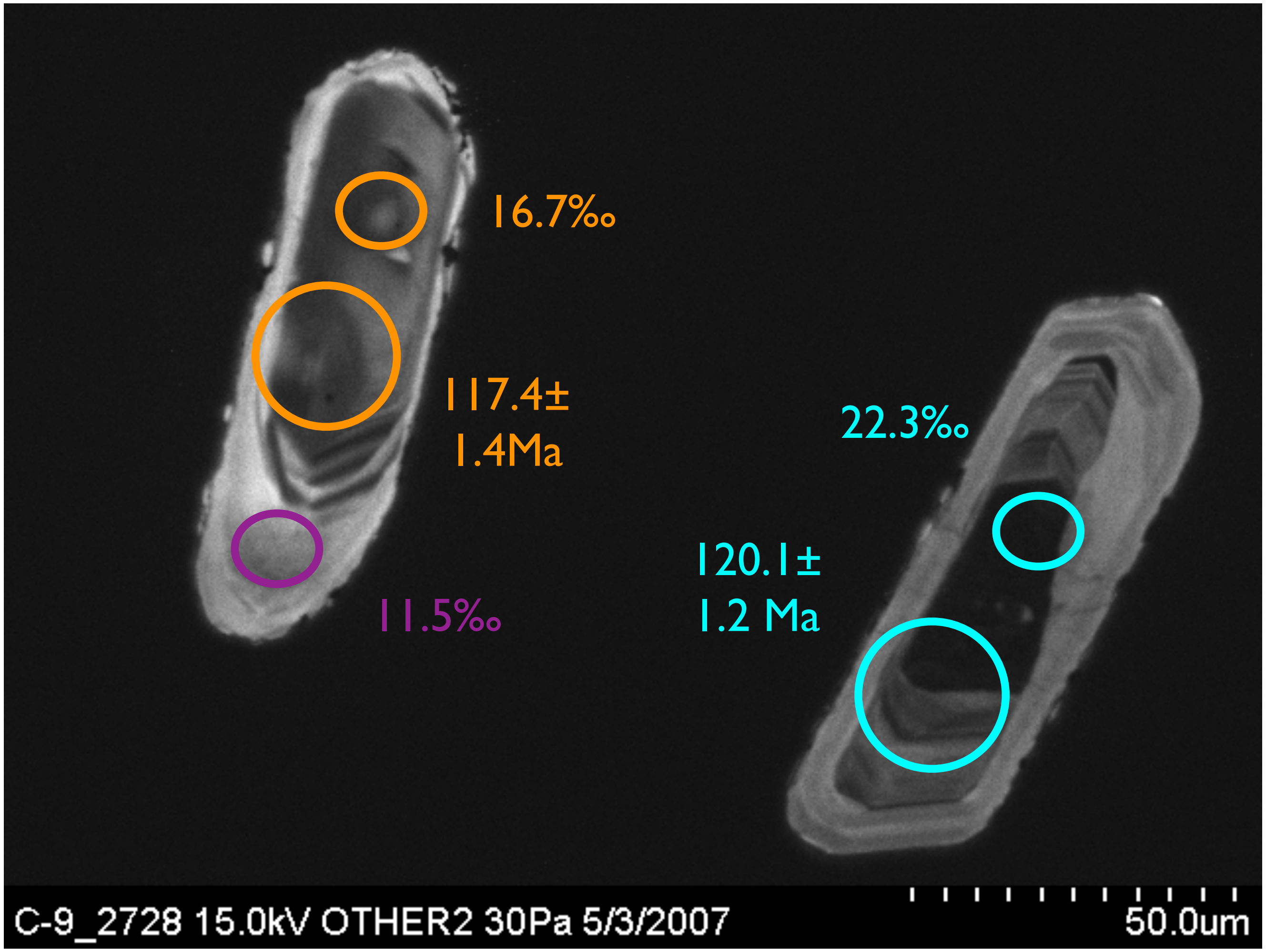

ZP-12 05C-9z29-30-a

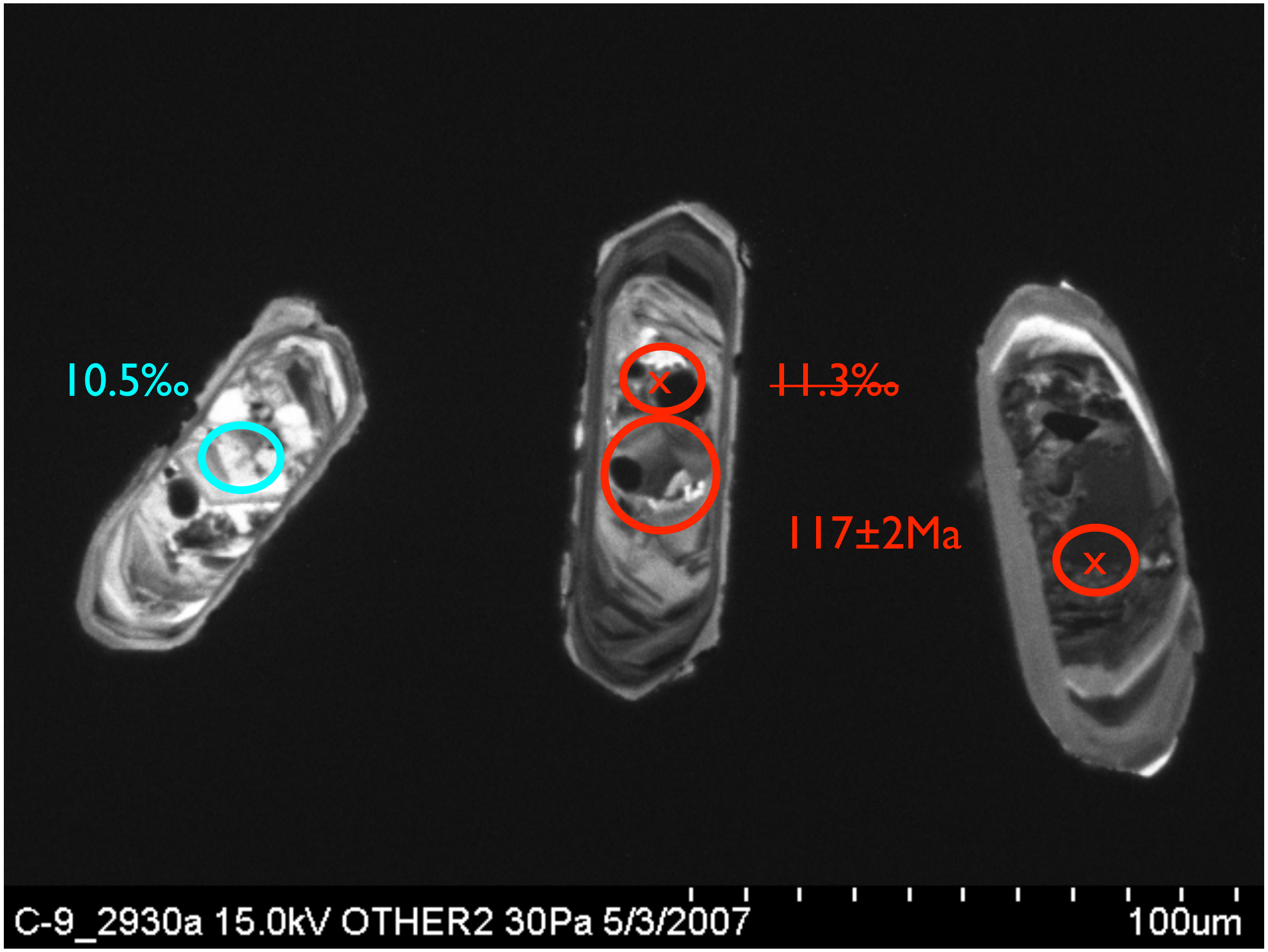

ZP-12 05C-9z31-33

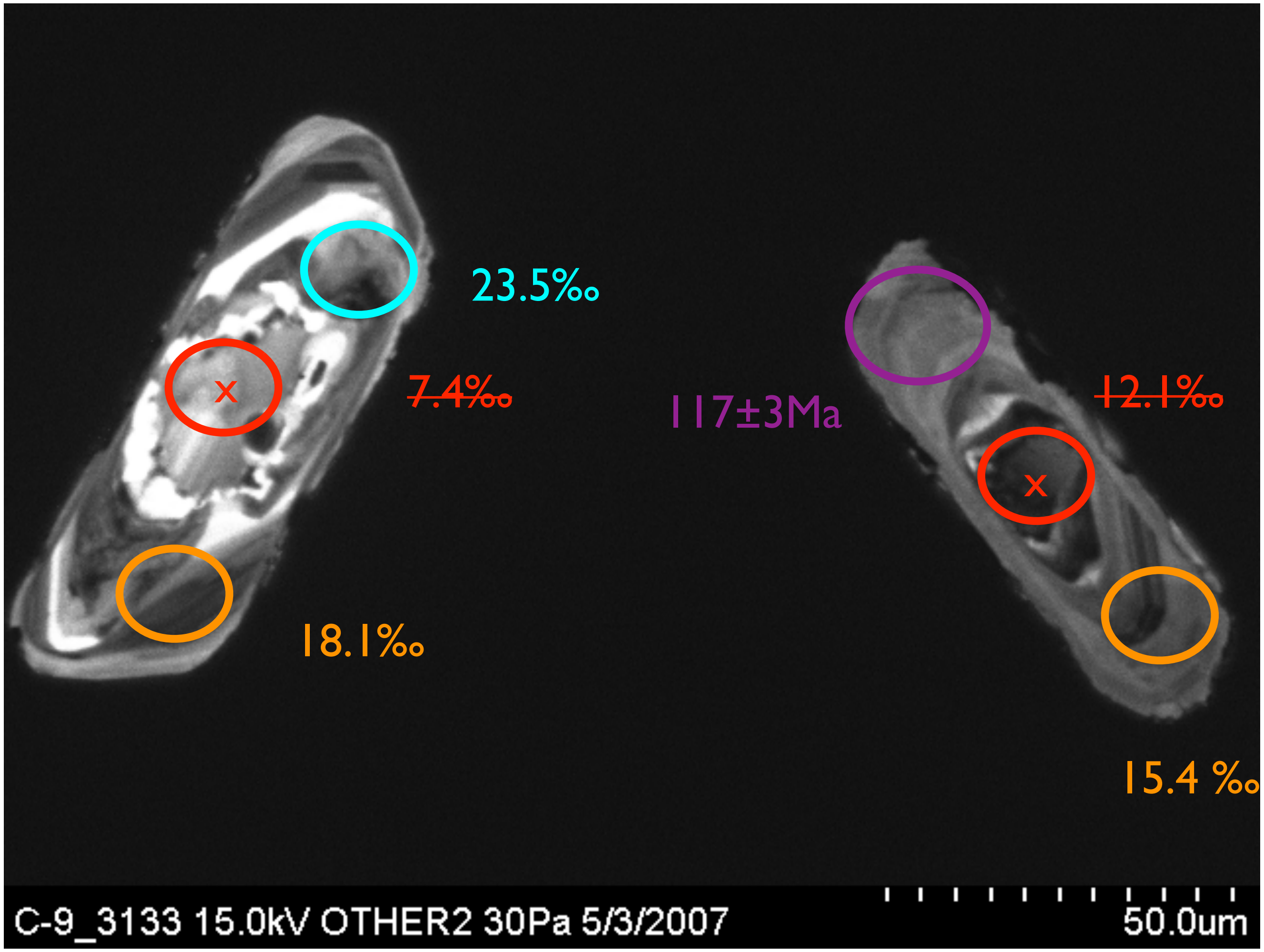

ZP-12 05C-9z32

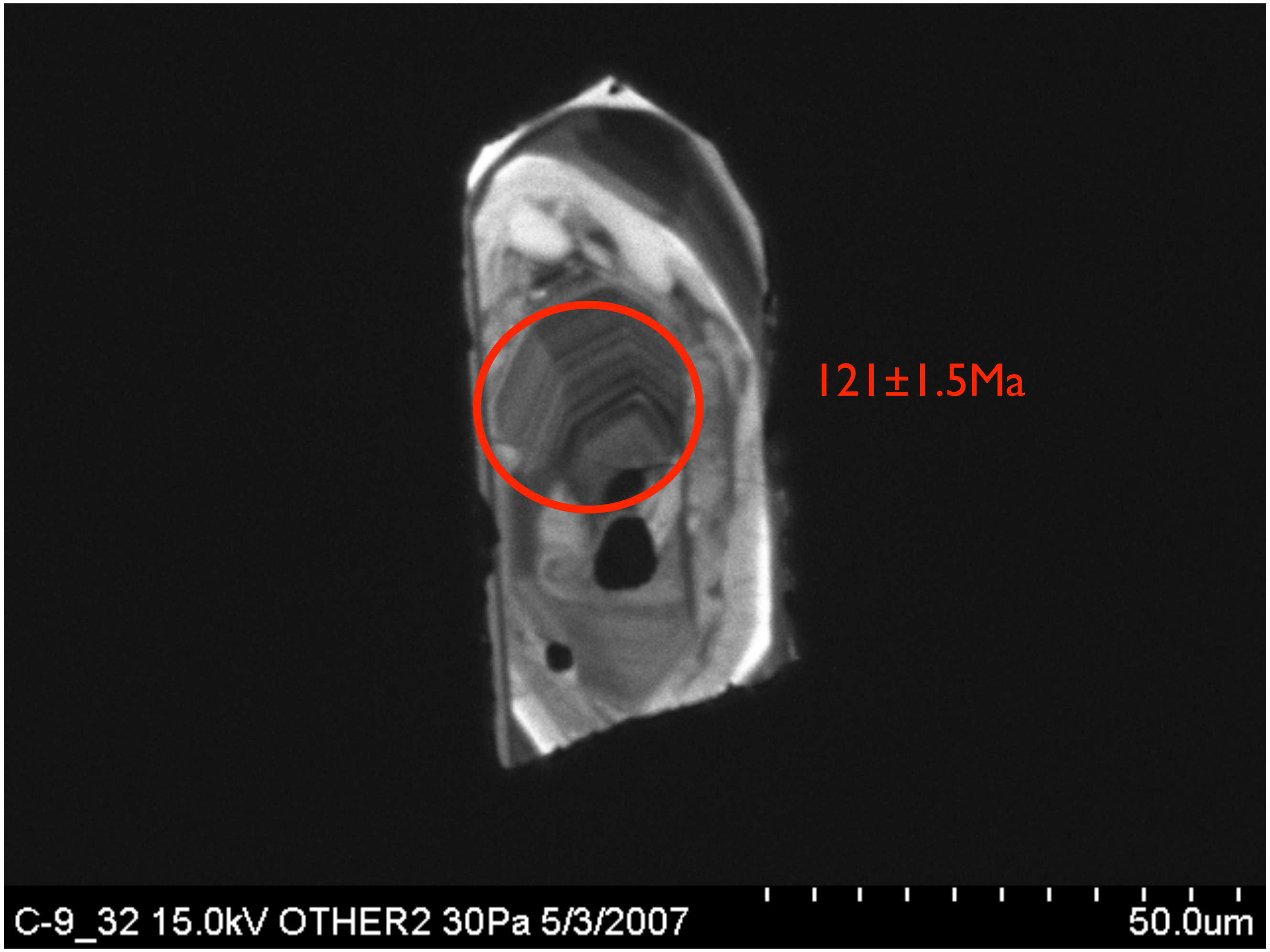

ZP-12 05C-9z34,37

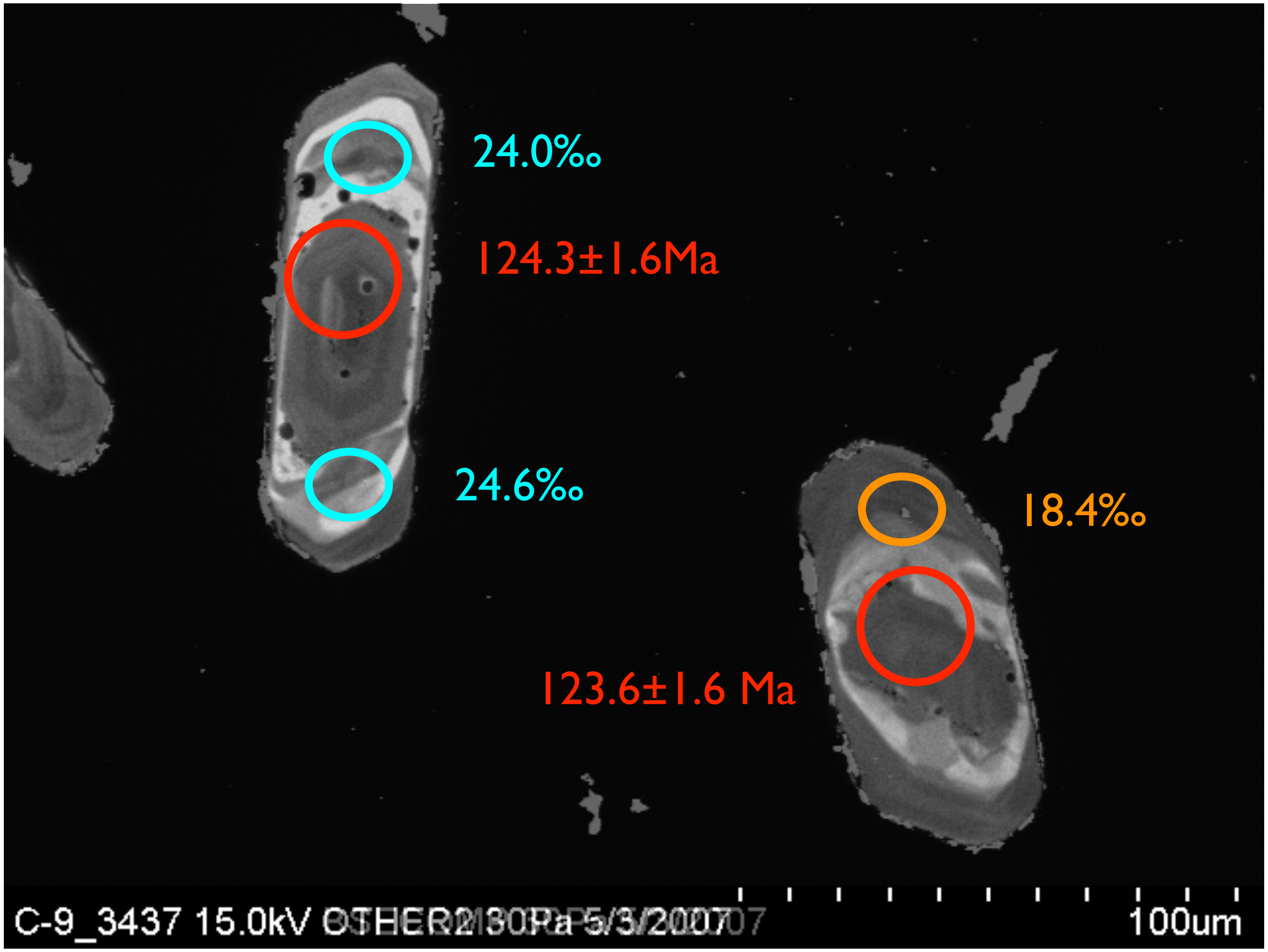

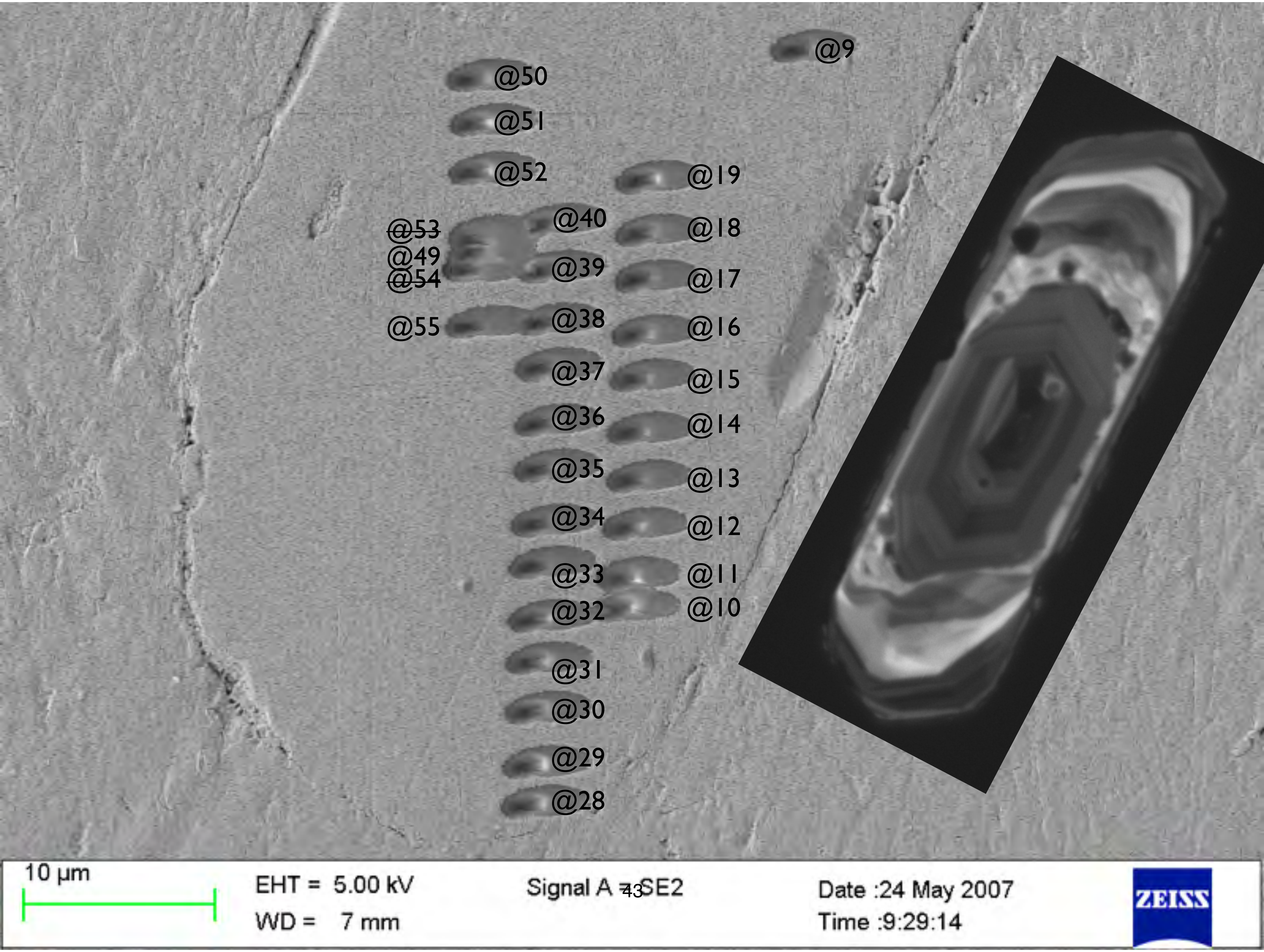
@9
@50
@51
@52
@19
~~@53~~
@40
@18
@49
@39
~~@54~~
@17
@55
@38
@16
@37
@15
@36
@14
@35
@13
@34
@12
@33
@11
@32
@10
@31
@30
@29
@28
10 µm
EHT = 5.00 kV
WD = 7 mm
Signal A = SE2
Date :24 May 2007
Time :9:29:14
ZEISS

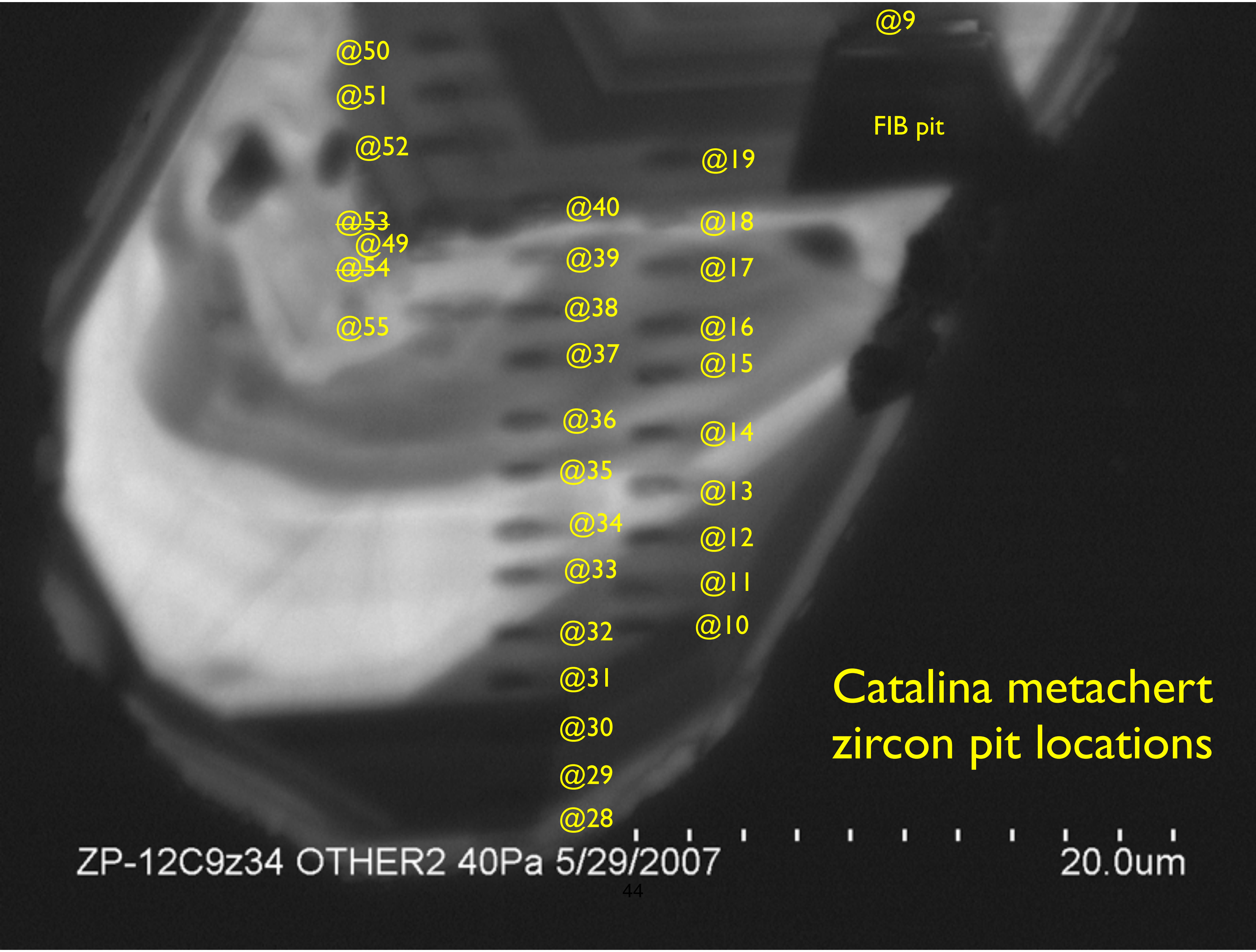
@9
FIB pit
@50
@51
@52
@19
@40
~~@53~~
@18
@49
@39
~~@54~~
@17
@38
@55
@16
@37
@15
@36
@14
@35
@13
@34
@12
@33
@11
@32
@10
@31
@30
@29
@28
Catalina metachert zircon pit locations
ZP-12C9z34 OTHER2 40Pa 5/29/2007
20.0um

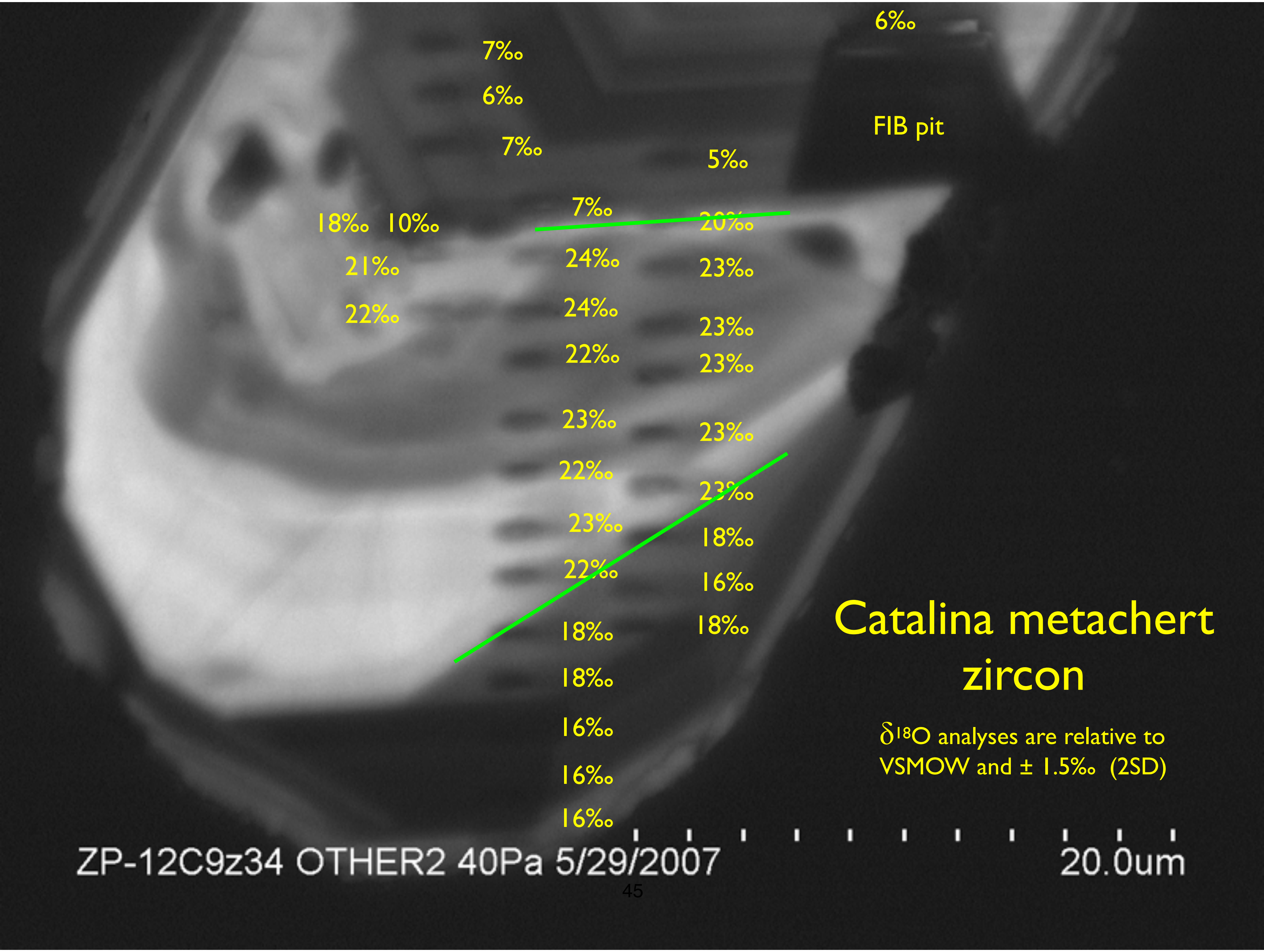
6‰
7‰
6‰
FIB pit
7‰
5‰
7‰
18‰
10‰
20‰
24‰
21‰
23‰
24‰
22‰
23‰
22‰
23‰
23‰
23‰
22‰
23‰
23‰
18‰
22‰
16‰
18‰
18‰
18‰
16‰
16‰
16‰
Catalina metachert
zircon
δ18O analyses are relative to
VSMOW and ± 1.5‰ (2SD)
ZP-12C9z34 OTHER2 40Pa 5/29/2007
20.0um

ZP-12 05C-9z35-36

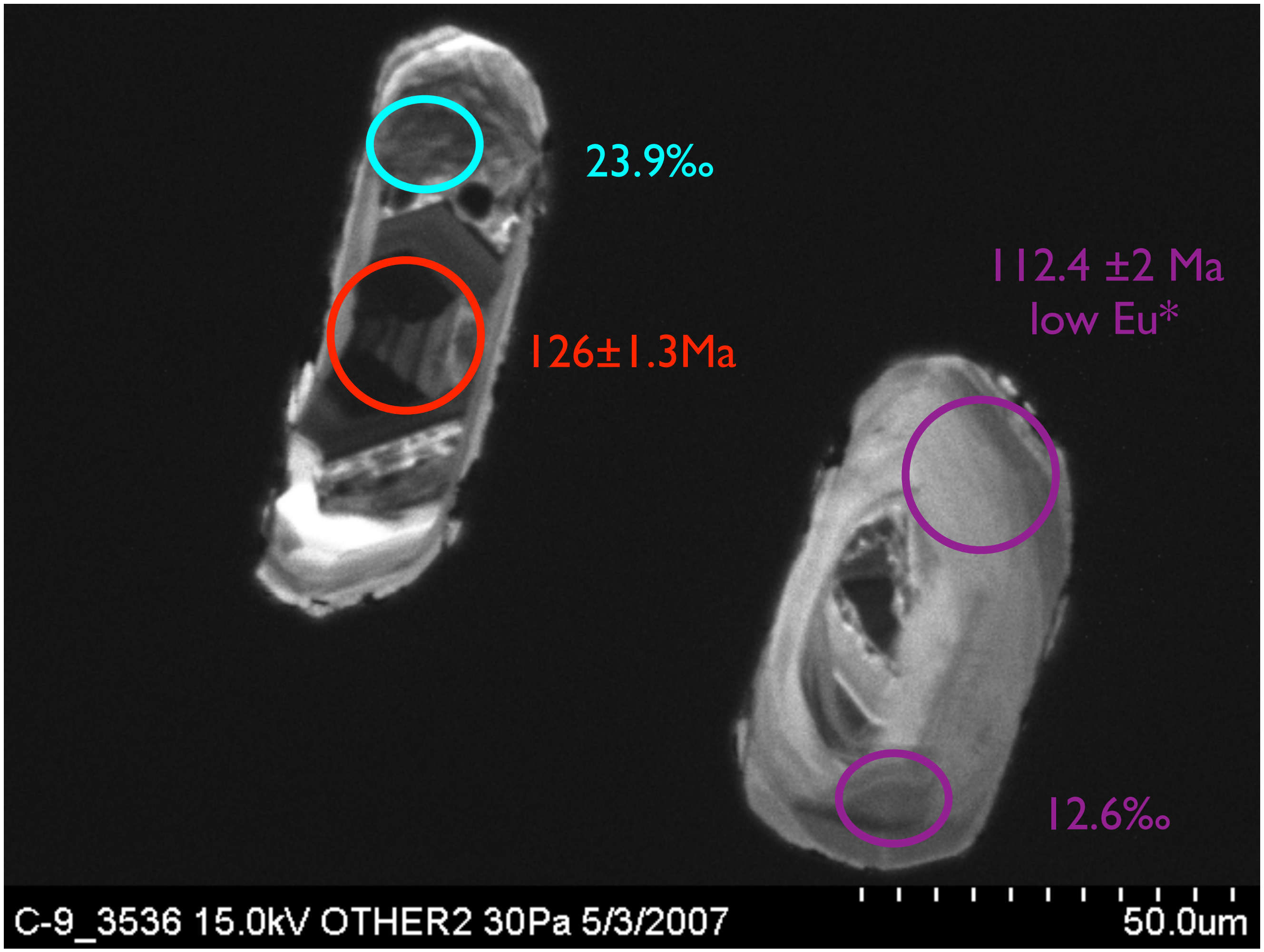

ZP-12 05C-9z38

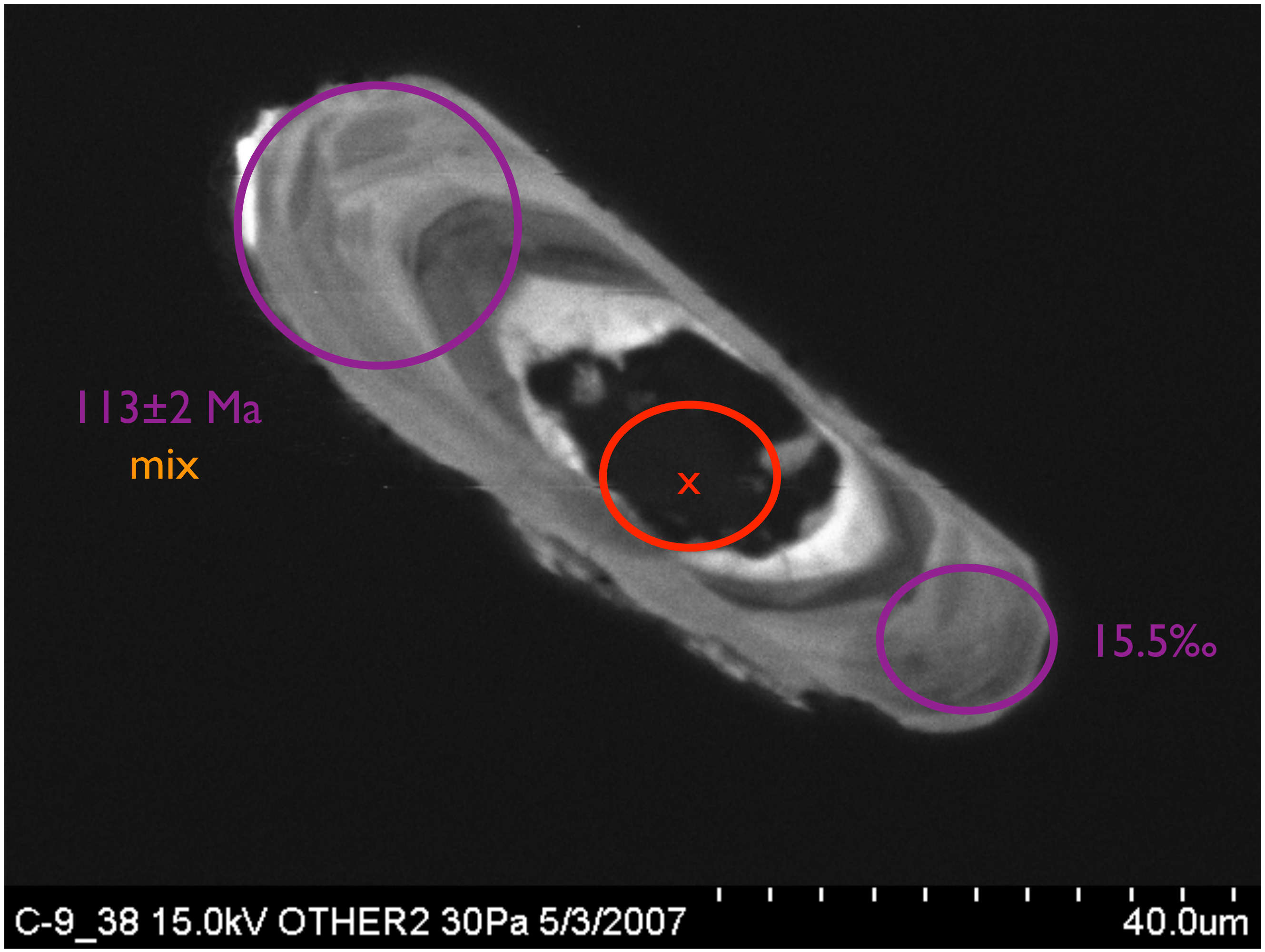

ZP-12 05C-9z39-40

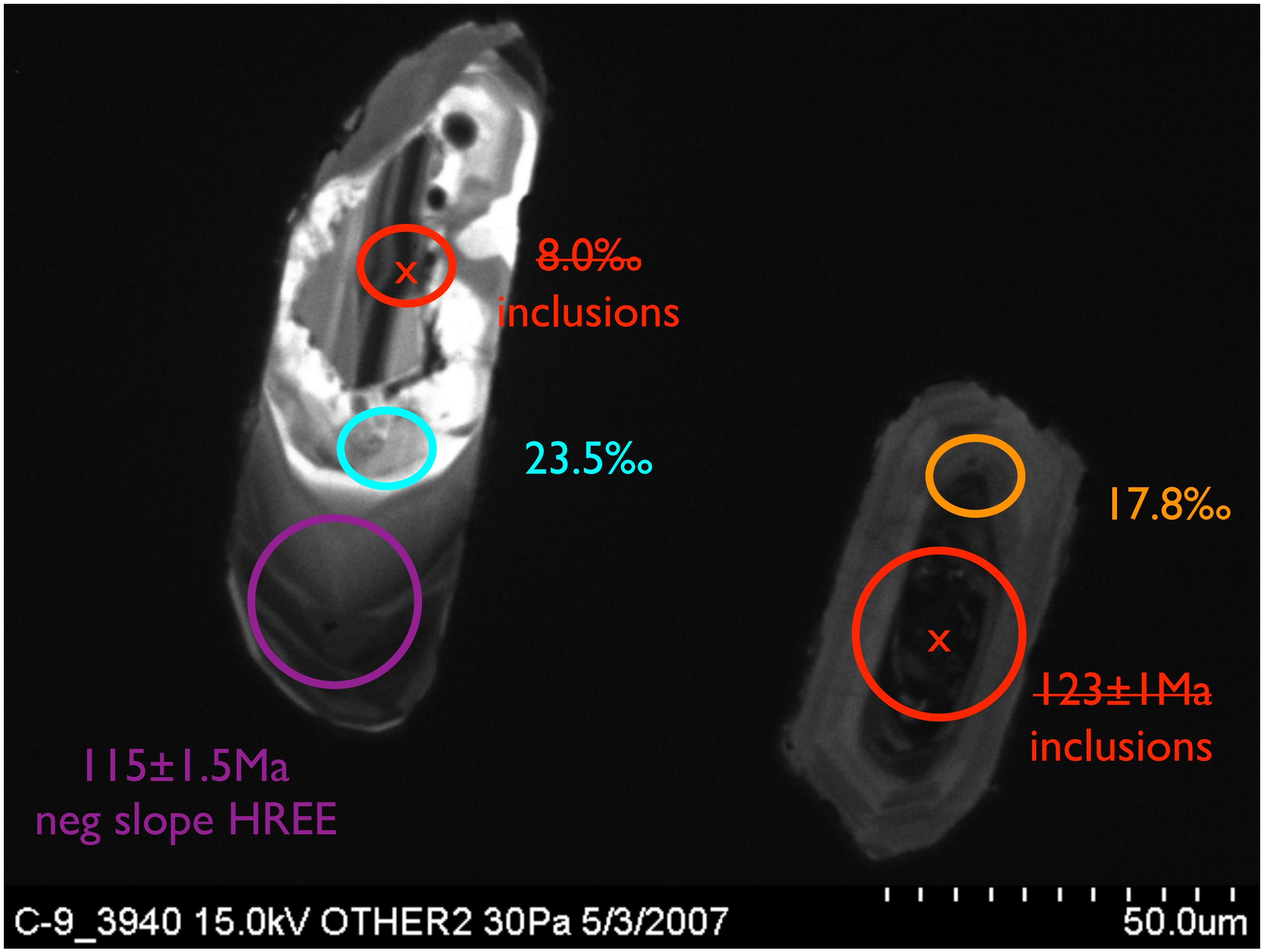

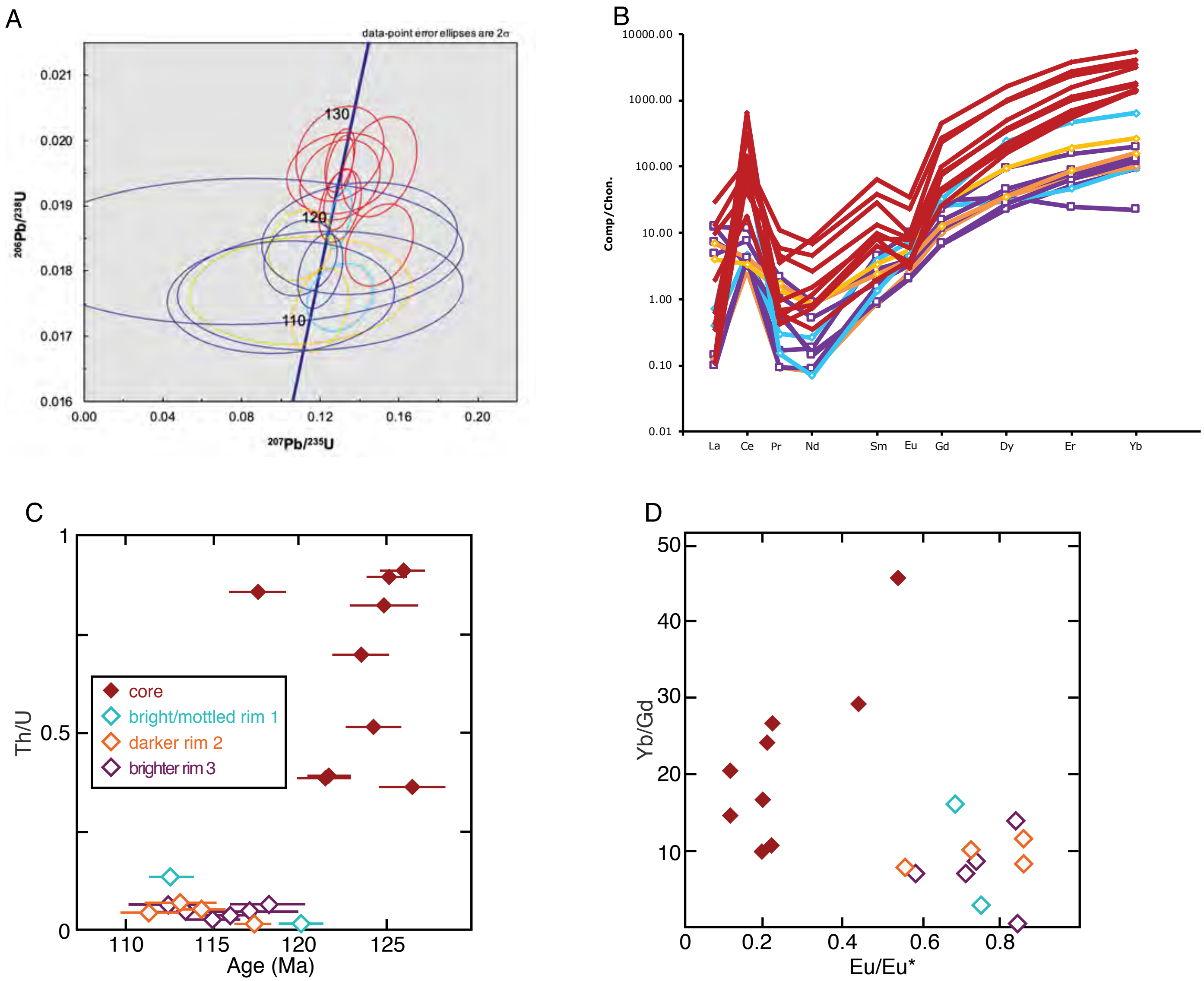

Figure DR-6 Trace element and U-Pb isotope analyses of Catalina quartzite zircons, colors indicate CL texture as in Fig. 3 A) 204Pb corrected concordia diagram of SHRIMP analyses. B) Chondrite-normalized REE diagram of combined isotope and Trace Element analyses. C) Th/U vs. ^{238}U-^{206}Pb age. High Th/U cores are older and likely detrital igneous zircon. All rim CL textures are indistinguishable in age and Th/U, both of which suggest metamorphic origin. D) Yb/Gd vs. Eu/Eu*. Detrital cores have steeper HREE patterns (greater Yb/Gd) and more prominent Eu anomalies (smaller Eu/Eu*) consistent with coexisting plagioclase (but not garnet) during formation. Rims have flatter HREE and smaller Eu anomalies, indicating growth in a plagioclase-absent, garnet-present environment.

Appendix DR-9 Back-scattered electron images of garnets analyzed for $\delta^{18}O$by ion microprobe. Pit diameter is ~10 μm.

The lower Z matrix mineral is quartz. Extremely bright BSE material in cracks and along grain boundaries is remnant gold coating .

Numbers in yellow below pits are $\delta^{18}O$ values in ‰ relative to VSMOW.

White numbers above pits are ion microprobe analysis number as recorded in Table DR-3. Strikethrough represents discarded analysis.

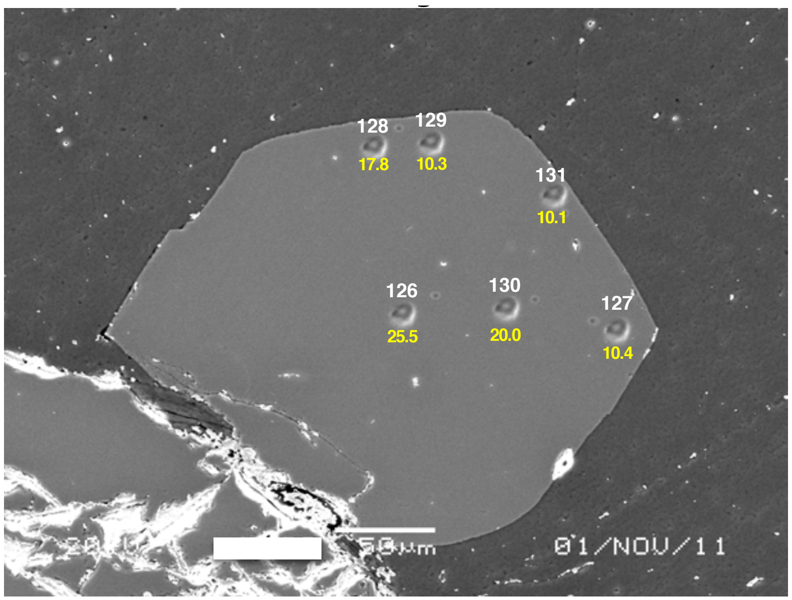

05C-09aOB
g1 baby

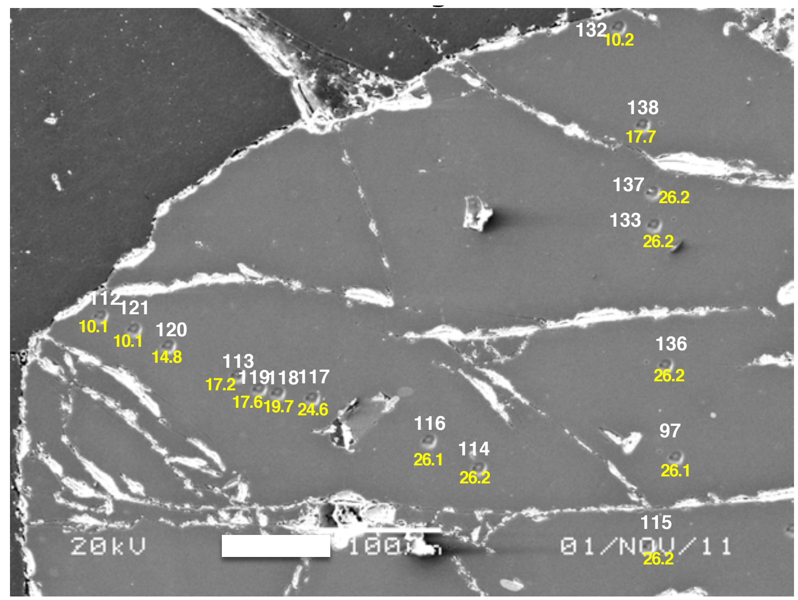

05C-09aOB
g1 NW pits

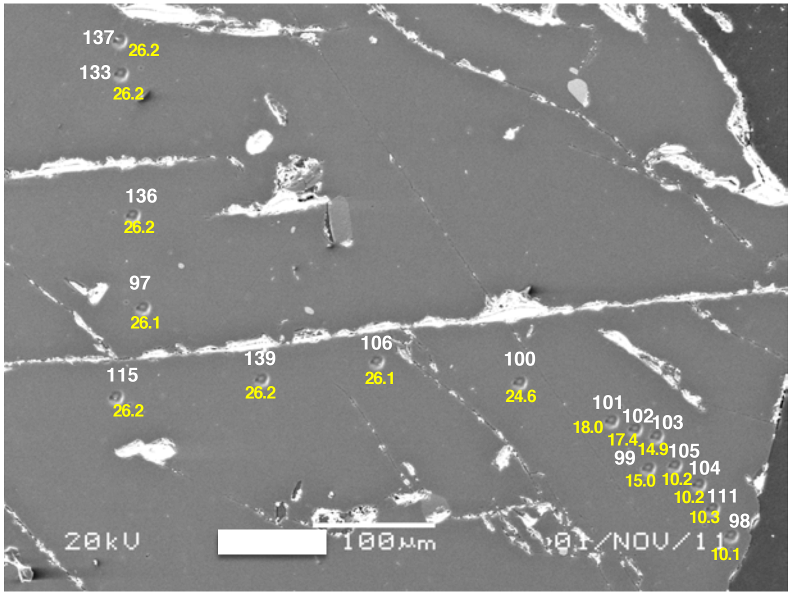

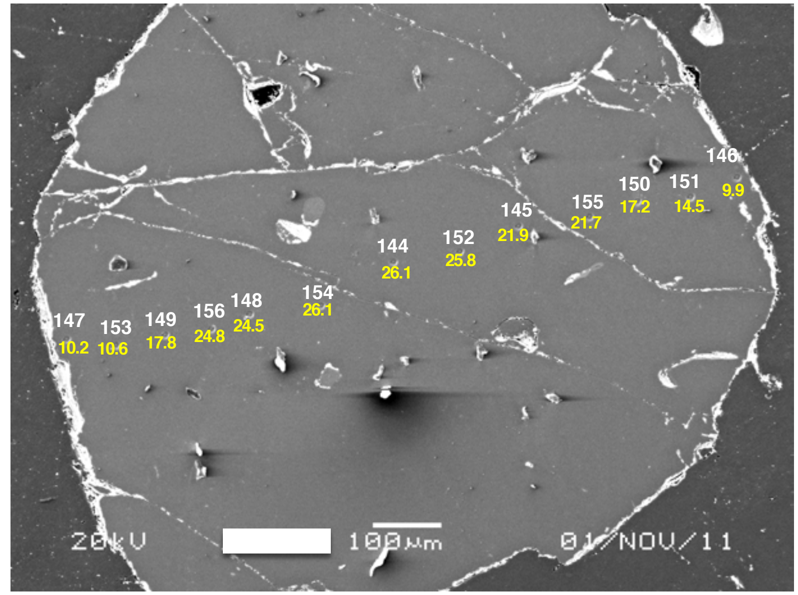

05C-09aOB
g1 SE pits

05C-09aOB
g2

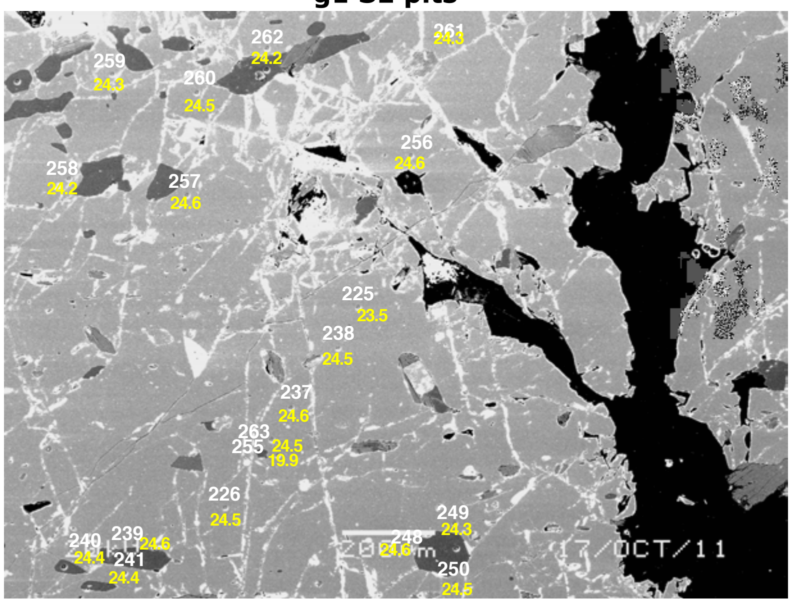

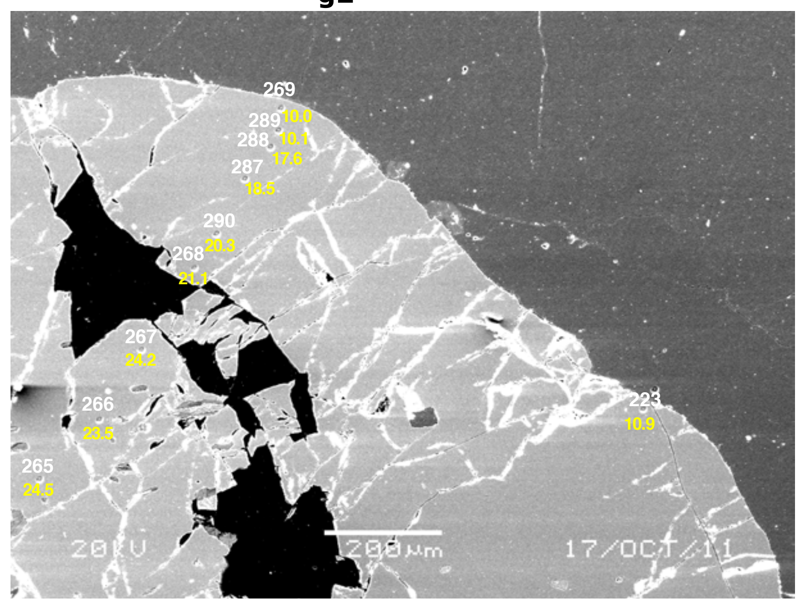

05C-09aUW g1
Center pits

05C-09aUW g1
NE pits

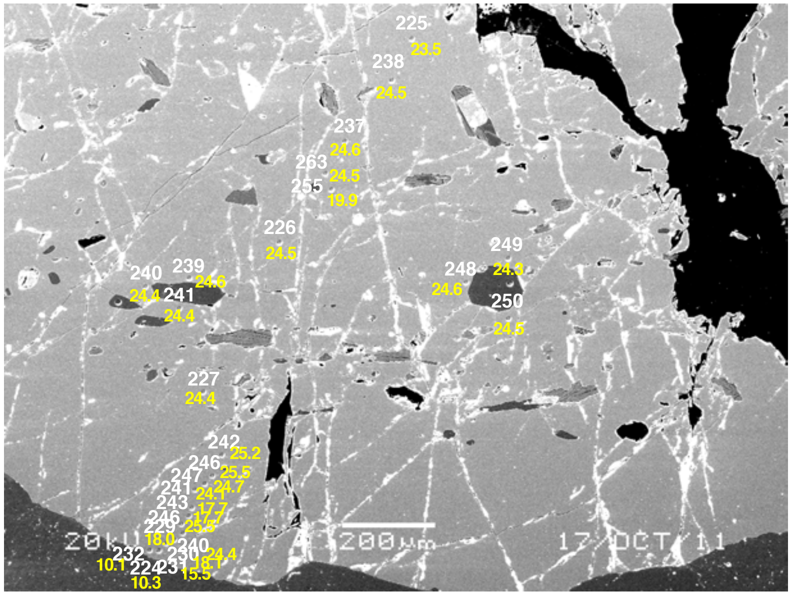

05C-09aUW g1
SW pits

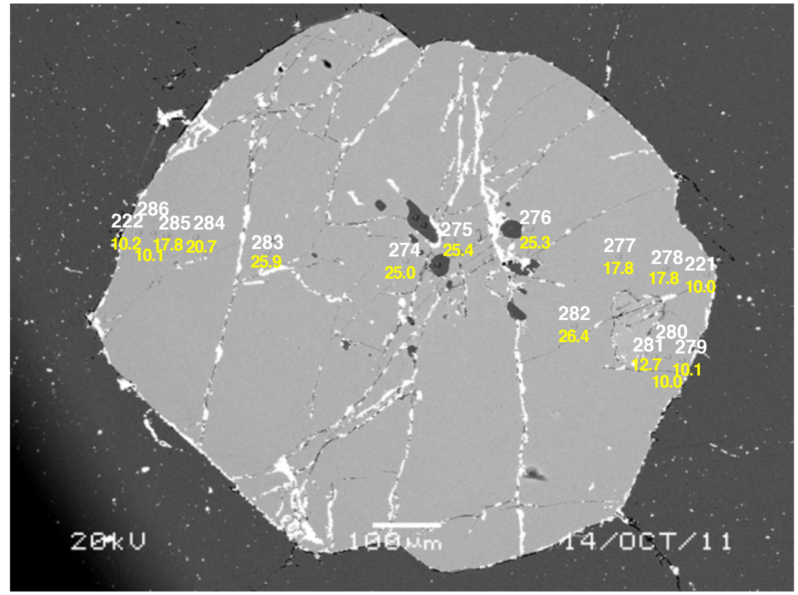

05C-09aUW g2